TRAFFICKING OF INTEGRAL MEMBRANE PROTEINS OF THE INNER NUCLEAR MEMBRANE CAN BE MEDIATED BY THE "SORTING MOTIF" OF *AUTOGRAPHA CALIFORNICA* NUCLEOPOLYHEDROVIRUS ODV-E66

A Dissertation

by

SHAWN T. WILLIAMSON

Submitted to the Office of Graduate Studies of
Texas A&M University
in partial fulfillment of the requirements for the degree of

DOCTOR OF PHILOSOPHY

August 2005

Major Subject: Microbiology

TRAFFICKING OF INTEGRAL MEMBRANE PROTEINS OF THE INNER NUCLEAR MEMBRANE CAN BE MEDIATED BY THE "SORTING MOTIF" OF *AUTOGRAPHA CALIFORNICA* NUCLEOPOLYHEDROVIRUS ODV-E66

A Dissertation

by

SHAWN T. WILLIAMSON

Submitted to the Office of Graduate Studies of
Texas A&M University
in partial fulfillment of the requirements for the degree of

DOCTOR OF PHILOSOPHY

Approved by:

Chair of Committee,	Max D. Summers
Committee Members,	Deborah A. Siegele
	Arne C. Lekven
	Arthur E. Johnson
	Sharon C. Braunagel
Head of Department,	Vincent A. Cassone

August 2005

Major Subject: Microbiology

ABSTRACT

Trafficking of Integral Membrane Proteins of the Inner Nuclear Membrane Can Be Mediated by the “Sorting Motif” of *Autographa californica* Nucleopolyhedrovirus ODV-E66. (August 2005)

Shawn T. Williamson, B.S., Texas A&M University

Chair of Advisory Committee: Dr. Max D. Summers

The amino-terminal 33 amino acids of the baculovirus integral membrane protein, ODV-E66, are sufficient for localization of fusion proteins to viral-induced intranuclear microvesicles (MV) and occlusion derived virus envelopes during infection, and has been termed the sorting motif (SM). When abundantly expressed, SM-fusions are also detected in the inner nuclear membrane (INM), outer nuclear membrane and endoplasmic reticulum of infected cells, suggesting proteins with the SM use the same trafficking pathway as cellular INM proteins to traffic to nuclear membranes. This study identifies the essential characteristics required for sorting of the SM to the INM of uninfected cells, and the MV and ODV envelopes of infected cells. These features are an 18 amino acid transmembrane sequence that lacks polar and charged amino acids (a.a.) with a cluster of charged a.a. spaced 5-11 residues from the end of the transmembrane sequence. A comparison of the a.a. sequence of these SM features with cellular INM proteins shows the features are conserved.

The model of INM protein sorting and localization predicts the only known sorting event during INM protein trafficking is immobilization/retention in the INM.

This study uses confocal microscopy and fluorescence recovery after photobleaching to compare the localization and mobility of lamin B receptor (LBR) fusions (which contain SM-like sequences) to a viral SM fusion when expressed in either mammalian or insect cells. The results show that immobilization is not necessarily required for accumulation of proteins in the INM. Furthermore, the results from infected cells show that an active sorting event, likely independent of immobilization, can distinguish the viral SM from cellular sequences similar to the SM.

The results of this study show that sorting of proteins to the INM can be mediated by the viral SM or INM protein SM-like sequences that can function either independent of, or in addition to, immobilization. These data combined with recent reports suggest that in addition to diffusion:retention a signal mediated mechanism for sorting and localization to the INM can occur.

DEDICATION

To my wife, Susan, for her compassion and support that kept me going.

ACKNOWLEDGEMENTS

First I need to thank my advisor, Dr. Max D. Summers, for his guidance and support. I also need to thank Dr. Sharon C. Braunagel. I truly appreciate the superb intellectual insight, guidance and assistance offered by both of these two wonderful scientists and people.

Additionally I would like to thank the members of my graduate advisory committee, Dr. Deborah Siegele, Dr. Arne Lekven, Dr. Arthur Johnson and Dr. Efithimos Skoulakis, for their time and help.

I thank: 1) Dr. Jan Ellenberg (EMBL Heidelberg, Heidelberg, Germany) for the phLBR 1TM-EGFP construct; 2) Yuanlong Shao and Suraj Saksena for the preparation of insect microsomal membranes [laboratory of Dr. Arthur Johnson (Department of Medical Biochemistry and Genetics, Texas A&M University, College Station, TX)]; 3) Dr. Paul Fisher (Department of Pharmacological Sciences, University of New York at Stony Brook, Stony Brook, NY) for providing the Adl67 anti-sera (*Drosophila* lamin); 4) Dr. Robert Possee (Center for Ecology and Hydrology, University of Oxford, Oxford, UK) for providing the BacPak viral variant used for production of recombinant virus; 5) Dr. Robert Burghardt and Rola Barhoumi-Mouneimne (Image Analysis Laboratory, College of Veterinary Medicine, Texas A&M University, College Station, TX) for their FRAP expertise and facilities.

I would also like to thank the members of the Summers laboratory, including: Dr. Zhenping Zhong, Dr. Qi Ding, Dr. German Rosas, Jared Burks,

Matthew Powers, Paula Shawver, and Genevieve Ledwell for their assistance and friendship.

Finally, I am indebted to my wife, Susan J. Williamson, for her support, love and understanding.

TABLE OF CONTENTS

LIST OF FIGURES

FIGURE Page

FIGURE Page

LIST OF TABLES

LIST OF ABBREVIATIONS

Abbreviation	Name
a.a.	amino acid
AcMNPV	*Autographica californica* multi-nucleopolyhedrovirus
AD	adenovirus
BAF	barrier to autointegration factor
β-gal	β-galactosidase
bp	base pair
BV	baculovirus budded virus
C. elegans	*Caenorhabditis elegans*
cDNA	coding DNA
C-terminal	carboxy terminal
C-terminus	carboxy terminus
$CaCl_2$	calcium chloride
CO_2	carbon dioxide
CHO-K1	chinese hamster ovary cells, clonal isolate k1
DAPI	4,6-diamidino-2-phenylindole
DMEM	Dulbecco's modified eagle media
DNA	deoxyribonucleic acid
DTT	dithiotheritol
EDMD	Emery-Dreifuss muscular dystrophy
EGFP	enhanced green fluorescent protein

Abbreviation	Name
EDTA	ethylene diamine tetra-acetic acid
EN	extra-nuclear
ER	endoplasmic reticulum
FBS	fetal bovine serum
Fig.	figure
FP	few polyhedra
FRAP	fluorescence recovery after photobleaching
gB	glycoprotein B of HSV
GDP	guanidine di-phospate
GlcNAC	N-acetyl glucosamine
GTP	guanidine tri-phospate
GFP	green fluorescent protein
GV	Granulovirus
HCl	hydrochloric acid
HP1	heterochromatin binding protein 1
h p.i.	hours post infection
HSV	herpes simplex virus
IN	intranuclear
INM	inner nuclear membrane
Kb	kilo-base
KOAc	potassium acetate

Abbreviation	Name
kDa	kilodalton
LAP	lamin associated polypeptide
LBR	lamin B receptor
LCM	light confocal microscopy
LdMNPV	*Lymantria dispar* multi-nucleopolyhedrovirus
LEM	LAP, Emerin, MANI nucleoplasmic binding domain
LMNA	lamin A gene
LMNB	lamin B gene
MDa	megadalton
mM	milli molar
M_r	relative molecular mass
MeOH	methanol
$Mg(OAc)_2$	magnesium acetate
mg	milli gram
ml	milli liter
MV	microvesicles
MW	molecular weight
µg	micro gram
µl	micro liter
µm	micro meter
N-terminal	amino terminal

Abbreviation	Name
N-terminus	amino terminus
NaCl	sodium chloride
$NaHCO_3$	sodium bi-carbonate
NE	nuclear envelope
NeleNPV	*Neodiprion lecontei* nucleopolyhedrovirus
NES	nuclear export signal
NLS	nuclear localization signal
nm	nano meter
NPC	nuclear pore complex
NPM	nuclear pore membrane
NPV	Nucleopolyhedrovirus
NST	glycosylation acceptor sequence
ONM	outer nuclear membrane
ODV	occlusion derived virus
OpMNPV	*Orgyia pseudotsugata* multi-nucleopolyhedrovirus
Orf	open reading frame
PBS	phosphate buffered saline
PCR	polymerase chain reaction
PE	polyhedra envelope
PM	plasma membrane
PMSF	phenylmethylsulfonylfluoride

Abbreviation	Name
RNA	ribonucleic acid
RT	room temperature
SeMNPV	*Spodoptera exigua* multi-nucleopolyhedrovirus
SDS	sodium dodecyl sulfate
SDS-PAGE	sodium dodecyl sulfate poly-acrylamide electrophoresis
Sf9	*Spodoptera frugiperda* IPLB-SF21 clonal isolate 9
SM	ODV-E66 INM sorting motif
SRP	signal recognition particle
TEA	triethanolamine
TM	transmembrane sequence
TNM-FH	*T. ni.* media – Frederick Hinks
TRAM	translocating chain-associating membrane protein
Tris	(hydroxymethyl) aminomethane buffer
v/v	volume/volume
w/v	weight/volume
wt	wild type
X-gluc	5-Bromo-4-chloro-3-indolyl β-D-glucopyranoside
XcGV	*Xestia c-nigrum* granulovirus
YA	young arrest protein

INTRODUCTION

Literature review

Baculovirus: General information, hosts and infection process. The *Baculoviridae* are a family of viruses with single or multiple enveloped rod-shaped nucleocapsids containing a circular, double stranded DNA genome ranging from 82 kb pairs [NeleNPV, (1)] to 179 kb pairs [XcGV, (2)] in length. They are classified into two types based on the type of viral occlusion formed during infection, granulovirus (GV) and nucleopolyhedrovirus (NPV). NPV is further classified into two subgroups, group I and II NPV, based on phylogentic data (3-5). Baculovirus is characterized by an unusual biphasic lifecycle that results in the production of two forms of progeny virus, budded virus (BV) and occlusion derived virus (ODV), both of which are essential for natural infection (6). The ODV form matures in the nucleus and is encapsulated in crystalline protein matrix structures termed viral occlusions. Infection is initiated when the viral occlusions are consumed by a susceptible larval host (7). Upon consumption, the occlusions are dissolved by the high pH of the insect midgut, releasing the enveloped ODV. ODV enters the cell by fusion of the ODV envelope with the microvilli of the gut cell epithelium, and infection initiates in the nucleus of the columnar cells (8-10). Early in infection, progeny nucleocapsids assemble in the nucleus and then transport to the basolateral plasma membrane

---

This dissertation follows the style and format of Traffic.

where they are enveloped and bud into the insect hemolymph as budded virus. BV is responsible for secondary infection throughout the remaining tissues of the larvae, by distribution in the hemolymph and through the tracheal system (11, 12). Alternatively, Granados et al. (7) observed nucleocapsids budding from the basolateral membrane prior to the production of BV (as early as 0.5 h p.i.). This observation suggests that parental ODV nucleocapsids are capable of directly initiating secondary or systemic infection of the host (7). As primary infection progresses the midgut cells die and are sloughed off. Secondary infection is initiated as BV infects the remaining cells of the insect. During secondary infection BV is also produced, however, during the later stages of infection nucleocapsids remain in the nucleus where they are enveloped forming ODV. The ODV form of the virus is occluded in a crystalline protein matrix, while in the nucleus [polyhedra (NPV)] or in the cytoplasm [granule (GV)] (6, 13). The major structural protein of NPV occlusions (polyhedra) is polyhedron and of GV occlusion (granule) is granulin. NPV occlusions may contain one to many virions, whereas GV occlusions only contain a single virion. As infection progresses, the insect host dies and upon death the larva liquefies. This liquefaction results in the release and spread of the viral occlusions into the surrounding environment ensuring transmission of virus among insect hosts (6).

To date over 500 NPV have been identified and isolated exclusively from arthropods (14), primarily from the order *Lepidoptera*, but also from *Hymenoptera, Diptera, Coleoptera, Neuroptera, Thysanura, Trichoptera* and the

crustacean order *Decapoda* (shrimp). GV have only been isolated from arthropods in the order *Lepidoptera* (6). In general, the baculoviruses have a limited host range, often only infecting one species of insect, however, some have been shown to have a broader host range but are limited to single order.

Autographa californica multi-nucleopolyhedrovirus, AcMNPV (type species), is the baculovirus used in this study. Unlike most baculoviruses, AcMNPV infects over 30 different species of insects in 12 families of the order *Lepidoptera*. Because AcMNPV has a large host range, it has been extensively studied as a "viral pesticide" (14). Additionally, AcMNPV was used in the development of the baculovirus expression vector system (15, 16). AcMNPV is also considered an important model system for the study of the molecular biology of baculovirus infection as it is easily studied in cultured cell systems (14).

Baculovirus: Genome organization, DNA replication and gene regulation

genome organization. AcMNPV has a circular, double stranded DNA genome of 133,894 bp. The genome sequence of AcMNPV (strain C6), the first baculovirus to be sequenced and annotated, was completed in 1994, and is comprised of 154 potential open reading frames (17). To date a total of 18 baculovirus genomes have been sequenced, including five GV (2, 18-21), ten *Lepidopteran* NPVs (17, 22-30), two *Hymenopteran* NPVs (1, 31), and one *Dipteran* NPV (32). Comparison of the sequenced genomes determined that 29 genes are common to all baculoviruses. Of these 29 genes, 20 have known

Table 1. Genes conserved in the baculoviruses

Gene Function	Genes present in all baculoviruses	Additional genes conserved in lepidopteran baculoviruses
Replication	lef-1(ac14), lef-2(ac6), dna pol(ac65), helicase(ac95)	dbp1(ac25), lef-3(ac67), IE-1(ac147), me53(ac139)
Transcription	p47(ac40), lef-8(ac50), lef-9(ac62), vlf-1(ac77), lef-4(ac90), lef-5(ac99)	Pp31/39k(ac36), lef-6(ac28), lef-11(ac37)
Structural proteins	ac23(ld130)(not in NeleNPV), gp41(ac80), odv-ec27(ac144), odv-e56(ac148), p6.9(ac100), p74(ac138), vp91/p95(ac83), vp39(ac39), vp1054(ac54)	FP25K(ac61), odv-e18(ac143), odv-e25(ac94), odv-e66(ac46), pk1(ac10), polh(ac8)
Auxiliary	alk-exo(ac133)	fgf(ac32), ubiquitin(ac135)
Unknown	38k(ac98), ac22, ac68, ac81, ac92, ac96, ac109, ac115, ac119, ac142	38.7k(ac13), ac29, ac38, ac53, ac66, ac75, ac76, ac78, ac82, ac93, ac106, ac110, ac145, ac146, p40(ac101), p12(ac102), p45(ac103)

Adapted from Herniou, et al., (2003)(33) and Lauzon, et al., (2004)(1)

functions, and include genes responsible for DNA replication and transcription as well as genes that encode structural proteins. In *Lepidopteran* baculoviruses an additional 32 genes, of known and unknown function, are conserved (33) [see Table 1 for summary of conserved baculovirus genes (1, 33)]. Some of the differences in genomic composition among the baculovirus strains are attributed to the acquisition of DNA sequences from the host cell and/or other viruses. It is speculated that baculoviruses have acquired host cell genes to gain selective advantages such as an increase in virulence or host range (34).

Viral DNA replication. AcMNPV DNA replication occurs in the host cell nucleus, utilizing both cellular and virus encoded replication machinery.

Replication is detected as early as 6 h p.i. (hours post infection) (35) and continues through 18 h p.i. with the viral DNA content doubling every 1.7 hours until budding of BV begins, after which the rate of synthesis declines (36, 37). Using an *in vitro* DNA replication system, six viral proteins are identified and required for viral DNA replication: helicase, DNA polymerase, IE-1, Lef-1, Lef-2, and Lef-3 (38). Additionally, 3 other proteins stimulate DNA replication, but are not essential: p35, Ie-2, PE-38. Five of the proteins required for replication (all except Lef-2) are identified structural proteins of the ODV, indicating the virus may be able to initiate DNA replication at the time of infection (39). Additionally, four of the six genes encoding the essential DNA replication machinery are conserved among the sequenced baculoviruses (Table 1) (33). Replication origins within the genome sequence of AcMNPV and OpMNPV are within the homologous repeat regions, however, several non-homologous repeat regions can also act as replication origins in AcMNPV and other baculoviruses (40, 41).

Regulation of viral gene expression. Baculovirus genes are temporally expressed and are divided into one of four classes: immediate early, delayed early, late and very late genes (42).

Early baculovirus gene expression: Purified viral DNA transfected into the host cell *in vitro* can initiate infection, thus virus encoded transcription factors are not required to initiate infection (43). Baculovirus early genes are transcribed prior to viral DNA replication (6 h p.i.) and are transcribed by the host cell RNA polymerase II (44, 45). These genes encode the proteins required for

viral DNA replication and transcription factors needed for late and very late gene expression (46, 47). The early genes are classified as either immediate early or delayed early. Five immediate early genes have been identified: IE-0 and IE-1 (48-56), IE-2 (57-61), PE-38 (61-63), and ME-53 (64, 65). The immediate early transcription consensus sequence, TATAtAa-$(N)_{19}$T-$(N)_4$-CAGT, was identified from the comparison of five baculovirus early genes (66). Several upstream regulatory sequences are required for transcription activation including the TATA box (43, 67), and the GATA motif (68, 69). Delayed early genes require IE1 for transcription (49), but have a similar transcription start sequence as the immediate early genes. In addition to the early transcription consensus sequence, homologous regions within the genome can also act as enhancers of transcription (49, 70).

Late baculovirus gene expression: The baculovirus late genes are characterized as those that are transcribed after viral DNA synthesis begins. The start of viral DNA synthesis is critical to late gene transcription, as a delay in DNA synthesis will result in a delay of late gene transcription. The late genes are divided into two groups, late and very late. Transcription of the late genes begins as early as 6 h p.i. and continues at high levels throughout infection. These genes typically encode the virus structural proteins. The very late genes differ by the timing of transcription, a requirement of vlf-1, a late gene (71), and the abundance of protein produced. The very late genes are expressed at very high levels from 18 h p.i. through the end of infection and encode polyhedrin,

p10 and granulin. Both the late and very late genes, require a virus encoded RNA polymerase (α-amanatin resistant) and several other virus encoded genes (44, 72-74). The late promoters have a conserved transcription initiation site, TAAG (34, 75). These promoters lack a TATA box, and no other upstream regulatory sequences have been identified (75). The very late genes, polyhedrin and p10, are transcribed from a consensus sequence, AATAAGATTTT (76). It remains unclear what factors regulate the timing and expression levels between late and very late genes.

Baculovirus: Structural composition of occlusions, virions, and viral envelopes. The two forms of progeny virus, BV and ODV, have the same genome and a similar nucleocapsid structure. Yet, the two forms differ in envelope morphology, source of viral envelopes, protein and lipid composition of the envelope, and the role in the infection process (77, 78).

Viral occlusion structural composition. Occlusion derived virus, ODV, is the form of the virus responsible for primary infection of the larval insect host. ODV is protected from the environment by encapsulation in viral occlusions called polyhedron for NPV, granules for GV. Viral occlusions are soluble at pH 9.5, which is similar to the pH of the insect midgut (6, 79). Occlusions can range in size from 0.5 μm to 15 μm and contain from one to many virions (6).

Polyhedron/granulin: Viral occlusions are composed primarily of a single ~29 kDa protein, polyhedron (NPV) or granulin (GV). Polyhedron is a highly conserved baculovirus protein; BlastP (80) shows a minimum amino acid (a.a.)

sequence identity of 78% and similarity of 85% when comparing the AcMNPV polyhedron protein sequence to full length *Lepidopteran* baculovirus polyhedron protein sequences (data not shown). Granulin is also very highly conserved having an a.a. similarity of 90% and identity of 81% among sequenced granulin proteins sequences (78). Polyhedron and granulin have about 49% a.a. sequence identity (81, 82). Polyhedron is expressed at very high levels during infection but is not essential in tissue culture. Because of the high levels of expression, the polyhedron promoter is used worldwide to express foreign genes (16) with the baculovirus expression vector system (83).

Polyhedra envelope/calyx: Surrounding the viral occlusion is an electron dense region termed the polyhedra envelope (PE) or calyx. Originally thought to be composed primarily of carbohydrates (84), the PE was determined to be sensitive to protease (85). The protein pp34 in AcMNPV (86), OpMNPV (87) and LdMNPV (88) was identified as the primary structural protein of the PE (85). Deletion of the pp34 gene resulted in electron dense structures surrounding polyhedra that were smaller and irregular in shape indicating the protein is required for proper formation of the PE (89-91). The polyhedra envelope function is unknown. Studies have shown that deletion of pp34 does not decrease the infectivity of the virus or offer protection against environmental factors (90, 92, 93).

p10: p10 is very highly expressed during infection. Because the p10 is not essential for virus replication in cell culture, the promoter is also used for the

expression of foreign genes in the baculovirus expression vector system (94, 95). The 3' un-translated region of p10 is important for efficient translation initiation and thus the expression levels of p10 or genes expressed from the p10 promoter (96, 97). Immunoelectron microscopy shows p10 forms intranuclear fibrillar structures that associate with pp34 in infected cell nuclei (82). These fibrillar structures disappear in p10 deletions mutants (89). Deletion mutagenesis has determined that both the N-terminal and C-terminal portions of the p10 are required for the formation of the fibrillar structures (98). The N-terminal portion contains a conserved coiled-coil domain and is believed to have an aggregation function (99). The C-terminal portion has been proposed to interact with cellular tubulin (100) and may also be associated with disintegration of the host cell nucleus (101).

Nucleocapsid structural composition. The two forms of progeny baculovirus, BV and ODV, have a similar nucleocapsid structure and protein composition. Nucleocapsids are rod shaped and measure 40-60 nm x 250-300nm (up to 500nm) and are bacilliform in structure (6, 102). Recently, a proteomics study of the composition of enveloped ODV was completed (39) and this study identified a number of viral proteins that had not been previously known to associate with ODV. Only the most well described of these proteins will be discussed further. A similar study of BV has yet to be completed. Figure 1 shows the BV and ODV structure and protein composition.

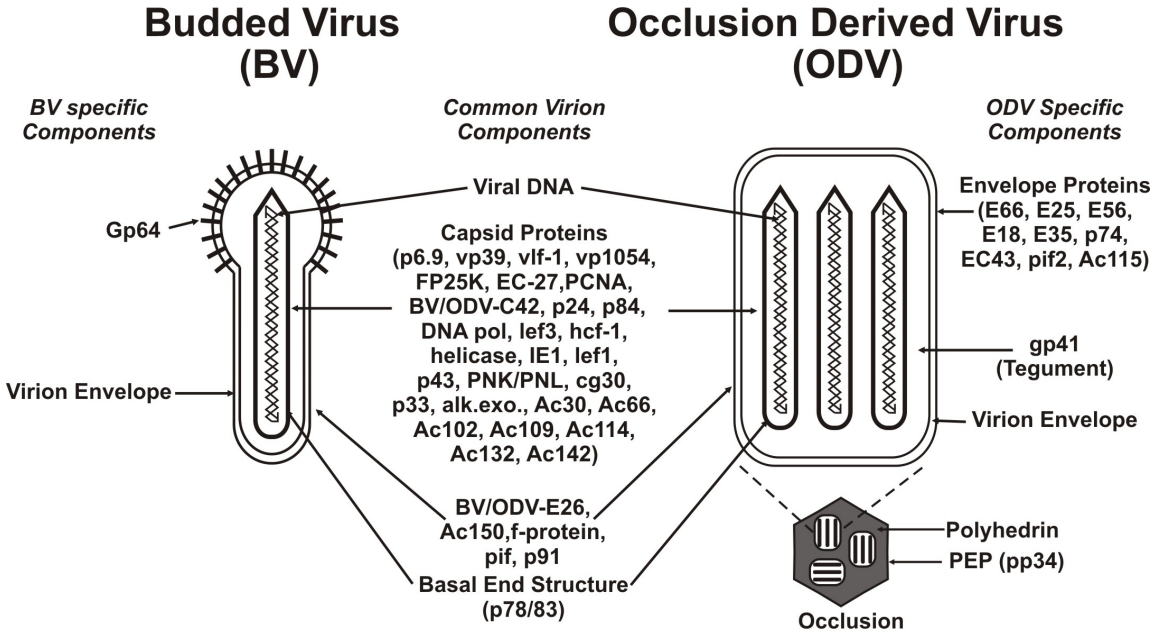

Figure 1. Budded virus and occluded derived virus structure and protein composition.

Adapted from Funk et al., (1997) (78).

p6.9: A DNA binding protein of the nucleocapsid composed of 40% arginine and 30% threonine or serine (78). This protein's a.a. content is similar to protamine, a protein involved in the condensation and packaging of DNA in sperm nuclei of mammals, fish and avian species (103, 104). Evidence suggests that p6.9 is responsible for the efficient packaging of viral DNA into nucleocapsids (105, 106).

vp39-Capsid: This protein is one of the most abundant proteins of the nucleocapsids (107). Immunoelectron microscopy shows that vp39 is uniformly distributed throughout the nucleocapsid structure (108). Comparison of the a.a. sequences of 23 vp39 proteins using Pfam (109) shows an average identity of 42% among the protein sequences.

vlf-1: A late protein of baculovirus, vlf-1 is produced from 15-24 h p.i. (western blot analysis). It is involved in the regulation of very late genes (71), and is a structural protein of the nucleocapsids. Efforts to generate a null mutant are not successful indicating this protein is likely essential (110). Computer assisted analysis of the a.a. sequence shows this protein is a member of the λ-phage integrase family of proteins (71). Experimental evidence suggests that integrase activity by vlf-1 is required to produce viable virus (110). By altering the time and level of vlf-1 expression, the timing and abundance of polyhedrin expression can be altered. This indicates that vlf-1 is a regulator of very late gene expression and may regulate the timing of occlusion assembly (111).

vp1054: This BV/ODV protein is expressed from multiple promoters from early to very late times through infection and was identified by marker rescue experiments using a temperature sensitive mutant that does not form nucleocapsids (112).

FP25K: Naturally occurring viral mutants that produce a “few polyhedra” phenotype (FP) were first observed by Hink and Vail, (113). Several unique mutations in the viral genome including insertions, deletions and a.a. substitutions produce the FP phenotype. Analysis of 9 FP viral isolates identify a gene that consistently contains mutations resulting in the FP phenotype (114, 115) termed *FP25K*. The function of FP25K is unknown, but the protein localizes in electron dense regions in the cytoplasm and the nucleus (116) and is a structural protein of BV/ODV nucleocapsids (117). Infection with FP mutant

viruses result nucleocapsids that are associated with intranuclear membrane structures, but are not fully enveloped. In the rare occasion that a nucleocapsid is fully enveloped, ultrastructural observations show the FP virus envelopes have a abnormal morphology as compared to wt ODV envelopes (116). Infection with a naturally occurring mutant virus, 480-1, which contain a N-terminal a.a. deletion within FP25K, results in accumulation of the envelope protein, ODV-E66, in the cytoplasm as compared to wt infection where ODV-E66 is detected in intranuclear microvesicles and ODV envelopes. Infection with 480-1 also results in a delay in the nuclear accumulation of another envelope protein, ODV-E25 (117). Deletion of *FP25K* reduces the steady state protein levels of ODV-E66 five fold, however, there are no detectable changes in transcription levels of *ODV-E66* when compared to wild type infection; suggesting that FP25K may be involved in regulating the translation of ODV-E66. Deletion of FP25K also results in E66 accumulation at the nuclear periphery, suggesting a role for FP25K in the trafficking of E66 to microvesicles and ODV envelopes (118). Finally, *in vitro* and *in vivo* protein cross-linking studies identified FP25K is proximal to ODV-E66 in ER derived membranes, further supporting a hypothesis that FP25K may be involved in the trafficking of ODV-E66 (119).

p78/83: This BV/ODV protein is expressed late in infection (17, 120). Taking advantage of the gene's genomic proximity to *polyhedrin*, and the fact that it is essential, Kitts and Possee (121) developed a selection system to

increase the yield of recombinant baculovirus with foreign genes inserted in the polyhedrin locus. Immunoelectron microscopy revealed that p78/83 is localized to the basal end of the nucleocapsid, oriented away from the virogenic stroma (during encapsulation), intranuclear microvesicles (during envelopment) and the nuclear envelope (during cytoplasmic budding) (122). Yeast two-hybrid screening and blue native gel electrophoresis identify this protein in putative complexes with BV/ODV-C42 and/or ODV-EC27 (123). In addition to the two viral proteins, p78/83 has also been shown to bind actin. This actin binding is suggested to be involved in actin polymerization, facilitating the transport of nucleocapids to the nucleus upon infection (124). Additionally, p78/83 associates with viral induced RNA polymerase, suggesting a role for p78/83 in the polymerase activity (125)

BV/ODV-C42 (C42): Expressed as a late gene product of orf 101 this protein is a structural component of BV/ODV nucleocapsids. At 24 h p.i., C42 localizes to the virogenic stroma, an intranuclear electron dense region associated with viral DNA replication. By 72 h p.i. C42 is dispersed evenly throughout the nucleus. Yeast two-hybrid and blue native gel electrophoresis identified p78/82 and/or EC27 in putative protein complexes with C42 (123).

ODV-EC27 (EC27): Both a capsid and envelope protein found only in ODV (126). The sequence from a.a. 80-110 of EC27 has a 25-30% similarity to the cyclin box sequence of several cellular cyclins (human/*Drosophila* cyclin B, Human cyclin D1, D2). Additionally, this protein co-immunoprecipitates with

cdc2 and/or cdk6 with kinase activity capable of phosphorylating histone H1 and retinoblastoma *in vitro*. These results indicate that EC27 may function as a multi-functional virus encoded cyclin [cdc2-EC27 (B like cyclin), cdk6-EC27 (D-like cyclin capable of binding PCNA)] (127).

Other nucleocapsid proteins: The proteins, p24 (128) and p87 (129) are structural components of nucleocapsids**,** although the function(s) of these two proteins are unknown. An exhaustive proteomic analysis of the ODV viral form identify several viral proteins as structural components of the nucleocapsid that have not been previously reported (39). The newly identified proteins are: DNA polymerase, lef3, hcf-1, helicase, IE1, lef1, p43, PNK/PNL, cg30, p33, alkaline exonuclease, and open reading frames Ac30, Ac66, Ac102, Ac109, Ac114, Ac132, Ac142. The functions of many of these newly identified proteins have been determined or postulated, but is beyond the scope of this review.

Tegument. The tegument is defined as the area between the viral envelope and the nucleocapsid in BV or ODV. Fractionation studies indicate GP41 fractionates with nucleocapsids and viral envelopes and, as such, has been termed a tegument protein (130). GP41 is a N-glycosylated protein of ODV (130). *GP41* is late gene transcribed from 12 to 36 h p.i. (131). Data from a temperature sensitive mutant of *GP41* show that BV is not produced at the non-permissive temperature suggesting a role for GP41 in BV maturation (132).

Budded virus envelope composition. The BV enters the cell by receptor mediated endocytosis (133). During endocytosis, the acidic pH of the endocytic

vesicle lumen activates fusogenic protein(s) in the virion envelope, which results in fusion of the envelope with the endosome membrane. This fusion releases the nucleocapsid in the cytoplasm. Two fusogenic proteins have been identified in BV envelopes, GP64 and F-protein (134, 135). At least three proteins reside in the envelope of both BV and ODV. These proteins will be discussed with the details of the ODV envelope proteins.

GP64/GP67: *GP64* is expressed as both an early and late gene (66, 136), and was the first protein identified as a fusion protein of BV envelopes (135). This protein localizes to the plasma membrane (PM) of infected cells (66) and the envelopment of the nucleocapsids appear to originate by budding from the GP64 rich PM regions. In BV, GP64 is a homotrimer localized in spike-like structures (peplomers) at one end of the virion (137). Antibodies directed against GP64 can block the membrane fusion activity thus decreasing the infectivity of the virus (138). Studies using a GP64 null mutant show that the protein is essential for cell to cell transmission of budded virus, although this null mutant virus does produce infectious occlusions (139). GP64 is both glycosylated and palmitoylated, with palmitoylation functioning in membrane anchoring, protein mobility within membranes, or regulation of trafficking in the cell (140, 141). Two domains within the protein are required for GP64 function. The fusion domain (a.a. 223-228) is required for pH activated membrane fusion of this protein (135, 138). The oligomerization domain (a.a. 327-335) constitutes a leucine zipper required to form the mature GP64 homotrimer (142).

Additionally, GP64 is likely involved with the establishment of secondary " pass through" infection by ODV derived virions (143).

Fusion protein/F-protein: Sequence analyses of the known baculovirus genomes reveal that several baculoviruses lack *GP64* (group II baculoviruses). Computer assisted analysis of the group II baculovirus, LdMNPV, identify a single protein, LD130, with a predicted transmembrane domain and signal sequence. LD130 accumulates in the plasma membrane of infected cells and induces membrane fusion at pH 5.0. Therefore, LD130 is considered a fusogenic or F-protein of the group II BV (134). A F-protein homolog has been identified in all of the group I and group II baculoviruses except NeleNPV (1), however for at least OpMNPV and AcMNPV (group I baculovirus), the F-protein homolog could not act as a pH-mediated fusion protein (144, 145). Recently, F-proteins from LdMNPV or SeMNPV (group II baculoviruses) were used to replace *GP64* in AcMNPV. The AcMNPV encoded F-protein homolog could not compensate for the *GP64* deletion alone (145), however the F-protein from either group II virus can act as a functional replacement for GP64 in the *GP64* null mutant AcMNPV BV virions (146). This data indicates that even though group I baculoviruses encode a F-protein homolog, it functions differently than the group II baculovirus f-protein.

Occlusion derived virus envelope composition. ODV nucleocapsids are assembled and enveloped in the nucleus. The source of the envelope is unique as it does not appear to be derived directly from the nuclear envelope, but

instead the envelope is apparently derived from viral-induced intranuclear microvesicles (MV) that bud from the INM (147, 148). Ultrastructural observations of membrane elements during *Dipteran* NPV envelopment suggests that the precursor membranes of viral envelopes are synthesized *de novo* during infection (149). However, ultrastructural observations during *Lepidoteran* NPV infection and envelopment shows perturbations in the nuclear envelope that are induced during infection suggesting that microvesicles may be produced by budding from the inner nuclear membrane (150). Additionally, when the ODV-envelope proteins, ODV-E66 (148) and ODV-E56 (151), are abundantly expressed (polyhedrin promoter) these proteins are detected in MV and viral envelopes as well as in the INM, ONM and ER. These observations led to the hypothesis that the virus-induced MV originate from the INM and act as precursors of the ODV envelopes (151).

ODV-E66 (E66): This late baculovirus ODV envelope protein was identified by N-terminal sequencing of a SDS-PAGE band unique to purified ODV envelope samples. *E66* is transcribed from 12 to 72 h p.i. This protein is expressed from 24 through 72 h p.i. Western blot and/or immunoelectron microscopy detects E66 in ODV envelopes and viral-induced intranuclear MV (148). Yeast two-hybrid direct cross assays identify the viral proteins FP25K, p39 and/or ODV-E25 may each interact with E66 independently (117). When *FP25K* is deleted from the genome, E66 is detected mostly in clusters in the outer nuclear membrane, and is not detected in the microvesicles or ODV

envelopes. This suggests that FP25K plays an important role in the trafficking of E66 during infection (118).

The N-terminal 33 a.a. of E66 constitute a hydrophobic, non-cleaved, Type I signal anchor sequence. This region of E66 is termed the sorting motif (SM) (119). When the SM is fused to green fluorescent protein (GFP) or β-galactosidase (β-gal), the fusion proteins localize to intranuclear microvesicles and ODV envelopes during infection. Additionally, when the SM-fusion proteins are abundantly expressed (polyhedrin promoter), they localize in the inner nuclear membrane (INM) and outer nuclear membrane (ONM), and ER membranes in close association with the NE (152). When the a.a. sequence of the SM is compared to the a.a. sequence of the known INM proteins, the chemical features of the SM are conserved. *In vivo* and *in vitro* crosslinking studies show the viral proteins, FP25K and BV/ODV-E26, are proximal to E66 in the ER, suggesting these proteins may regulate the trafficking of SM prior to localization in the MV and viral envelopes (119). A detailed discussion of the SM features is found in the specific aims section of this thesis. A comprehensive study of the chemical features of the E66 SM, and the possible role(s) in sorting integral membrane proteins to the INM is the major goal of this study.

ODV-E25 (E25): E25 is a late baculovirus protein. It was identified in *Op*MNPV by screening λgt11 expression libraries using antibodies generated against ODV virions. A monospecific antibody detects E25 as a doublet on

western blots, and detects the protein in ODV envelopes when used for immunoelectron microscopy (153). Hong et. al. (152) determined that the E25 N-terminal 24 a.a., which are chemically similar to the E66 SM, are also sufficient to direct a GFP fusion to intranuclear MV and ODV envelopes, as well as the INM, ONM and ER membranes in close association with the NE (152). While E25 trafficking to the nucleus is delayed in naturally occurring *FP25K* mutants (480-1) (117), the trafficking is apparently not affected in the *FP25K* deletion virus (118).

ODV-E56 (E56): E56 is a baculovirus late protein, with the gene transcribed from 16 to 72 h p.i. and protein produced from 36 to 96 h p.i. (151, 154). This protein was identified through screening λgt11 expression libraries from AcMNPV infected cells using antibodies generated against ODV or BV (151). E56 is an ODV envelope protein (immuno-electron microscopy) that is also detected in virus-induced MV and the INM and ONM (151, 154). By replacing the C-terminal 204 a.a. of E56 with β-gal, the fusion protein localizes to nucleocapsids of ODV, but not viral envelopes or microvesicles. This data indicates that the C-terminus of the protein contains the sequence(s) required for membrane association and localization to ODV envelopes and microvesicles (155).

ODV-E18 (E18) and ODV-E35 (E35): *E18* is transcribed as a late gene (transcripts are detected from 16 h p.i. thru 72 h p.i.) and the protein is detected from 24 h p.i. thru 72 h p.i. It was identified by N-terminal sequencing of an 18

kDa band from purified ODV envelopes, however the gene encodes a predicted 9.5 kDa protein. *In vitro* translation produces only a 9.5 kDa form, indicating that the protein is likely a dimer in infected cells (126).

Translation of both E18 and EC27 (envelope and capsid protein of ODV, putative viral cyclin) is initiated from the same mRNA. The E35 protein is proposed to be translated from this mRNA product as a result of ribosomal frame shifting at the 3' end of the *E18* coding sequence, which takes the *E18* stop codon out of frame, and places the *EC27* coding sequence in frame (126). N-terminal sequencing shows that E35 has the same N-terminal sequence as E18. Both the E18 and EC27 antisera detect E35 on western blots of purified viral envelopes, indicating E35 is likely a structural protein of the ODV envelope. Using E18 antisera, immuno-electron microscopy was used to determine that E18 and/or E35 is present in the viral-induced microvesicles and ODV envelopes (126).

<u>p74:</u> p74 is an ODV envelope protein (156). The gene was identified as an open reading frame (orf) positioned 3' to the *p10* open reading frame. Deletions in the C-terminus of the p74 yields viral occlusions unable to infect larvae by feeding (157). Deletion of full-length p74 has the same affect, however injection of virions purified from the mutant occlusions are infectious. These studies show that p74 is required for primary infection of the insect midgut (156-158). This protein localizes in the intranuclear MV of infected cells, and in the membrane fraction of infected cell lysates. A microscopy study showing the

effects of deletions within p74 demonstrate that the C-terminal 65 a.a. are required for membrane association and localization specific to the intranuclear MV (159). p74 mediates binding of the virus to the gut epithelium of infected larvae suggesting that like BV, ODV requires specific receptor binding for viral adhesion and entry into the host cell (160).

ODV-EC43 (EC43): A late protein, EC43 is a structural component of both the nucleocapsid and envelope of ODV. EC43 is transcribed from 24 h p.i. through 96 h p.i. and the protein is detected from 36 h p.i. through 96 h p.i. Computer predictions do not identify a signal peptide or TM sequence encoded within the protein. Fractionation studies show that while EC43 is present in both capsid and envelopes preparations, the majority of the protein is in the capsid fraction (161).

p91: The p91 protein is detected late in infection, and is present in both ODV and BV envelopes (39, 162). It was identified by screening λgt11 expression libraries using antibodies directed against ODV virions. Immunoelectron microscopy shows p91 is present in both the envelope and capsid of ODV, but extraction by NP40 detect the protein only in the capsid fraction. These results suggests that p91 maybe a capsid associated protein and that if it is present in the envelope, it is also linked to the capsid in a manner that is resistant to detergent or reducing conditions (162).

BV/ODV-E26 (E26): BV/ODV-E26 is another protein reported that is detected in the envelopes of both BV and ODV (163). *E26* is only found in the

group I baculoviruses and is likely an essential gene of these viruses (164). This protein is expressed and detected beginning at 4 h p.i. and continuing throughout the infection process. E26 is detected in foci of both the cytoplasm and nucleoplasm prior to 16 h p.i. (163, 164). The E26 detected in the nucleus co-localizes with IE1 in the nucleus through at least 20 h p.i. (164). Additionally, at 24 h p.i., E26 is detected in intranuclear microvesicles and ODV envelopes (163). Biochemical assays show that E26 binds nucleic acids (164). Co-immunoprecipitation experiments and/or yeast two-hybrid assays predict FP25K and/or cellular actin can interact with E26 (163). *In vitro* and *in vivo* crosslinking studies show that E26 is proximal to the E66 SM in the ER suggesting a possible role in protein trafficking of ODV envelope proteins (119).

Pif, "per os infectivity factor": Pif is a late protein that is expressed at relatively low levels (165). The N-terminus of pif has a SM-like sequence with a similar chemical structure as the E66 SM (Braunagel, personal communication). The pif protein was identified by studies of a SeMNPV mutant virus that produces occlusion bodies not capable of infecting larvae by feeding (*per os*) (166). Western blot analysis shows the protein fractionates as a ODV envelope protein (166). A recent study (Braunagel, personal communication) shows that pif is also a BV envelope protein.

Pif2: Like Pif, this protein was identified as a protein responsible for loss of *per os* infectivity by a SeMNPV mutant virus with a deletion of orfs 29-35. Computer assisted analysis identifies a late gene promoter, suggesting *pif2* is

likely a late gene (167). Like pif, the N-terminus of pif2 has a SM-like sequence with chemical characteristics similar to the E66 SM (Braunagel, personal communication). The presence of this SM-like sequence suggests pif2 is likely an envelope protein.

Ac150: Ac150 is an envelope protein of both BV and ODV. Deletion of *Ac150* combined with a deletion in *Ac145* results in virus that has a 39-fold decrease in *per os* infectivity. Since deletions still result in the production of virus, *Ac150* is considered to be non-essential (168).

Other ODV envelope proteins identified by a proteomic analysis of ODV: With the exception of a few of proteins (E26, pif, and Ac150) an exhaustive proteomics study of AcMNPV ODV proteins confirmed the identity of all the previously described envelope proteins of the ODV envelope. Additionally, gp41 and F-protein were both identified as structural proteins of the ODV envelope (39). Previous reports identify gp41 as a tegument protein (130), and as such this protein would likely contaminate envelope preparations. However, F-protein is the fusogenic protein of group II NPV and GV baculoviruses that was only found in BV prior to the proteomic study (134, 146). The function of F-protein in the ODV envelope is unknown.

Nuclear envelope: Structure and function. The nuclear envelope (NE) is a specialized membrane system in eukaryotes that separates the nucleus from the cytoplasm and maintains the biochemical identities of the two compartments (169). In addition, the NE is involved in “communication” between the cytoplasm

and nucleoplasm through the nuclear pores and also is involved in the regulation of DNA replication, gene expression and mitosis. The NE is made up of two membrane bilayers, the ONM and the inner nuclear membrane INM. These membranes are joined at the nuclear pore complexes

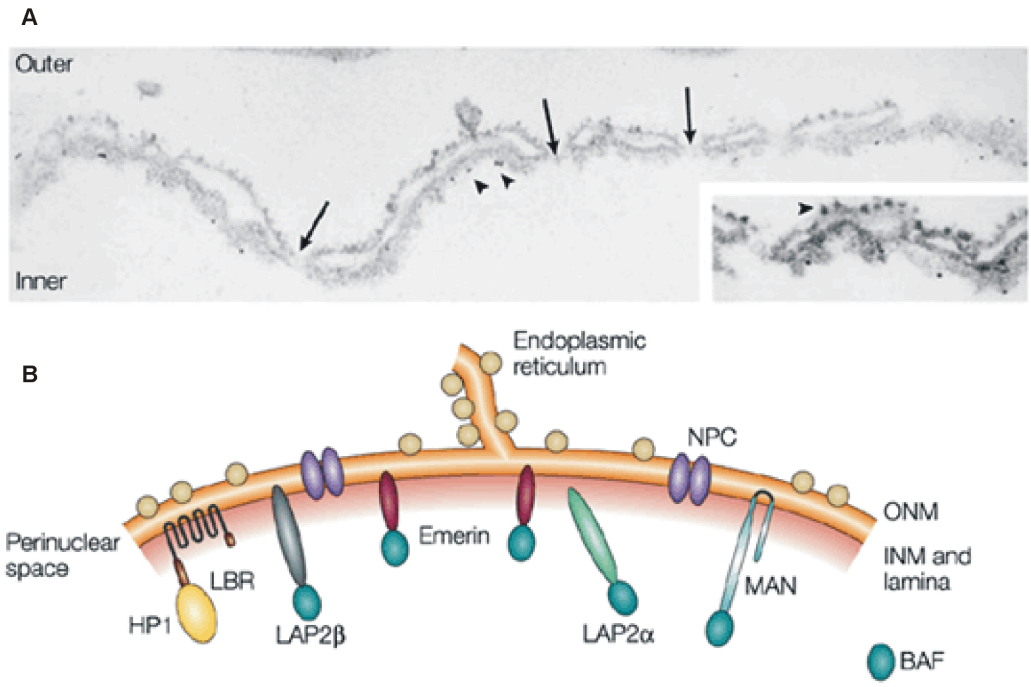

Figure 2. Structure of the nuclear envelope. A.) Electron micrograph of the NE from rat liver nuclei. The outer and inner membranes are clearly visible as are the junctions of these two membranes at the nuclear pores (arrows). The inset image shows ribosomes attached to the ONM (170). B.) Illustration showing the proteins of the nuclear envelope, and its general structure (170). Abbreviations are listed in the abbreviations section of this thesis (pp. xiv-xiii). This figure is reprinted with the permission of the copyright holder, Nature Publishing Group.

(NPC) via the nuclear pore membrane (NPM) (171). Figure 2A illustrates this continuity. The INM is lined with a network of proteins called the nuclear lamina that act as a structural framework for the nucleus and also may be involved in the regulation of chromatin structure and condensation and/or the localization of proteins to the INM (172). A group of diseases termed the laminopathies are characterized by mutations in the lamina proteins and/or the lamina associated proteins (170, 173).

Outer nuclear membrane. The ONM is functionally and structurally continuous with the ER. Ribosomes are even observed docked at the cytoplasmic face of the ONM (Fig. 2A) (170). The ONM is connected to and continuous with the INM via the NPM.

Nuclear pore complex, nuclear pore membrane. The nuclear pore complex (NPC) separates the ONM and the INM and is anchored in the NPM by the integral membrane nucleoporin proteins of the pore complex (171). The NPC acts as a gateway to control the exchange of macromolecules and macromolecular complexes between the nucleoplasm and the cytoplasm via signal-mediated transport (174). NPCs are large protein complexes of 125 MDa in vertebrate cells (175) and ~66 MDa in yeast (176). Despite the size differences, the yeast and vertebrate nuclear pores have the same general structure and likely use similar mechanisms for both soluble and membrane-mediated protein transport. The protein composition of the yeast nuclear pore and the specific localization of these proteins within the pore were analyzed

using mass spectrometry and immunoelectron microscopy (176). From these analyses, the yeast nuclear pore complex is predicted to consist of 29 nucleoporins. The vertebrate NPC is believed to consist of approximately 50 nucleoporins (177). The specific function(s) of each nucleoporin is unknown and currently under investigation.

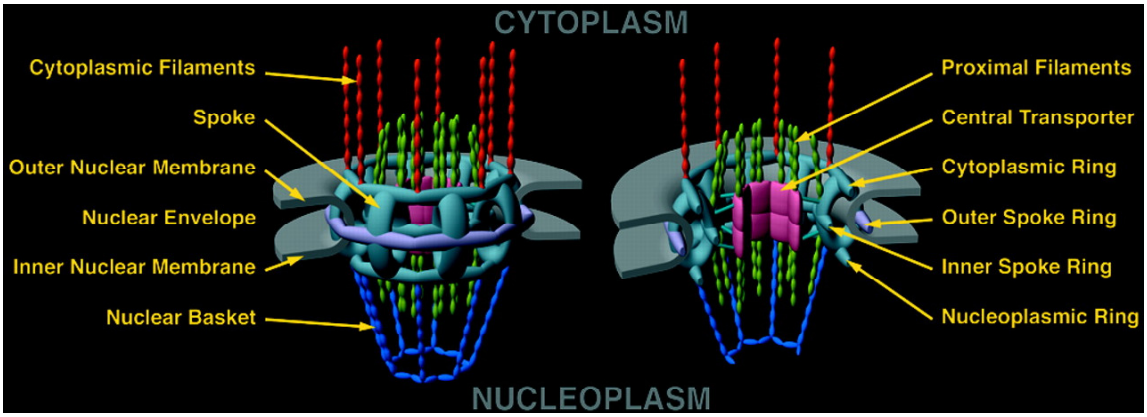

Figure 3. Schematic of the structural organization of the nuclear pore complex. This figure is reprinted with permission from the Journal of Biological Chemistry (178).

NPCs (see Fig. 3, schematic) display an octagonal rotational symmetry. The core of the NPC is composed of the central transporter and the spoke/ring complex. The central transporter forms the channel connecting the nucleoplasm and cytoplasm and interacts with nuclear import and export complexes as they traverse through the center of the NPC. The transporter is embedded in the octagonally symmetric spoke/ring complex, which also anchors the NPC in the pore membrane. The cytoplasmic and nucleoplasmic coaxial rings flank the

spoke ring complex, and these coxial rings anchor the cytoplasmic filaments and nuclear basket to the NPC, respectively (179). The cytoplasmic coaxial ring is composed of three separate components, the star ring, the thin ring and internal filaments. The star ring is the central structure of cytoplasmic ring. Cytoplasmic filaments, which act as docking sites during signal mediated import and export of macromolecules (180), attach in eightfold symmetry to the star ring via the thin ring. The star ring joins the spoke/ring complex to the NPC core by eight internal filaments, arranged in a hub and spoke conformation. The nucleoplasmic coaxial ring is anchored to the nucleoplasmic side of the of the spoke-ring complex and like the rest of the pore, displays an eightfold symmetry. Filaments protrude from nucleoplasmic coaxial ring and join a smaller nucleoplasmic ring to form the nuclear basket (179, 181). Current evidence suggests that the nuclear basket is involved in nuclear export of both protein and RNA (182, 183) as well as being involved in the termination of nuclear protein import (184).

Transport of macromolecules through the NPC. There are three methods for transporting macromolecules through the NPC: free diffusion, signal-mediated transfer (import and export), and integral membrane protein trafficking.

Free diffusion: The NPC appears to allow free diffusion of some macromolecules. Microinjection of labeled dextrans of various sizes show that the rate of diffusion is controlled by the molecule's size; larger molecules diffuse at a slower rate than smaller molecules. These experiments also show that free

diffusion is limited to macromolecules smaller than 50 kDa. Free diffusion is believed to occur through the 8 peripheral channels located around the nuclear pore between the spokes of the spoke-ring complex, and not through the central transporter (185, 186). These peripheral channels are shown to be 10 nm in diameter (175), which concurs with the size of the molecules that freely diffuse. However, many proteins that are small enough to diffuse, such as histones, still use signal-mediated transfer (187).

Signal-mediated transfer: Molecules that are too large to diffuse through the NPC, and many small macromolecules, use signal-mediated transfer to translocate across the nuclear pore. Import and export each utilize unique signals, NLS (nuclear localization signal) and NES (nuclear export signal), respectively (180). The “classical NLS” identified in SV40 large T-antigen contains a sequence of basic a.a., KRKK or similar (188). In addition, a bipartite NLS, composed of two basic sequences of a.a. separated by a 10 a.a. spacer was identified in nucleoplasmin (189). The NES contains a leucine rich a.a. sequence (190, 191).

Nuclear import is accomplished in three steps: docking, translocation and dissociation. In the docking step, NLS containing cargo binds a soluble import carrier protein, importin β or another karyopherin, in the cytoplasm. The NLS cargo may bind the carrier protein either directly (importin β or transportin), or indirectly (importin β) via adaptor proteins such as importin α. These adaptor proteins may regulate nuclear import as each adaptor can bind a particular NLS

with higher or lower affinities compared to other adaptors [reviewed in Macara, (192)]. Once the import complex is assembled, it is targeted to the nuclear pore, facilitated through interactions with the cytoplasmic fibers of the pore complex. Translocation results in the movement of the import complex across the nuclear pore through the central transporter. This process requires the small G-protein Ran. The majority of Ran is found in the nucleus, in the form of Ran-GTP, whereas the cytoplasmic pool of Ran is in the form of Ran-GDP. The RanGTP-RanGDP gradient facilitates the translocation of substrates across the pore, as import complexes assemble in the presence of cytoplasmic Ran-GDP, and disassemble in the presence of the nucleoplasmic Ran-GTP. During the process of translocation, import complexes bind Ran-GDP via the importin, and through (putative) interactions with the FG repeats of nucleoporins (193), the entire complex translocates through the pore. Once the complex has reached the nucleoplasmic side of the pore, the import complex dissociates. Ran-GDP is then converted to Ran-GTP by RCC1 (Ran GDP-GTP exchange factor) and Ran-GTP and the importins are recycled to the cytoplasm. When Ran-GTP is in the cytoplasm, it is hydrolyzed to Ran-GDP.

Proteins and substrates (RNA, RNA/protein complexes) are exported from the nucleus following a similar pattern. The NES-containing molecule binds an exportin (i.e. Crm1) in the presence of Ran-GTP, and the entire complex translocates to the cytoplasm where it dissociates in combination with the

hydrolysis of Ran-GTP to Ran-GDP (191) [Reviewed in Kaffman and O'Shea, (194) and Macara, (192)].

Inner Nuclear Membrane (INM). The INM is continuous with the ONM via the NPM. The INM has a unique protein complement as compared to the NPM or ONM. Proteins of the INM are involved in regulation of DNA replication, mitosis, chromatin, apoptosis and nuclear structure [reviewed in Worman and Courvalin, (195)].

Sorting, localization and accumulation of membrane proteins to the INM. Accumulation of membrane proteins in the INM is not as well characterized as the accumulation of soluble proteins to the nucleus. The accepted model for localization of proteins to the INM is "diffusion:retention" (196, 197). This model predicts: following insertion, INM proteins randomly diffuse within the continuous membranes of the ER and NE and once in the INM, are immobilized and retained through binding interactions with either immobilized nucleoplasmic components, and/or other resident INM proteins (195-198). Therefore, localization to the INM can be regulated by both the limits of diffusion through the NPC and well as the ability of a protein to become immobilized via binding interactions at the INM.

The INM and ONM are continuous membranes connected through the peripheral channels of the NPC via the nuclear pore membrane. According to diffusion:retention, proteins which diffuse from the ONM to the INM must have cytoplasmic/nucleoplasmic domains that are small enough to pass through the

10nm peripheral channels. Thus proteins with domains larger than 45-70 kDa should not be able to diffuse from the ONM to the INM, and are thus excluded. Most of the INM proteins studied to date have domains smaller than 45-70 kDa (199-201) supporting the idea that diffusion may be sufficient for protein trafficking to the INM. However, recently one group of INM proteins have been identified that contain cytoplasmic/nucleoplasmic domains up to 1mDa in size (202-204), suggesting that in addition to diffusion, there may be additional steps in trafficking proteins to the INM.

Once a membrane protein is located in the INM, diffusion:retention predicts that only those proteins that are immobilized via binding nuclear ligands or other immobilized INM proteins will be retained in the INM. In fact, the model predicts that integral membrane proteins destined for other cellular locales may be localized transiently in the INM. However, because these proteins lack a binding domain for immobilized nucleoplasmic components, they would continue to diffuse within the continuous membrane systems of the ER and NE, and therefore not concentrate in the INM to detectable levels. Ligand binding assays (201, 205-212) and FRAP experiments (198-201) show that not only do several INM proteins bind to nuclear ligands, but they are immobile in the INM. While a considerable amount of data suggests that binding immobilized nuclear ligands is required for accumulation in the INM, there is a small pool of data that suggests that binding these nuclear components is not necessary (196, 198).

One major objective of this study is to determine if immobilization in the INM is required for accumulation.

Protein composition of the inner nuclear membrane (Fig. 2B, pg. 24).

Lamin B Receptor (LBR). LBR is an integral membrane protein, p58, which localizes in the INM (205). Sequence analysis of the *LBR* cDNA shows the calculated molecular mass of the protein to be 73,375 kDa (621 a.a.) although the SDS-PAGE M_r is 58 kDa . The protein contains a 208 a.a. N-terminal region followed by 8 transmembrane (TM) sequences. The region of the LBR from 208-621 has a high homology with human, plant and yeast sterol reductase (213). LBR rescues sterol reductase activity in both yeast (214) and *Neurospora crassa* (215) that are both deficient in sterol reductase activity. It is currently unknown if LBR acts as a sterol reductase in mammalian cells (216). The N-terminal 200 a.a. region of LBR contains three DNA binding motifs and two conserved protein kinase phosphorylation sites. *In vitro* and *in vivo*, the protein is phosphorylated, regulating lamin B binding. Binding of the N-terminal segment of LBR to lamin B binding suggests the N-terminus is oriented toward the nucleoplasm (217).

When the N-terminal 200 a.a. region of LBR is fused to the N-terminus of type II integral membrane proteins, the chimeric fusion proteins sort to the INM. When this region of LBR is fused to soluble cytoplasmic proteins, the fusion proteins are sorted to the nucleoplasm (197, 218). When the N-terminal 238 a.a. of LBR (N-terminal binding domain and first TM sequence) are fused to GFP and

expressed in mammalian (199) or plant (219) cells, the fusion protein localizes to the INM. These data suggest that the amino-terminal 200 a.a. are necessary for INM protein localization. However, when the N-terminal 192 a.a. of LBR is replaced with β-gal, the resulting fusion protein accumulates in the INM as well as a distinct set of cytoplasmic membranes. Additionally, deletion of the first 190 a.a. of LBR results in protein accumulation in the INM. Finally, when the TM sequences 2-8 are deleted, the truncated LBR also accumulates in the INM (196). Thus, these data suggest that the first TM sequence of LBR is sufficient for accumulation of proteins to the INM. The first TM sequence of LBR is chemically similar to the ODV-E66 SM. One goal of this study is to determine if the viral SM or the SM-like sequence of LBR is sufficient for accumulation of protein in the INM.

FRAP (fluorescence recovery after photo-bleaching) studies show that when the N-terminal 238 a.a. of LBR are fused to GFP, the protein is immobile in the INM, but remains mobile in the ER (199). LBR binds lamin B (205, 206), DNA (206), chromatin (207) and HP1, a chromatin binding protein (208) via the nucleoplasmic, 200 a.a. N-terminal domain. Binding to one or more of these nucleoplasmic components is the accepted mechanism for sorting and immobilization (retention) of LBR in the INM. This binding data along with the FRAP data support the fundamental basis of the hypothesized diffusion:retention model of INM protein sorting and localization.

Lamin Associated Polypeptides (LAP). The LAP proteins consist of two types, LAP1 and LAP2. Each type has several variants that differ in sequence(s), function(s), and/or localization(s). LAP1 proteins are Type II integral membrane proteins consisting of three variants: LAP1A, 1B and 1C (220). High stringency hybridization studies indicate that each isotype of LAP1 is a splice variant of the same gene (221, 222). All three LAP1 forms interact with lamin A, mitotic chromosomes (209), lamin B and a protein kinase (220). These protein interactions are likely significant in maintaining nuclear structure and organization. Localization studies of LAP1B using deletion mutants fused to GFP show that the LAP1B TM sequence is required for localization in the nuclear envelope and ER. Together, the TM sequence and C-terminal segment of the nucleoplasmic domain function as the sorting and localization determinants for LAP1B (223).

The LAP2 protein variants are mostly Type II integral membrane proteins, and exist in six different forms, LAP2 α, β, ε, δ, γ, and ξ. LAP2β binds lamin B and the chromatin binding protein BAF (barrier to auto-integration factor) and is believed to be responsible for in nuclear reformation and organization at the end of mitosis (224). LAP2β has a large hydrophilic nucleoplasmic region, followed by a C-terminal, 24 a.a. TM sequence, which acts to anchor the protein in the membrane. When the lamin binding domain of the LAP2 N-terminus (a.a. 298-373) is fused to a Type II membrane protein (chicken hepatic lectin), the resulting fusion protein sorts and localizes to the NE (225). LAP2α is a soluble

form of the LAP2 protein family, and as such lacks the C-terminal TM sequence of LAP 2β. It localizes uniformly in the nucleoplasm and interacts with lamin A, lamin B and chromatin and is believed to be important for nuclear assembly and structural organization (226). LAP2 isoforms have a conserved 40 a.a. sequence in the N-terminal region of the proteins termed the LEM domain. The LEM domain is found in at least two other INM proteins, emerin and MANI (227). This domain interacts with BAF (224).

Emerin. Mutations in emerin are responsible for X-linked autosomal dominant Emery-Dreifuss muscular dystrophy (EDMD). Additionally, studies in C. elegans suggests that emerin may be involved in cell division (228). Emerin is a Type II integral membrane protein of 254 a.a., and contains a single TM sequence, 11 residues from the C-terminus, that anchors emerin in the INM. The N-terminal region (a.a. 1-188) of emerin interacts with the lamina (210). When the N-terminal 219 a.a. of emerin are fused to GFP, the resulting fusion protein localizes uniformly in the nucleus, but not in the INM (229). When this region is fused to the type II integral membrane protein, chicken hepatic lectin, the fusion sorts and localizes to the INM (200). When the C-terminal region (a.a. 197-254) of emerin (includes the TM sequence) is fused to GFP, the fusion localizes in the ER (200). These results suggest that the TM sequence of emerin is not sufficient to sort the protein to the INM, but that the N-terminal 219 a.a. of emerin contains the sorting determinants (200, 229). The N-terminal 219 a.a. of emerin also contains the conserved LEM domain as discussed for LAP2

(201). In addition, the N-terminal 219 a.a. of emerin binds A type lamins (211, 212, 230), and FRAP data shows a significantly slower mobility in the INM than the ER (200). These data suggest that sorting and retention of emerin in the INM is consistent with the diffusion:retention model.

MAN I. The MAN antigens were identified using auto-antibodies from an individual with collagen vascular disease. One of the proteins identified in this screen, MAN I, localized to the INM (201). MAN I is a 82.3 kDa protein, with a N-terminal region of 476 a.a. followed by two putative TM sequences and a 252 a.a. C-terminal tail. The N-terminal domain contains the conserved 40 a.a. LEM domain (201). A fusion of the first 538 a.a. of MAN I (N-terminal region plus the first TM sequence) to GFP is sufficient to sort and localize GFP to the INM. Additionally, when the N-terminal domain of MAN I (without the first TM sequence) is fused to chicken hepatic lectin, this fusion sorts and localizes in the INM. These results indicate that the N-terminal region of MAN I is necessary to direct membrane proteins to the INM (231). Localization studies using the only TM sequence of MAN I have yet to be reported. Studies in *C. elegans* suggest that MAN I is likely involved in cell division (228).

Nurim. Nurim was identified by screening a GFP fusion library for yeast proteins that localized to the NE. Nurim contains five putative transmembrane sequences, however immunoprobing and protease protection assays show that Nurim spans the membrane six times (232). However, Nurim lacks the large hydrophilic domain at the N-terminus that is present in the other known INM

proteins and has been shown to bind immobilized nuclear ligands. Despite the apparent lack of a binding sequence, FRAP data shows that Nurim is immobilized in the INM. This immobilization is predicted to occur by binding with other immobilized resident integral membrane proteins (198). However, biochemical fractionation studies using conditions which extracted lamins A/C did not result in a release of Nurim from the insoluble (membrane) fraction (232). Mutational analysis shows that several regions of Nurim appear to be important for localization to the INM. These include the second and third TM sequences as well as regions within the loops connecting the TM sequences of the protein. While the function of Nurim is currently unknown, sequence similarities suggest Nurim may have a isoprenylcysteine carboxymethyltransferase enzymatic function (232).

Nesprins. Nesprin (204), Myne I (203), and Syne I (202) are all members of an emerging class of INM proteins termed the Nesprins. This family of proteins is characterized by having series of spectrin repeats up to one MDa in size resulting in proteins with very large nucleoplasmic regions (204, 233). Other known cellular proteins with spectrin repeats function in both structural and signaling roles at the plasma membrane (234). Thus it has been proposed that nesprins may have structural and/or signaling roles in the nucleus. Nesprins co-localize with LAP1, emerin and lamin at the NE (204) and contains a LEM-like domain found in these proteins. The presence of the LEM domain

suggests that the nesprins may bind lamin(s) A or C (203), and therefore could potentially be associated with one or more of the laminopathies (233).

Other integral membrane proteins of the INM. Several other integral membrane proteins of the INM have been identified but not studied in detail. The ring finger binding protein is a type IV ATPase that has nine TM sequences, the most of any INM protein. It contains a conserved ring finger binding motif common in several transcription factors, suggesting a role in transcriptional regulation (235). Luma is a 45 kDa INM protein identified in a proteomic analysis of rat liver nuclei that likely interacts with the nuclear lamina (236), however little else is known. In the same screen, UNC 84 was identified. In *C. elegans*, UNC 84 is involved in nuclear migration during cell division (237). UNC 84 requires lamin for correct localization to the INM (238). It binds to, and is required for localization of UNC 83, another protein involved in nuclear migration during cell division, to the INM (239). UNCL contains five TM sequences and binds poly G RNA. This protein contains a LEM-like domain, however binding to BAF and/or lamin has not been tested (240). While characterization of these proteins is in the early stages, their identification illustrates the wide range of possible functions associated with INM proteins, many of which are yet to be discovered.

Peripheral membrane proteins of the INM. Two proteins have been identified in *Drosophila* as peripheral membrane proteins (241, 242) of the NE, Otefin (243) and YA (young arrest)(244). YA is only expressed in ovaries and

early embryos (244), and interacts with chromatin (245) and lamin (242). These interactions are hypothesized to contribute to nuclear structure and organization by mediating the association of chromosomes with the nuclear lamina (241). Otefin is a 45 kDa protein (407 a.a.) that contains a 390 a.a. nucleoplasmic domain followed by a C-terminal 17 a.a. hydrophobic tail, which is required for localization of the protein to the NE. Amino acids 173-372 are also required for localization in the NE and a.a. 35-172 further stabilize the interaction between otefin and the NE (241). Otefin interacts with the *Drosophila* lamina which is suggested as the mechanism used to sort otefin to the NE and/or lamina (242).

Other viral proteins that sort and localize to the INM. Prior to release from the PM, herpes viruses acquire a viral envelope by budding through specific domains in the INM remodeled by the virus. This nuclear budding process suggests that Herpes envelope proteins are sorted to the NE during infection. Envelope protein gB1 (904 a.a.) localizes to the NE of HSV-1 infected cells. The gB1 protein is not specifically targeted to the modified patches where HSV buds, but instead distributes evenly throughout the INM (246). The 21 a.a. TM sequence (774-795) localizes chimeric proteins to the INM and the ER (247). Epstein Barr Virus gp350/220, another herpes virus envelope protein, also localizes in the INM, but unlike HSV gB, sorts specifically to regions of the INM where virus budding occurs. However, the sequence of gp350/220 that specifies sorting and localization to the INM budding patches is yet to identified (248). Adenovirus 2 AD2-11.6 protein is an 11.6 kDa glycoprotein protein of

unknown function. This protein localizes to the NE of infected cells, has a single 21 a.a. hydrophobic sequence, and is predicted to be a Type I membrane protein (249).

Other proteins of the NE. Using multidimensional protein identification technology and "subtractive proteomics", 67 uncharacterized integral membrane proteins of the nucleus were recently identified. Of these newly identified proteins, 23 map to chromosomal regions that are linked to several dystrophies. Microscopy shows that eight of these proteins localize to the NE. Therefore, the authors predict the remaining 59 uncharacterized proteins also localize to the NE. This study suggests that only a small portion of the total proteins of the INM have been characterized (250).

Nuclear lamina. The nuclear lamina acts as a structural framework of the nucleus and is directly juxtaposed to the INM on the nucleoplasmic side of the membrane. The lamina is involved in cell cycle regulation, chromatin organization, DNA replication, cell differentiation, and apoptosis (172). The primary components of the lamina are two types of intermediate filament proteins, type A and type B lamins (251). Like all intermediate filament proteins, the lamins have variable N-terminal and C-terminal domains, but contain a conserved central, coiled-coil, rod domain. This rod domain mediates the formation of head to tail lamin dimers (252, 253). Lamins are unique when compared to other intermediate filament proteins because the C-terminus

contains both a nuclear localization signal (188) and a CaaX motif that acts as a site for prenylation (254).

The B-type lamins are expressed in virtually all somatic cells (169) and three different forms are produced from two genes. Lamin B_1 is encoded by the *LMNB1*, lamin B_2 is encoded by the *LMNB2* gene (255), and lamin B_3 is a splice variant of *LMNB2* (256). Lamin B_1 and B_2 are two minor forms of the lamin B family and associate with membranes by isoprenyaltion (254). The major form of B-type lamin is soluble lamin B_3. Depletion of lamin B_3 results in the loss of DNA replication *in vivo,* however addition of B_3 to depleted extracts will rescue DNA replication (257).

There are two primary forms of A-type lamins, lamin A and C. The *LMNA* gene encodes both the A and C forms. The amino terminal 566 a.a. of lamins A (646 a.a.) and C (572 a.a.) are identical, however alternative RNA splicing, yields two lamins with unique C-termini (258). The lamin A, 98 a.a., C-terminal tail contains a CaaX sequence which is isoprenylated (254). Lamin A is produced initially as a pre-lamin A before it is endoproteolitically cleaved, removing the last 18 a.a. including the farnesyl group (259). Lamin C has a 6 a.a. C-terminal tail which is not isoprenylated (254). The A-type lamins are expressed in most somatic cells, however they are absent in undifferentiated cells of early embryos, some neuron cells and epithelial cells, and certain types of cancer cells (173). While deletion of these proteins does not affect cell growth *in vitro*, at the organismal level the effects result in several laminopathies.

The only insect lamin system characterized is from *Drosophila*. Two lamins, Lamin Dm_0 (260) and Lamin C (261), have been identified. The two lamins have a 46% sequence identity with each other, but have less than a 30% sequence homology with lamins from other species: Lamin B (*Xenopus*) and Lamin C (mammalian). Despite the low sequence homologies, Lamin Dm_0 is considered an analog to the B-type lamins, while Lamin C is an analog of the A-type lamins (262).

Diseases related to the nuclear envelope. The laminopathies (table 2) are a group of inheritable diseases that are characterized by defects in proteins of the nuclear lamina or lamina associated proteins (170) and are the most characterized group of diseases associated with the NE. The laminopathies are part of three different classes of inherited disorders: muscular dystrophies,

Table 2 – Inherited disorders related to the nuclear envelope

Disease Type	Disorder	Gene Mutation
Muscular Dystrophy		
	X-Linked Emery-Dreifuss Muscular Dystrophy	*Emerin* (263)
	Autosomal Recessive Emery-Dreifuss Muscular Dystrophy	*LMNA* (264)
	Dilated Cardiomyopathy	*LMNA* (265)
	Limb Girdle Muscular Dystrophy	*LMNA* (266)
Lipodystrophy		
	Dunnigan Type Familial Partial Lipodystrophy	*LMNA* (267)
	Mandibuloacral dysplasia	*LMNA* (268)
Neuropathy		
	Charcot-Marie Tooth Disorder type 2B1	*LMNA* (269)

References for each disease are listed next to the gene mutated.

partial lipodystrophy, and neuropathy. Most of these diseases have been mapped to defects within the A-type lamins, however at least one of the laminopathies is associated with mutations in the lamin-associated INM protein, Emerin. Two forms of Emery Dreifuss muscular dystrophies have been identified as laminopathies, X-linked autosomal dominant EDMD (Emery-Dreifuss muscular dystrophy), and autosomal recessive EDMD. Autosomal dominant EDMD has been mapped to mutations in Emerin (263). To date, over 50 different pathogenic mutations have been described in Emerin. Most of these mutations result in truncated products which are not expressed, however some of these mutations yield Emerin that no longer localizes to the INM (230). Autosomal recessive EDMD, and the other laminopathies previously mentioned have been linked to mutations in the Type A lamin gene, *LMNA*. These mutations yield proteins that are not expressed or are assembly defective. Mutations within the lamins are also characterized by mislocalization of emerin to the ER as well as a diminished or absent heterochromatin layer in the nucleus (270). In most cases, alterations in the integrity of the NE or the underlying structure of the lamina is believed to be the cause of the laminopathies, however, defects in nuclear positioning, or gene expression may also affect disease progression (170).

Membrane proteins: Integration, orientation and sorting. This study focuses on the sorting and localization of integral membrane proteins to the INM or ODV envelopes. In general, biochemical fractionation techniques are used classify

membrane proteins as either peripheral or integral membrane proteins. Peripheral membrane proteins can be released from the membranes using gentle extraction conditions that leave the lipid bilayer intact (high ionic strength, extreme pH changes). Peripheral membrane proteins associate with membranes either through ionic interactions with integral membrane proteins and/or phospholipids, amphipathic helices and/or covalent modification of a protein with fatty acids. While proteins with fatty acid modifications are generally considered peripheral membrane proteins, during detergent fractionation they may fractionate as with either the detergent or aqueous phase, depending on the acyl modification and/or other interaction with the lipid bilayer. While there are a few examples of INM and ODV envelope proteins that are likely peripheral membrane proteins [eg. Otefin (242), Lamin B (254), ODV-E26 (163)], most are integral membrane proteins [eg. LBR (217), ODV-E66 (148)]. Integral membrane proteins can associate with membranes by two methods: membrane spanning β sheet structures [commonly in the form of a β barrel; eg. Omp A, (271)] or membrane spanning α helices [eg. bacteriorhodopsin, (272, 273)]. Release of integral membrane proteins from the membrane requires extraction conditions that disrupt the lipid bilayer (detergents) and/or denature the proteins (urea, SDS) (274).

Membrane proteins may be integrated into membranes either co- or post-translationally. Most membrane proteins of the eukaryotic cell are inserted into the ER membrane co-translationally. However, proteins that are anchored by C-

terminal TM sequences [reviewed in Borgese et al. (275)], lipid modifications and/or amphipathic helices integrate into the membrane post-translationally.

Co-translational integration of membrane proteins into the ER is mediated via a protein conducting channel called the translocon [reviewed in Johnson and van Waes, (276) and Alder and Johnson, (277)]. The translocon is a multifunctional heterotrimeric complex consisting of Sec61 α,β,γ and forms a gated, aqueous pore in the ER bilayer. Other proteins can be associate with the translocon including: TRAM (translocating chain-associating membrane protein) (278), BiP and signal recognition particle (SRP).

Membrane proteins are translated by cytosolic ribosomes. As an integral membrane protein TM sequence (signal sequence) emerges from the ribosomal tunnel, the nascent chain and ribosome are bound by the SRP and translation is slowed or paused. The SRP/ribosome/nascent chain complex is targeted to the translocon where SRP binds its receptor via a GTP dependent interaction. Following ribosome docking, SRP is released and translation resumes. While in the translocon, the TM sequence is oriented with the N-terminus either toward the lumen or the cytoplasm. The process of how a TM sequence adopts a particular orientation is not well understood, although experimental evidence has identified several features of the protein sequence that may regulate membrane protein orientation (discussed further on page 46). TM sequence integration into the bilayer occurs either co-translationally or following translation termination and ribosome release. Experimental evidence suggests that the timing of

integration may be dependent on whether the TM sequence acts as a signal sequence or a signal anchor. Following release from the translocon, the membrane protein may be modified (signal sequence cleavage, etc.) before being sorted to the final destination in the cell.

Integral membrane proteins may be initially targeted to membranes by either a cleaved signal sequence or a signal anchor sequence. Regardless of the method of targeting, the general consensus in the literature classifies mature single spanning membrane proteins as either Type I (eg. ODV-E66) or Type II (eg. emerin) dependent on the orientation of the mature protein within the membrane (Fig. 4). Polytopic membrane proteins (eg. LBR) can be further classified, but the literature presents no accepted consensus for classification of these proteins.

The orientation of the TM sequence of a membrane protein determines what part of the protein is exposed to the cytoplasm or organelle lumen. The final orientation of the protein in the membrane may determine what post-translational modifications can be made to the protein or what the protein can interact with or access. Several factors are involved in determining the orientation that a particular membrane protein may assume including: charges flanking the TM sequence, the folding of the N-terminal domain, and/or the hydrophobicity of the TM sequence (279).

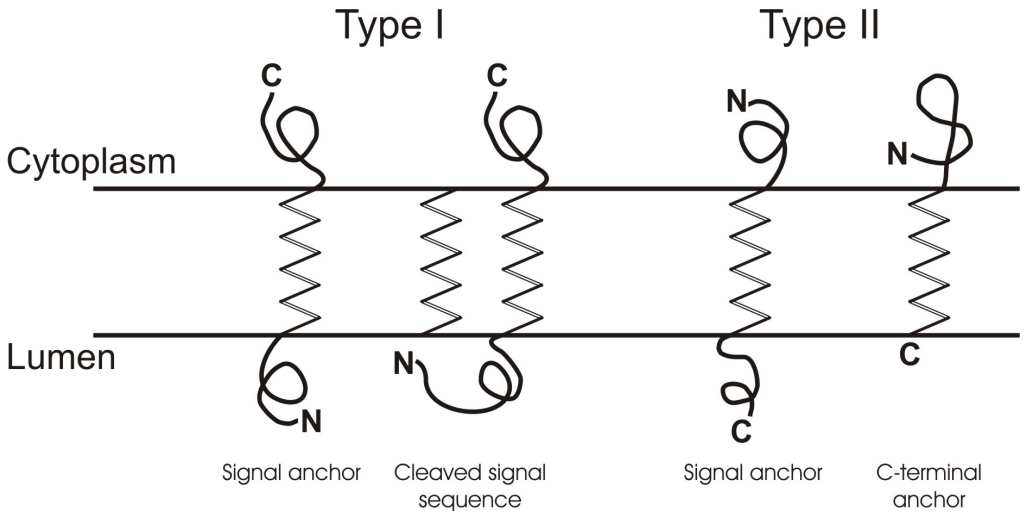

Figure 4. Diagram of the types of single spanning membrane proteins (280).

Statistical analysis of bacterial membrane proteins established the "positive inside rule." For bacterial membrane proteins, positive charges are more likely to be oriented on the cytoplasmic loops (281) of the proteins. Studies of eukaryotic proteins show similar results; the sequence flanking the TM that has a larger net positive charge is oriented on the cytoplasmic side of the membrane (282).

Proteins with internal signal anchor sequences may have the N-terminal region exposed in the cytoplasm prior to translation of the TM sequence. Thus, the N-terminal region can fold and assume a secondary structure prior to the SRP-mediated targeting of the nascent chain to the translocon (283). This folding may inhibit the translocation of the N-termini of these proteins, resulting in the these proteins adopting a Type II orientation [reviewed in Goder and Spiess, (279)]. In fact, experimental evidence shows that truncations of the N-

terminal domain of a Type II membrane protein can result in the protein adopting a Type I orientation (284).

Hydrophobicity and length of the TM sequence within a membrane protein also affects the orientation of the TM sequence. Increasing the length of the TM sequence with hydrophobic a.a., can change the orientation of a Type II membrane protein to the Type I orientation (285). Evidence suggests that as the overall hydrophobicity of a TM sequence increases, the greater the chance that the TM sequence will adopt a Type I orientation (286). Finally, the gradient of hydrophobicity along a TM sequence may also have an effect on the orientation. The more hydrophobic end of the TM sequence is oriented on the lumenal side of the membrane (287).

Sorting can be mediated by a.a. sequences encoded within the membrane protein [reviewed in van Vliet et al., (288) and Emanuelsson and von Heijne (289)], post translational modifications [reviewed in Chatterjee and Major (290)], oligomeric state [reviewed in Martin and Evans (291)], and/or TM sequence characteristics [reviewed in van Vliet et al., (288); Killian (292)]. Targeting signals encoded within a membrane protein can regulate sorting to specific organelles/membranes: ER [di-lysine motifs: Type I protein retention and retrieval sequence (293, 294), N-terminal +2 to +5 di-arginine motifs:Type II protein retrieval and retention sequence (295)] or the plasma membrane [YXXΦ motif (where Φ is any aromatic amino acid)(296-298) or di-leucine motif: basolateral sorting in polarized cells (299)]. Membrane proteins may also be

sorted as a result of post-translational modification: glycosylphosphatidylinositol anchors [apical PM sorting via lipid raft association (290, 300)] or N- or O-linked glycans [apical PM sorting (301)]. For some membrane-bound golgi enzymes, oligomerization is also suggested as a mechanism of retaining these enzymes in the correct compartment of the golgi (302, 303).

The TM sequence of a membrane protein can contain sorting determinants. TM sequence length, hydrophobicity, and the flanking sequences can all influence the localization of membrane proteins in the cell. Lipid bilayer thickness and cholesterol concentrations increase in membranes from the ER to the PM (304, 305). Matching this increase in membrane thickness and/or increase in cholesterol content, TM sequences of PM proteins are an average of 5 a.a. longer than TM sequences of golgi proteins. Increasing the length of a golgi membrane protein TM sequence can result in protein sorting to the PM (306-308). Experiments with an ER tail anchored protein showed that increasing the length of the TM sequence from 17 a.a. to 21 or 26 a.a. results in sorting of the protein to the golgi or PM, respectively (309). Studies conducted in plants also show that lengthening or shortentening the length of a TM sequence can modulate the localization of a type I membrane protein between the ER, Golgi and PM (310). These studies suggest that TM sequence length can act as a sorting determinant of some membrane proteins.

The chemical character of the TM can also regulate the sorting of membrane proteins. A computational analysis of golgi and PM membrane

proteins shows that the overall hydrophobicity of a TM sequence can regulate the sorting of proteins between the golgi and PM; the higher the hydrophobicity, the greater the likelihood the protein will sort to the PM (311). Experimental evidence supports the computational analysis, showing that a replacement of nonhydrophobic a.a. in the middle of an ER membrane protein's TM sequence with hydrophobic a.a. causes the protein to sort to the PM (312). In addition to overall hydrophobicity, changing the polarity of the linear hydrophobicity gradient within the TM sequence of an ER membrane protein results in sorting of the protein to the PM (312). The same study shows that altering the a.a. sequence flanking the TM sequence can also influence ER membrane protein sorting; mutating the positively charged or polar a.a. to hydrophobic a.a. results in the protein sorting to ER-Golgi intermediate transport vesicles. The a.a. sequence characteristics used to predict the sorting and localization of most cellular membrane proteins do not apparently apply to proteins destined for the INM or ODV envelopes. Figure 5 shows a summary and comparison of several INM proteins and the viral SM sequence. This comparison shows that examples of both type I and type II membrane proteins can be found in the INM or the ODV envelope. The proteins of these membranes can be anchored by internal TM sequences or N-terminal or C-terminal signal anchors. Prediction of localization based on the length of the TM sequence also cannot be applied to these proteins, as the length varies from 18 to 22 a.a. Infact, the nuclear pore membrane protein, POM121, has a predicted TM sequence of 44 a.a., yet spans

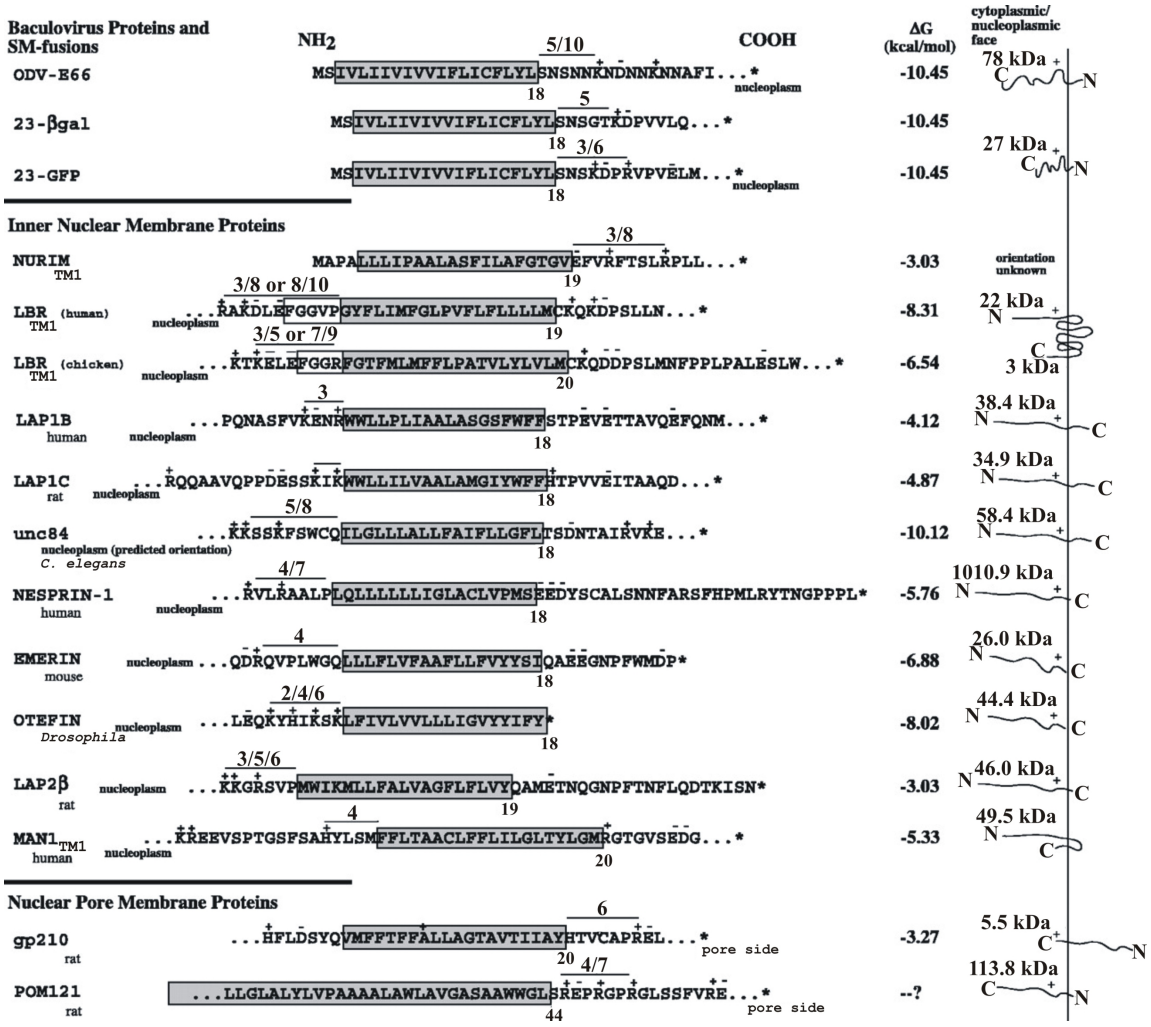

Figure 5. Comparison of the E66 SM a.a. sequence with cellular INM proteins. The TM and flanking sequences most likely to influence INM localization are shown. Reprinted in accordance with Copyright ©1993-2004 by The National Academy of Sciences of the United States of America, all rights reserved (119).

the membrane only once (313). Hydrophobicity cannot be used to predict the localization: the overall hydrophobicity of the TM sequence varies greatly among the INM and ODV envelope proteins. Additionally, cytoplasmic/nucleoplasmic domain size cannot be used to predict if a protein will be excluded from the INM

as the nesprin family of INM proteins contain a cyto/nucleoplasmic domain of one MDa (204). However, there are features identified in the viral SM sequence that are apparently conserved among the known ODV envelope and INM proteins: a TM sequence (with a single or no polar a.a. and no charged a.a.) with a cluster of charged a.a. spaced 5-8 a.a. from the nucleoplasmic side of the TM. The goal of this study is to interrogate the conserved features of the viral SM to determine which features are essential and their role in protein sorting to the INM.

Specific aims

Hypothesis. *Sorting and localization of integral membrane proteins to the inner nuclear membrane can be mediated in part by the sorting motif sequence identified in AcMNPV ODV-E66.*

As described, the current model for sorting and localization of integral membrane proteins to the INM is “diffusion:retention”. This model predicts: integral membrane proteins randomly diffuse within the continuous membranes of the ER and NE and once localized in the INM, the proteins are immobilized and retained through interactions with either immobilized nucleoplasmic ligands, and/or other resident INM proteins (195-198). Therefore, immobilization in the INM is the only mechanism for sorting INM proteins at the INM. The amino terminal 33 a.a. of ODV-E66, termed the sorting motif (SM) (Fig. 6), are sufficient for localization of GFP, β-gal fusions, or E66 to viral-induced intranuclear microvesicles and ODV envelopes during infection. When

abundantly expressed, in addition to intranuclear microvesicles and ODV envelopes, the SM-fusion proteins are also detected in the INM, ONM and ER (152). This localization pattern suggests that the SM-fusion proteins use a pathway similar to INM proteins to sort and localize to the INM, while viral-specific events further sort these proteins to MV and ODV envelopes (151, 152). The chemical characteristics of the E66 derived SM are: 1) An 18 a.a. TM sequence (type I orientation) with no charged or polar a.a.; 2) A cluster of aromatic a.a. located at one end of the TM sequence; 3) A group of 5 polar a.a. at the C-terminal end of the TM sequence followed by 4) A cluster of charged a.a. spaced 6 a.a. residues from the last aromatic a.a. of the TM sequence. A comparison of the E66 SM with cellular INM proteins shows most of the chemical features of the SM are conserved within the INM proteins whose sorting determinants have been identified (119) (the polar a.a. of the SM are not

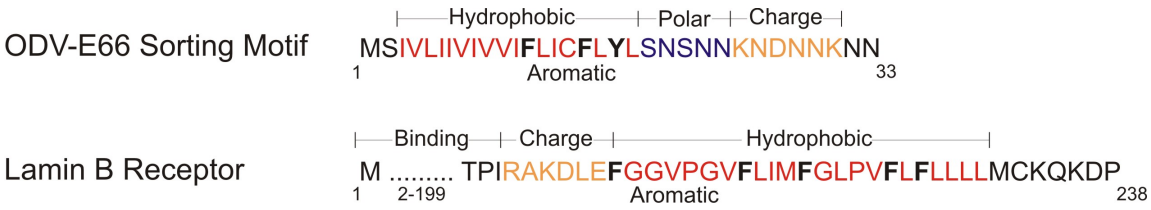

Figure 6. Predicted functional features identified in the ODV-E66 SM and lamin B receptor.

conserved among the cellular INM proteins). The primary goal of this study is to gain insights into the essential features of the SM or SM-like sequences in the sorting and localization of proteins to the INM or ODV envelope.

What are the essential features of the ODV-E66 "sorting motif?" To determine which of the predicted features of the ODV-E66 SM are essential for sorting, directed mutations within the SM will be developed. These mutations will remove or alter: 1) the aromatic a.a. of the TM; 2) the polar a.a.; and/or 3) the spacing a.a. residues separating the cluster of charged a.a. and the TM sequence of the SM (Fig. 6). These SM mutants will be expressed as GFP fusion proteins. In addition, comparative studies will be performed with LBR to determine if the cellular SM-like sequences sort proteins like the viral SM. The LBR nuclear ligand-binding sequence and the N-terminal charged a.a. associated with the TM sequence in the first 238 a.a. of LBR will be deleted and the mutant LBR expressed as GFP fusions. Intracellular localization, protein orientation and membrane association (in Sf9 cells) will be determined for all the SM- and LBR-fusion proteins.

To further address if SM function correlates with the placement of presence of the charged a.a., one or more of the charged a.a. within the SM of E66 will be replaced with alanine or a different charged a.a. Intracellular localization and membrane association of the mutant E66 protein in uninfected and infected Sf9 cells will be determined.

Are SM or SM-like sequences functional in vertebrate cells? To determine if the SM is sufficient to sort fusion proteins to the INM of vertebrate cells, the E66 SM-GFP and LBR-GFP fusions will be expressed in CHO-K1 cells and intracellular localization and protein orientation of the fusion proteins will be determined.

Can sorting and localization to the inner nuclear membrane be independent of immobilization? To determine if immobilization is required for concentration of proteins with SM or SM-like sequences in the INM, FRAP experiments will be performed to measure the mobility of the LBR- and SM-GFP fusion proteins in the INM and ER of CHO-K1 and Sf9 cells.

Are viral SM sequences recognized differently than cellular SM-like sequences during infection? During infection, viral envelope proteins localize to INM derived viral-induced microvesicles (MV) and ODV envelopes. One could predict that if cellular INM proteins with SM-like sequences are immobilized in the INM of insect cells, then, during infection, these proteins should not localize in microvesicles/ODV envelopes. However, if the resident INM proteins are mobile in the INM, and the only active sorting event at the INM is immobilization, then it is possible that these proteins will accumulate in MV and ODV envelopes. To determine if cellular SM-like sequences are distinguished from the viral SM sequence, the LBR- and SM-fusion proteins will be expressed during infection and localization determined using light confocal and immunoelectron microscopy.

MATERIALS AND METHODS

Plasmid cloning and DNA sequencing

General plasmid cloning protocols are described by Sambrook et. al., (314). Polymerase chain reaction (PCR) was performed using a MJ Research DNA Engine Peltier Thermal Cycler, PTC-200 (MJ Research, Inc., Reno, NV). DNA was transformed into strain DH5α *E. coli* cells by electroporation using a Bio-Rad Gene Pulser II (Bio-Rad Laboratories, Inc., Hercules, CA). Double stranded DNA sequencing was performed using the ABI PRISM Big Dye Terminator Cycle Sequencing Core Kit with Amplitaq® DNA Polymerase. Sequencing reactions were analyzed using an ABI 373 XL or 377 XL DNA sequencer (Applied Biosystems Inc., Foster City, CA). DNA was sequenced on both strands to check for errors using oligonucleotides appropriate for the specific clone. Enzymes were purchased from either Promega (Madison, WI) or New England Bio-labs (Beverly, MA) unless otherwise noted.

Cell culture and virus infection

Spodoptera frugiperda IPLB-SF21 (315) clonal isolate 9 (Sf9) cells (16) were cultured as both suspension and adherent cultures at 27^{o}C in TNM-FH medium supplemented with 10% FBS and 1.0% F-68 (Complete TNM-FH). AcMNPV strain E2 was used as the wild type (wt) control virus. All infections were performed at a multiplicity of infection of 10, with time zero set at the time of virus addition. A proline auxotroph clone of a Chinese Hamster Ovary cell line (CHO) (American Type Culture Collection, Manassas, VA, catalog number CCL-

61), termed CHO-K1, was cultured as an adherent culture in Dulbecco's Modified Eagle Medium (DMEM) (Invitrogen Corporation, Carlsbad, California) supplemented with 2 mM Proline, 10% FBS, and 3.7g/L $NaHCO_3$ (37^oC + 5.0% CO_2 in a humidified incubator).

Expression in uninfected Sf9 cells

Expression studies were conducted using uninfected Sf9 cells with various DNA constructs. Transfection of Sf9 cells was conducted using calcium phosphate transfection method described in Summers and Smith (83). Briefly, Sf9 cells were seeded at a density of 1.0×10^6 cells per well in 6 well culture dishes. After allowing attachment, the cells were washed with 2.0 ml Grace's Antheraea medium (Graces) (316) + 10 % FBS leaving 0.75 ml of the medium on the cells. Transfection mixes were prepared by adding 10 μg of pIE1 plasmid DNA containing the appropriate construct to 0.75 ml of transfection buffer (25mM HEPES, pH 7.1, 140 mM NaCl, 125 mM $CaCl_2$). The transfection mix was added to 1 well of cells drop wise, and the cells were incubated at 27^oC for 4 hours. Following incubation, the cells were washed with 2.0 ml complete TNM-FH, and incubated with 2.0 ml complete TNM-FH at 27^oC for 48 hours.

Immunofluorescence confocal microscopy

Infected (48 hours post infection, h p.i.) or transfected Sf9 cells were harvested. The harvested cells were collected by centrifugation (500 x g, three minutes) and resuspended in Graces media and 2.8×10^5 cells were transferred to a one well cytofuge container (Statspin Technologies, Norwood, MA.) on an

Esco No. 2960 slide (Erie Scientific, Erie, PA). After allowing attachment at room temperature (RT) for five minutes, the cells were fixed with 3.7% paraformaldehyde in PBS (phosphate buffered saline) at RT for 10 minutes. Following fixation, the cells were washed three times with PBS. Following the washes, fixed cells were incubated with 100% Methanol (MeOH) for 10 minutes at RT followed by 0.5%Triton X-100 for 10 minutes at RT. Following both incubations, the cells were washed as previously described, and incubated in blocking solution (1.0% porcine serum, 3.0% bovine serum albumin, PBS) for one hour at RT. Primary antibodies were diluted in blocking solution, added to the fixed cells and incubated at 4^{o}C for overnight. The fixed cells were washed and incubated with secondary antibodies (Alexa Fluor conjugates, Molecular Probes, Inc., Eugene, OR) diluted at 1:2000 in blocking solution for two hours at RT. Following incubation with secondary antibody, the cells were washed. When DNA staining was required, the cells were incubated with DAPI (4', 6' diamidino-2-phenylindole) diluted at 0.1 μg/ml in PBS for five seconds and washed three times in PBS. Following the final washes, all solutions were removed, and 10 μl of DAKO Fluorescent Mounting Medium (DAKO Corporation, Carpinteria, CA) was added and covered with a number 1.5 1-ounce cover slip (VWR, West Chester, PA, catalog number 48366 227). Cover slips were sealed with nail hardener and stored in the dark at 4^{o}C until ready for viewing. Slides were viewed using a Zeiss Axiovert 135 (Carl Zeiss MicroImaging, Inc. Thornwood, NY) with a CARV confocal module (Atto

Bioscience, Rockville, MD). After viewing at least 20 fields, representative cells/fields were collected using either the CARVer software (Atto Bioscience), or Zeiss Axiovision ver. 3.1 (Carl Zeiss MicroImaging, Inc., Thornwood, NY). Confocal sections were collected at 0.75 μm intervals and the section representing the middle of the cell shown in each case. Three-dimensional reconstruction and image deconvolution was conducted using either Zeiss KS400, ver. 3.0 or Zeiss Axiovision ver. 3.1.

CHO-K1 cell transfection and microscopy

The DNA used for transfection of CHO-K1 cells was isolated using a Qiagen Endo Free Plasmid Maxi Kit (Qiagen, Inc., Valencia, CA, catalog number 12362). Transfection of foreign DNA constructs into CHO-K1 cells was accomplished using LipofectAmine® reagent following the manufacturer's protocol (Invitrogen Corporation, Carlsbad, California, catalog number 18324-012). CHO-K1 cells were seeded at a density of 1.0×10^5 cells/well in a 6 well plate in complete DMEM and incubated overnight at 37°C. The cells were washed with 2.0 ml of Opti-MEM® (Invitrogen Corporation, Carlsbad, California, catalog number 22600050) before adding the transfection mix. Transfection mix was assembled by mixing 3.0 μg of plasmid DNA, 12.5 μl of LipofectAmine, and 200 μl of Opti-MEM. This solution was incubated for 30 minutes at RT and then diluted with 800 μl of Opti-MEM. The dilute transfection mix was added to the washed cells and incubated overnight at 37°C. Following incubation, the transfection mix was removed, and replaced with complete DMEM (time zero).

At 48 hours post transfection, the cells were detached by trypsinization, and reseeded onto chambered slides (Nalge Nunc International, Rochester, NY, catalog number 154461) at a density of 7.0 x 10^4 cells/well in DMEM and incubated overnight at 37^{o}C. Following transfection, the cells were processed for microscopy, and representative cells captured as previously described.

Quantifying fluorescence from confocal images

Utilizing a custom macro (Appendix A) written for Zeiss KS400, ver. 3.0, the amount of E66 fluorescence label in the intranuclear space, nuclear envelope, or the extra-nuclear space of infected cells was quantified. A schematic of the macro is shown in figure 7. This macro allows the user to load images of a specific confocal section corresponding to the three separate channels of fluorescence plus a brightfield image. Briefly, the macro allows the user to trace the outside of the cell (from the brightfield image) to identify the plasma membrane. Once completed, the blue channel was used to identify the region directly beneath the nuclear envelope by allowing the user to trace fluorescence label. Once the trace was complete, the software identified the nuclear envelope and segregated this region from the intranuclear and extra-nuclear space. Once completed, the software then calculated the total fluorescence intensity units (grey values) per cell, the total fluorescence intensity units in each region, as well as the total area/pixel^2 and total area/pixel^2 for each region. The blue channel of fluorescence corresponded to the lamin antibody label [Adl67, (242)]. The green channel of fluorescence corresponded to the

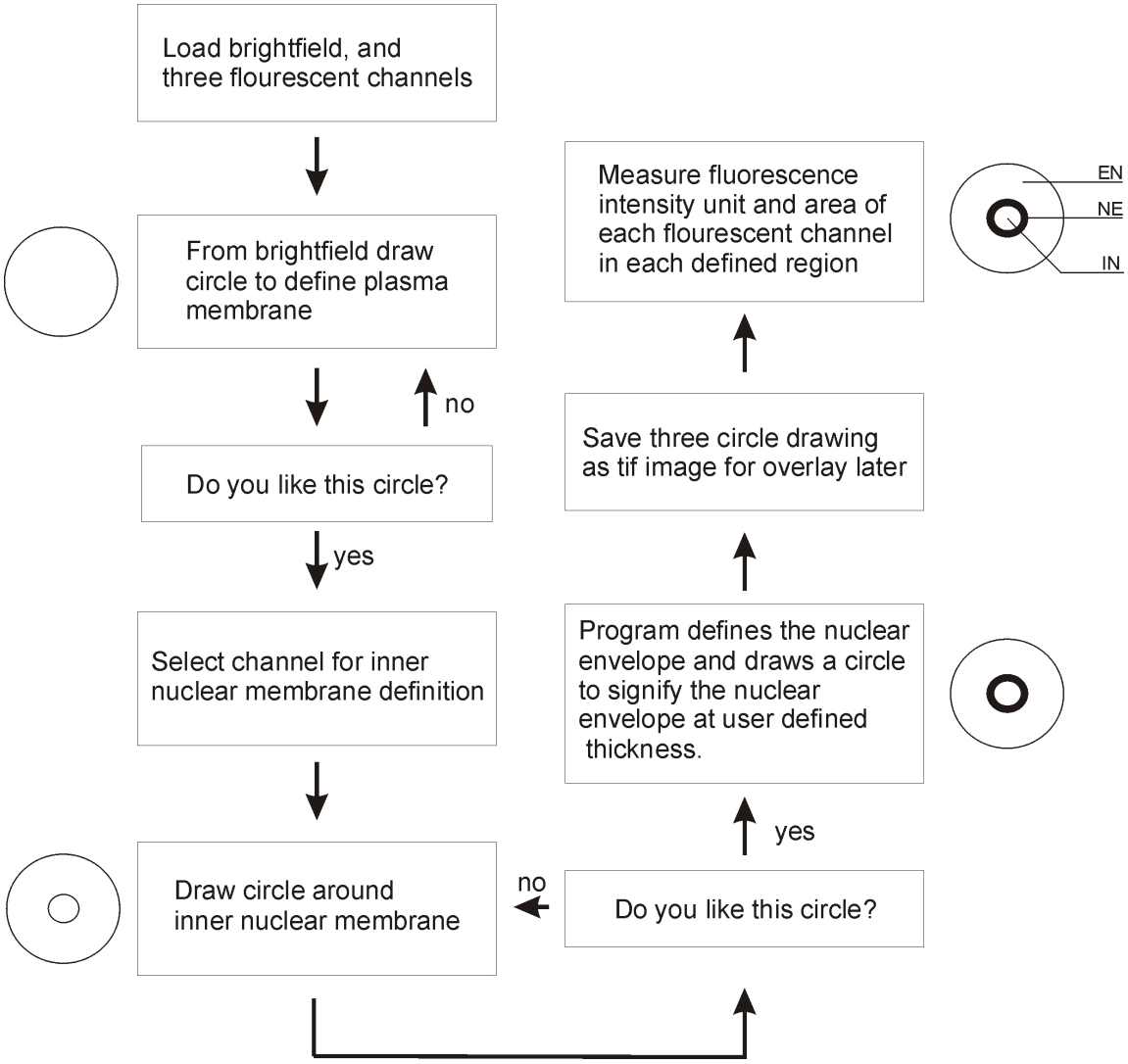

Figure 7. KS400 macro schematic. Schematic drawing of the macro used for regional quantitation experiments. EN-extranuclear, NE-nuclear envelope, IN-intranuclear.

GFP auto fluorescence. The red area/pixel^2 and total area/pixel^2 for each region. The blue channel of fluorescence corresponded to the lamin antibody label [Adl67 (242)]. The green channel of fluorescence corresponded to the GFP auto fluorescence. The red channel of fluorescence corresponded to the

label of the quantified protein. For each cell, only those sections that displayed a prominent rim of fluorescence around the nucleus when viewing the lamin label were quantified. Once the raw quantitation was accomplished by KS400, the data was imported to Microsoft Excel for analysis. To analyze, the sum of the fluorescence intensity units per each region for each section was calculated, along with the area/pixel^2 per each region for each section. Following those calculations, the percentage of label and the percentage of area for each section were calculated. A density ratio was calculated by dividing the percentage of fluorescence intensity units per region by the percentage of area/pixel^2 per region (% grey/% area) for each cell. For each construct tested, the fluorescence of 7-10 cells was quantified, and the density ratios were used to calculate an average density ratio for each fusion protein tested. These average ratios were normalized to 100% for each fusion protein tested, and plotted on a bar graph using Microsoft Excel. Error bars represent standard deviation for the noted number of determinations (n).

Assay of membrane protein integration by Triton X-114 extraction

Triton X-114 extractions assays were performed as described by Bordier et al. (317) and Rosenberg et al. (318). Briefly, 2.0 ml of Triton X-114 (Fluka, Buchs SG, Switzerland) was pre-cleared with 100 ml of PBS, pH 7.0 resulting in a ~11.4% v/v Triton X-114 solution, this solution was used as the stock Triton X-114 throughout the experiment. Transfected or infected (48 h p.i.) Sf9 cells (~5.0 x 10^6) or transfected CHO-K1 cells (~5.0 x 10^6) were collected by

centrifugation (500 x g, three minutes). The cell pellet was resuspended in 1.0 ml of lysis buffer (1.0% Triton X-114, PBS) and incubated with agitation at 4^{o}C. The solution was cleared by centrifugation (16,000 x g, 10 minutes), and the supernatant loaded on a100 µl sucrose cushion (6.0%sucrose, 0.06% Triton X-114 in PBS). Following incubation at 37^{o}C for 3 minutes, the phases were separated by centrifugation (500 x g, three minutes) at 37^{o}C. Following centrifugation, the aqueous and detergent phases were separated into separate fractions. The aqueous fraction was re-extracted with 50 µl of the 11.4% Triton X-114 stock, and the detergent fraction was re-extracted with 1.0 ml PBS. Each fraction was incubated and centrifuged as previously described to separate the phases. Only the aqueous phase was saved after re-extracting the initial aqueous fraction and only the detergent phase was saved after re-extracting the initial detergent fraction. The final extracted fractions were adjusted to 1.0 ml with PBS. An equal volume of SDS-PAGE sample buffer (4% w/v SDS, 10% v/v Glycerol, 0.50 mM Tris, 2.0% β-mercapthoethanol, 0.04% Bromophenol blue, pH 6.8) was added to each sample and incubated at 65^{o}C for 15 minutes. Following SDS-PAGE (35 µl of the total sample) and western transfer, the samples were analyzed by incubating the immunoblot with the appropriate antibodies.

Digitonin permeabilization assay for INM localization

Digitonin permeabilization was utilized as described in Adam et al. (319). The protocol was slightly modified for Sf9 cells. Briefly, transfected Sf9 cells

(~2.8 x 10^5) were re-seeded in 1 well cytofuge container (Statspin Technologies, Norwood, MA.) on an Esco No. 2960 slide (Erie Scientific, Erie, PA). After allowing attachment for one hour a RT, the cells were washed three times with Graces media and fixed with 3.7% paraformaldehyde (PBS) for 10 minutes (RT). Fixed cells were washed three times with PBS, and incubated with 30 μg/ml digitonin (Calbiochem, La Jolla, CA; PBS) for 10 minutes at RT. The cells were washed with PBS, and incubated with blocking solution (RT, 10 minutes). Following the incubation, the fixed cells were incubated with primary and secondary antibodies as previously described for immunofluorescence microscopy. For CHO-K1 cells, the protocol was modified as described in Wu et al. (231). Transfected cells were washed three times in PBS, and fixed in 2.0% paraformaldehyde (PBS) for 30 minutes on ice. The cells were washed three times with PBS and incubated with pre-cooled digitonin, diluted to 40 μg/ml (PBS), for 10 minutes on ice. The cells were washed three times with PBS and incubated with blocking solution (RT, 10 minutes). Following the blocking reaction, the fixed cells were incubated with primary and secondary antibodies as previously described for immunofluorescence microscopy.

Fluorescence recovery after photo-bleaching

DNA was transfected into CHO-K1 or Sf9 cells as previously described, however, the cells were not fixed or exposed to antibodies. Prior to the day of FRAP experiments, the cells were transferred to number 1 chambered cover glasses (Nalge Nunc International, Rochester, NY, catalog number 155380).

The transfected Sf9 cells (1.0×10^5 cells/well) or CHO-K1 cells (7.0×10^4 cells/well) were allowed to attach overnight under normal culture conditions. If DNA staining was required the cellular DNA was stained for five minutes using Hoechst 33342 (Molecular Probes, Inc., Eugene, OR, catalog number H-3570) diluted to 0.1 μg/ml (PBS). Following staining, the cells were washed three times with PBS followed by incubation with complete medium. Prior to viewing, the cells were washed once [Sf9; Graces medium + 10%FBS, CHO-K1; Leibovitz L-15 Medium (Invitrogen Corporation, Carlsbad, CA, catalog number 21083027)] with 2.0 ml of the medium left on the cells. The FRAP algorithm was used to achieve photo-bleaching of either the NE or ER (1.3 μm spot) of a cell with the scanning laser strength adjusted to 300 microwatts and photo bleaching laser strength set at two milli-watts. Following bleaching, the area was scanned every three seconds for up to four minutes and fluorescence recovery was recorded over time. Lateral mobility in cell membrane was then computed according to the method of Yguerabide et al. (320).

Protein orientation using an *in vitro* glycosylation assay

Orientation of the LBR-fusion proteins in insect and mammalian cell membranes was determined using an *in vitro* glycosylation assay (321, 322). This assay involved *in-vitro* translation in the presence of microsomal membranes followed by determination of glycosylation state. All mRNAs were transcribed from PCR generated templates using the AmpliCap™ SP6 High Yield Message Maker Kit (Epicentre Technologies). *In vitro* translation was

performed using rabbit reticulocyte lysate (Promega) labeling the protein with ^{35}S-methionine (MP Biomedicals). To generate the mRNAs for the LBR-GFP fusions with amino-terminal NST sequences, oligonucleotides were designed to generate templates that had the SP6 promoter, a Kozak consensus sequence, an ATG start codon, and a consensus glycosylation acceptor sequence (NST) on the 5' end of the coding sequence. If spacer a.a. were required ($_{200\text{-}238}$LBR, $_{208\text{-}238}$LBR), they were added between the NST and the start of the gene coding sequence. To add the carboxy terminal NST and required spacer a.a., PCR was used to generate LBR gene sequences with a 5' SP6 promoter and Kozak sequence, and a 3' NST and required spacing sequences. The final sequences of the engineered proteins are shown in the figure (pg. #). *In vitro* translation reactions were performed in the presence or absence of canine (Promega) or Sf9 cell derived microsomal membranes. For each construct, one translation reaction containing microsomes was incubated with endoglycosidase H (New England Biolabs; manufacturers instructions). The proteins were separated using SDS-PAGE and the translated product viewed by autoradiography. Sf9 derived microsomal membranes were isolated as reported in Saksena et al. (323). Sf9 cells were collected by centrifugation (1,200 x g, 10 minutes) and diluted with 4.0 ml per gram of cell mass in buffer A [50 mM TEA (pH 7.5), 50 mM KOAc, 6 mM $Mg(OAc)_2$, 1.0 mM EDTA, 1.0 mM DTT, and 0.5 mM PMSF]. The resuspended cells were homogenized with 10 strokes using a motor driven drill homogenizer, avoiding foam formation and heating. This homogenate was

centrifuged (1,000 x g, 10 minutes) and the supernatant re-centrifuged (10,000 x g, 10 minutes). Microsomes were collected by centrifugation of the 10,000 × g supernatant (140,000 x g, 2.5 hours) through a 1.3 M sucrose cushion (buffer A). Microsome pellets were resuspended in buffer B [250 mM sucrose, 50 mM TEA (pH 7.5), and 1 mM DTT] by manual dounce homogenization to a concentration of 50 A_{280} units/ml (1 equivalent/ml). The microsomes were considered competent if they targeted and translocated pre-prolactin (rabbit reticulocyte lysate) at levels comparable with canine microsomes. In addition to the glycosylation assay, orientation was also confirmed using protease protection following the protocol of Hong et al. (148).

SDS-PAGE, western and immunoblotting

Sodium dodecyl sulfate polyacrylamide gel electrophoresis, SDS-PAGE, was performed as described by Laemmli (324). Unless otherwise stated a 12.5% separating gel with 3.0% stacking gel was used. Samples were denatured using an equal volume of 4x SDS-PAGE sample buffer and incubated at 65^{o}C for 15 minutes. Following electrophoresis, gels were either stained with Commassie blue (0.1%Comassie R-250, 10%MeOH) and destained/fixed (45% Acetic Acid, 10%MeOH), or transferred to Immobilon-P membrane (Millipore, Billerica, MA, catalog number IPVH 000 10) using the tank transfer method (314). Blots were analyzed by incubating in blocking solution (3% nonfat dry milk, 50 mM Tris-HCL, 150 mM NaCl, 0.05% Tween 20, pH 7.4) for 30 minutes at RT, then incubated with primary antibody (diluted in blocking solution) for

either two hours at RT, or overnight at 4^{o}C. Blots were washed three times (5 minutes per wash, RT) with TBS-T (50 mM Tris-HCl, 150 mM NaCl, 0.05% Tween 20, pH 7.4), followed by incubation with secondary antibody conjugated to horseradish peroxidase (HRP) (1:10000, blocking solution; 1hour, RT). The blots were washed four times with TBS-T, and developed using the Western Lightning™ chemiluminescence reagent kit (Perkin Elmer, Boston, MA, NEL100) and Kodak X-Omat Blue XB-1 film (Eastman Kodak Company, New Haven, CT).

DNA constructs

ΔXbaI, NarI pUC18 (Appendix B1, page 162). Numerous constructs were developed using a modified version of the pUC 18 vector. This modified version lacks the restriction enzyme recognition sites, NarI (bp235) and XbaI (bp423). Both of these sites were removed by first digesting with the appropriate enzyme, then filling the resulting overhangs with T4 DNA polymerase to generate blunt ends. The digested/filled DNA vector was ligated and amplified. The NarI site was destroyed first, generating ΔNarI pUC18. This modified pUC was digested to destroy the XbaI site generating ΔXbaI, NarI pUC18.

ΔXbaI, NarI pUC18 EGFP/Alt. EGFP (Appendix B2, page 163). Enhanced green fluorescent protein (EGFP) (BD Biosciences Clontech, Palo Alto, CA) fusions were utilized throughout this study. To generate the fusion protein constructs, restriction enzyme sites had to be added in frame to EGFP. In addition, a variant of EGFP that lacked the charged amino acids between a.a. 2-7 was designed and constructed (Alt. EGFP). For subsequent cloning, the

restriction enzyme sites BamHI, XbaI, and NarI (5' to 3') were added to the 5' end of the EGFP/Alt. EGFP DNA sequence. PCR was utilized for the addition of the sites and for the modifications to EGFP (Appendix B2). The PCR products were cloned into ΔXbaI, NarI pUC18 using the BamHI sites. The two resulting clones are termed ΔXbaI, NarI pUC18 EGFP and ΔXbaI, NarI pUC18 Alt. EGFP (Appendix B2).

Sorting motif scanning constructs (Appendix B3, page 164). To dissect the essential features required for INM localization of the E66 sorting motif (SM), a series of EGFP fusion proteins were generated (Fig. 8). Mutations in the coding sequence of the E66 SM fused to EGFP were constructed using complementary oligonucleotides (Appendix B3) cloned into the XbaI and NarI sites of the ΔXbaI, NarI pUC18 EGFP/Alt. EGFP vectors. Complementary oligonucleotides were annealed by mixing equimolar amounts of each oligonucleotide, incubating at 95^{o}C for 5 minutes, and then cooling to room temperature at 0.1^{o}C per second. Constructs "A" and "B" are native E66 sequences, and constructs "C" and "D" have the aromatic a.a. codons replaced with a leucine codon. Constructs "A" and "C" were fused to the EGFP sequence, whereas, constructs "B" and "D" were fused to Alt. EGFP (Appendix B3). For expression in uninfected Sf9 insect cells, the constructs were inserted in the BamHI site of pIE1-3 (Novagen, Madison, WI, catalog number 69090-3). To production of recombinant baculovirus, the constructs were inserted in the BamHI site of pBACgus-1 (Novagen, Madison, WI, catalog number 70054-3). Finally, for mammalian cell

expression, the constructs were placed into the BamHI site of pcDNA3.1/Zeo(+) (Invitrogen Corporation, Carlsbad, CA, catalog number V860-20).

A.a.: 1	18 25 33
E66	MSIVLIIVIVVI**F**LIC**F**L**Y**LSNSNNKNDANKNNAFID – E66
SM1A	MSIVLIIVIVVI**F**LIC**F**L**Y**LSNSNNKNDANKNNAGAM – EGFP
SM1C	MSIVLIIVIVVI**L**LIC**L**L**L**LSNSNNKNDANKNNAGAM - EGFP
SM2A	MSIVLIIVIVVI**F**LIC**F**L**Y**LKNDANKNNAGAM – EGFP
SM2C	MSIVLIIVIVVI**L**LIC**L**L**L**LKNDANKNNAGAM – EGFP
SM3A/B	MSIVLIIVIVVI**F**LIC**F**L**Y**LSNSNNAGAM – EGFP/Alt.EGFP
SM3C/D	MSIVLIIVIVVI**L**LIC**L**L**L**LSNSNNAGAM – EGFP/Alt.EGFP
SM4A/B	MSIVLIIVIVVI**F**LIC**F**L**Y**LAGAM – EGFP/Alt.EGFP
SM4C/D	MSIVLIIVIVVI**L**LIC**L**L**L**LAGAM – EGFP/Alt.EGFP
ΔCSM1A	MSIVLIIVIVVI**F**LIL**F**L**Y**LSNSNNKNDANKNNAGAM – EGFP

Figure 8. A.a. sequence resulting from the sorting motif mutations. The transmembrane sequences are shown in red. The aromatic a.a. or the leucines substituted in their place are bolded. The polar a.a. are shown in blue. The charged cluster of a.a. is shown in purple. The EGFP of Alt.EGFP sequences are shown in green. The leucine substituting the cysteine in ΔC SM1A is underlined.

Charge mutations in full length E66 (Appendix B4, page 166). Several constructs were built that mutated the codons encoding the charged a.a. of the SM within the full length *E66* gene (Fig. 9 for final a.a. sequence). PCR (Appendix B4 for the oligonucleotides) was utilized to generate the *E66* gene sequence with the charge mutations. Following PCR amplification, the mutated

E66 genes were cloned into the SacI/MluI sites of a pGEM-4z construct containing *E66* which lacks the coding sequence for the amino terminal 33 a.a. These charge mutated constructs were cloned into the BamHI sites of pIE1-3, pBACgus-1, and pcDNA3.1/zeo (+).

A.a.: 1		**37**	**704**
E66	MSIVLIIVIVVIFLICFLYLSNSNNKNDANKNNAFID	–	E66
E66	MSIVLIIVIVVIFLICFLYLSNSNN**G**N**G**AN**G**NNAFID	–	E66
E66	MSIVLIIVIVVIFLICFLYLSNSNN**A**N**A**AN**A**NNAFID	–	E66
E66	MSIVLIIVIVVIFLICFLYLSNSNN**K**N**K**AN**K**NNAFID	–	E66
E66	MSIVLIIVIVVIFLICFLYLSNSNN**D**N**D**AN**D**NNAFID	–	E66
E66	MSIVLIIVIVVIFLICFLYLSNSNN**A**N**D**AN**K**NNAFID	–	E66
E66	MSIVLIIVIVVIFLICFLYLSNSNN**K**N**D**AN**A**NNAFID	–	E66
E66	MSIVLIIVIVVIFLICFLYLSNSNN**A**N**D**AN**A**NNAFID	–	E66
E66	MSIVLIIVIVVIFLICFLYLSNSNN**R**N**D**AN**R**NNAFID	–	E66
E66	MSIVLIIVIVVIFLICFLYLSNSNN**K**N**E**AN**K**NNAFID	–	E66
E66	MSIVLIIVIVVIFLICFLYLSNSNN**R**N**D**AN**R**NNAFID	–	E66

Figure 9. N-terminal sequence of E66 with mutated charge residues. The mutated a.a. of the SM are shown in bold.

N-terminal 125 a.a. of E66 with the SM charge mutations fused to EGFP (Appendix B5, page 168). PCR (Appendix B5 for oligonucleotides) was utilized to amplify the sequence of the first 125 amino acids from the pGEM E66 genes containing the directed mutations at the charged a.a. described in appendix B4 (a schematic of the clones is shown in figure 10). The products were placed into

the XbaI/NarI sites of ΔXbaI, NarI pUC19 EGFP (Appendix B5). Once sequence confirmed, the 125 E66 EGFP clones were digested with BamHI, and the fragments ligated into the BamHI site of pIE1-3.

Figure 10. Schematic of the N-terminal 125 a.a. of E66 with the SM charge mutations fused to EGFP.

Mammalian expression of the sorting motif (Appendix B6, page 169). For expression in mammalian cells, a consensus Kozak sequence (325) was added 5' of the initiator methionine codon of the SM-GFP constructs using PCR (forward oligo – 125FW (ori), Appendix B6, reverse oligo – EGFP reverse, Appendix B2). Once amplified, the PCR products placed into the AflII/BamHI sites of pcDNA3.1/Zeo (+) (Appendix B6).

Lamin B receptor. Three lamin B receptor (LBR) clone constructs (Fig. 11) were used in this study. The first construct, phLBR 1TM-EGFP ($_{1\text{-}238}$LBR-GFP) (199), construct obtained from Jan Ellenberg (European Molecular Biology Laboratory, Heidelberg, Germany). This construct contains the cDNA sequence for a.a. 1-238 of LBR fused to EGFP and includes the N-terminal nuclear ligand-binding sequence as well as the first transmembrane domain. This fusion construct was excised and inserted into the BamHI/NotI sites of pIE1-3 (insect expression), pGEM-4z (in vitro transcription), and

pBACgus (recombinant baculovirus). Two additional LBR base constructs containing deletions in the N-terminal a.a. were generated using PCR (Appendix B7, page 166). The first construct lacked the sequence encoding the nuclear ligand-binding sequence of LBR ($_{200\text{-}238}$LBR-GFP, Fig. 11B), while the second construct lacked the nuclear ligand-binding sequence and the sequence encoding the charged a.a. flanking N-terminal side of the transmembrane sequence ($_{208\text{-}238}$LBR-GFP, Fig. 11C) (Appendix B7 for oligonucleotides). The PCR generated products were inserted into the BamHI/HindIII sites of pUC18. Both constructs were then cloned into the BamHI/HindIII sites of the mammalian expression vector, pCMVBlue (Pharmingen, San Diego, CA). Additionally, each construct was cloned into the BamHI/NotI sites of pIE1-4 (insect expression, Novagen, Madison, WI, catalog number 69090-3) and pBACgus-1 (recombinant virus).

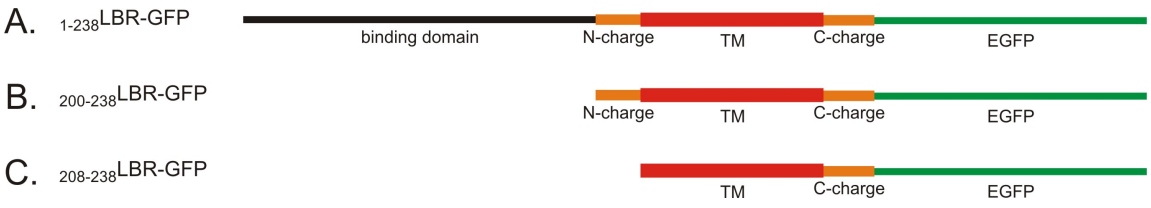

Figure 11. Schematic of LBR-GFP base constructs. A.) The phLBR 1TM-EGFP clone obtained from J. Ellenberg. B.) The LBR-GFP fusion generated lacking the nucleoplasmic 200 a.a. of phLBR 1TM-EGFP. C.) The LBR-GFP fusion generated lacking the nucleoplasmic 208 a.a. of phLBR 1TM-EGFP.

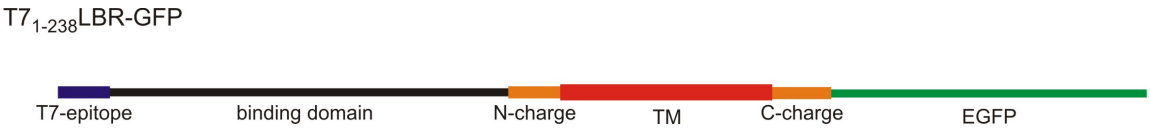

Figure 12. Schematic of T7$_{1-238}$LBR-GFP construct.

For expression in mammalian cells, a consensus Kozak sequence (325) was added 5' of the initiator methionine codon of the N-terminal deleted LBR-EGFP fusions (oligonucleotides and clone map, Appendix B8, page 167). The PCR products were inserted into the BamHI/NotI sites of pcDNA3.1/Zeo(+).

Digitonin permeabilization assays required that the $_{1-238}$LBR-GFP fusion have a unique epitope tag at the N-terminus (Fig. 12). PCR (clone map and forward oligonucleotides, Appendix B9, reverse oligonucleotides, Appendix B8) was used to generate the cDNA encoding T7$_{1-238}$LBR-GFP (Appendix B9, page 168). This PCR product was cloned into the BamHI/NotI sites of pcDNA3.1/Zeo(+) and pIE1-4 for mammalian and insect cell expression respectively.

Recombinant virus production

Recombinant virus expressing the sorting motif fusion proteins. To develop recombinant viruses that expressed the SM-GFP constructs (figure 7) under control of the polyhedrin promoter, the pBACgus SM clones were co-transfected with Bsu361 digested BacPak AcMNPV genomic DNA (gift of Robert D. Possee, Center for Ecology and Hydrology, University of Oxford, Oxford, UK) as described in Summers and Smith, (83). Recombinant virus was selected

through three rounds of plaque assay and positive plaques were detected using the chromagen X-gluc [40 mg/ml X-gluc (5-bromo-4-chloro-3-indolyl β-D-glucopyranoside); incubated at RT for 4-8 hours for the chromagenic reaction]. Blue plaques were picked into 500 µl of complete TNM-FH, vortexed for 30 seconds and incubated at RT for 1 hour. Passage 1 virus was generated from the third round plaques by inoculating 1.0 x 10^6 cells in a final volume of 2.0 ml with 100 µl of the viral stock. Infections proceeded for 7 days at 27^{o}C and the media supernatant collected to harvest recombinant virus. PCR was used to verify that each recombinant virus had the appropriate SM-GFP clone inserted into the polyhedrin locus. Briefly, 750 µl of the passage 1 virus stock was mixed with an equal volume of precipitation solution (20% polyethylene glycol, 8000 MW and 1M NaCl) and centrifuged at 16,000 x g for 20 minutes at room temperature. The supernatant was removed, the pellet resuspended in 100 µl of disruption buffer (10mM Tris, 1mM EDTA, 0.25% SDS, pH 7.6, 1.0 mg proteinase K) and incubated overnight at 37^{o}C. Following incubation, phenol:chloroform (1:1) extraction was performed and centrifugation (1,200 x g) used to separate the phases. The viral DNA was precipitated from the aqueous phase and resuspended in 10 µl of sterile water. PCR was performed using 5.0 µl of the purified viral DNA [forward oligonucleotides: SM4A sense strand (Appendix B3), reverse oligonucleotides: EGFP reverse (Appendix B2)]. Production of a ~900 bp product verified the insertion of the appropriate SM-GFP fusion into the polyhedron locus.

Recombinant virus expressing the lamin B receptor fusion proteins. Lamin B receptor recombinant viruses were constructed using the pBACgus-1 Lamin B receptor clones (Fig. 11). Techniques to produce the virus were the same as for the recombinant viruses expressing the SM fusions. PCR verification was done using EGFP forward and EGFP reverse (Appendix B2).

Antibodies. The antibodies used in this study are listed in table 3.

Table 3 – Antibodies used for dissertation study

Antibody	Company/Researcher	Location	Catalog Number	Dilution
Nuclear Pore (mAB414)	Berkley Antibody Company	Richmond, CA	MMS-120P	1:500 (microscopy)
Calreticulin	Affinity Bioreagents	Golden, CO	PA3-900	1:500 (microscopy)
GFP	Molecular Probes	Eugene, OR	A11122	1:1000 (immunoblotting) 1:500 (microscopy)
GFP	Rockland	Gilbertsville, PA	600-101-215	1:2500 (immunoblotting)
GFP	Chemicon International	Temecula, CA	AB16901	1:1000 (microscopy)
Calnexin	Stressgen Biotechnologies	Victoria, BC Canada	SPA-860	1:1000 (immunoblotting) 1:500 (microscopy)
Lamin	Paul Fisher, Southern University of New York	Stony Brook, NY	ADL 67 (242)	1:500 (microscopy)
ODV-E66	Max D. Summers, Texas A&M University	College Station, TX	ODV-E66 (148)	1:2500 (immunoblotting) 1:1000 (microscopy)

RESULTS

The essential features of the ODV-E66 sorting motif

To determine the essential features of the SM, fifteen E66 SM-GFP fusion proteins containing mutations within the SM sequence were constructed (Fig. 13). These fusions proteins were expressed under the IE1 promoter in uninfected insect cells and expressed under the polyhedrin promoter in infected insect cells. These SM fusions: 1) Mutated the aromatic a.a. to leucines; 2) Mutated the cysteine to leucine; 3) Removed the cluster of polar a.a.; 4) Removed the cluster of charged a.a. in the SM; 5) Removed the EGFP N-terminal charged a.a.; and/or 6) Shortened the SM transmembrane sequence. EGFP was altered to remove the N-terminal charged a.a. and is termed Alt. EGFP. Cells expressing these SM fusions were imaged using light confocal microscopy. Antibodies directed against the soluble endoplasmic reticulum (ER) protein, calreticulin, were used as a marker to identify ER, and the DNA stain, DAPI, was used to identify the nucleus. In addition, membrane association of the mutated SM-GFP fusions was assayed using Triton X-114 extraction. When expressed in uninfected cells, the SM fusion proteins pattern of localization allowed for the classification of each fusion into one of four groups. When the control GFP protein was expressed in Sf9 cells, it localized uniformly throughout the nucleus and the cytoplasm (Fig. 14). This pattern of localization allowed for the conclusion that the specific localization of the SM-GFP fusion

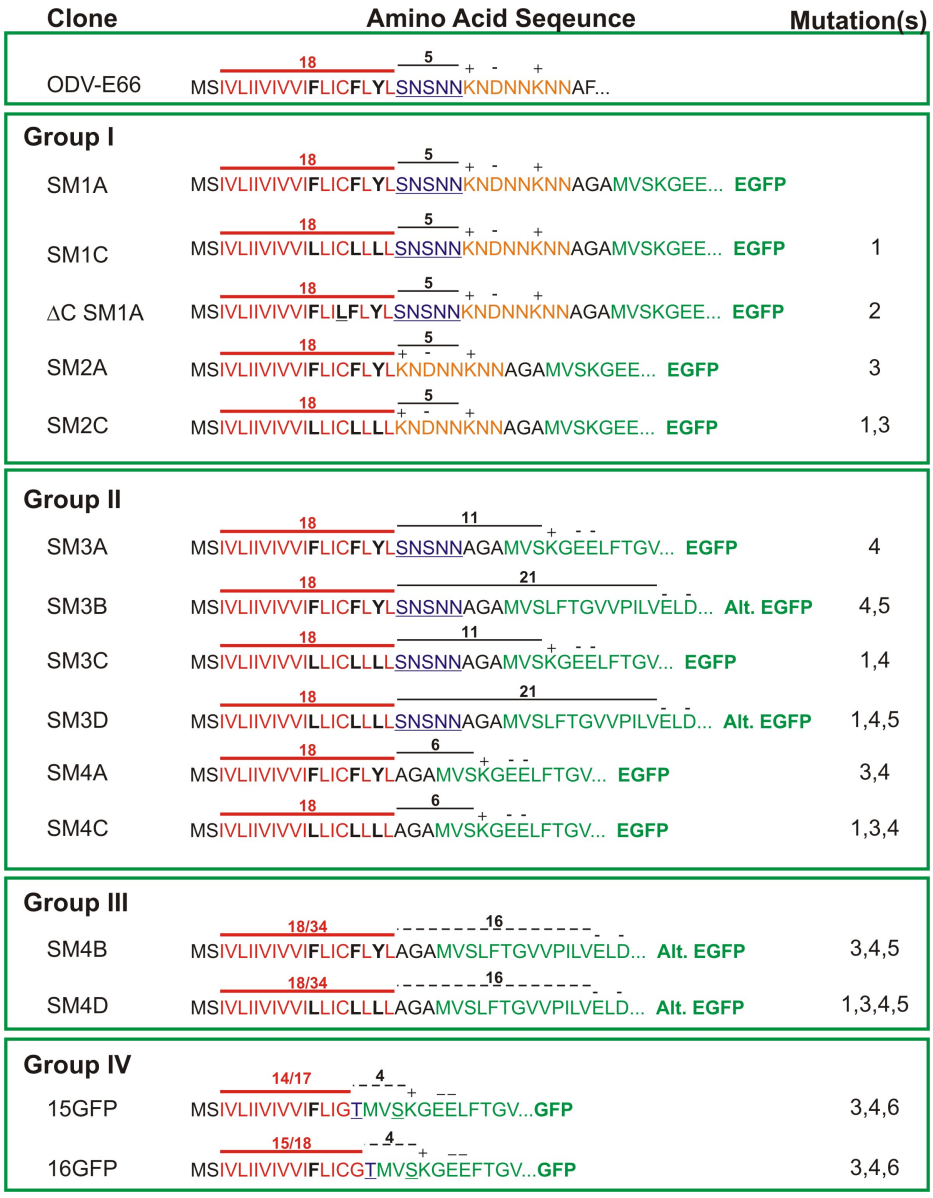

Figure 13. Fusion proteins generated to identify the minimal functional features of the ODV-E66 sorting motif. The TM sequence is denoted with a red bar and text, the aromatic a.a. are black and bolded, the polar a.a are blue and underlined, the C to L mutation of ΔC SM1A is black, bolded and underlined, and the GFP sequence is in green. Mutations within the clones are noted as follows: 1) Aromatic a.a. mutated to leucines; 2) Cysteine mutated to leucine; 3) Cluster of polar a.a removed; 4) Cluster of charged a.a. within the SM removed; 5) EGFP N-terminal charged region removed; and/or 6) SM transmembrane sequence shortened.

proteins could be attributed to the fused SM sequence(s).

When the WT SM sequence was fused to GFP (SM1A) and expressed in uninfected cells, it was detected colocalizing with the ER marker calreticulin and also showed a pronounced nuclear rim of fluorescence (Fig 14). This GFP fusion, and the GFP fusion proteins which showed a similar pattern of localization were all classified in Group I. These Group I fusion proteins included the SM fusions which mutated: 1) the aromatic amino acids to leucine; 2) the cysteine to a leucine; or 3) removed the polar amino acids of the SM. In each case the spacing from the C-terminus of the TM sequence to a charged amino acid remained 5 residues. The Group II SM fusion proteins were also detected colocalizing with calreticulin and showed a pronounced nuclear rim. However, the relative ratio of protein detected in the cytoplasmic membranes was higher in the cells expressing the Group II fusion proteins (Fig 15). These fusion proteins increased the distance from the C-terminus of the TM sequence to the first charged amino acid. Furthermore, in the case of SM3B and SM3D, the first charged amino acid was changed from a lysine to a glutamic acid. The Group III SM fusions showed no pronounced fluorescent nuclear rim, but instead these fusions were detected either in the plasma membrane (SM4B) or in the ER (SM4D) (Fig. 16). These fusion proteins likely increased the length of the TM sequence and changed the first charged amino acid from a lysine to a glutamic acid . The Group IV SM fusion proteins also showed no fluorescence rimming the nucleus but instead were detected only colocalizing with the ER

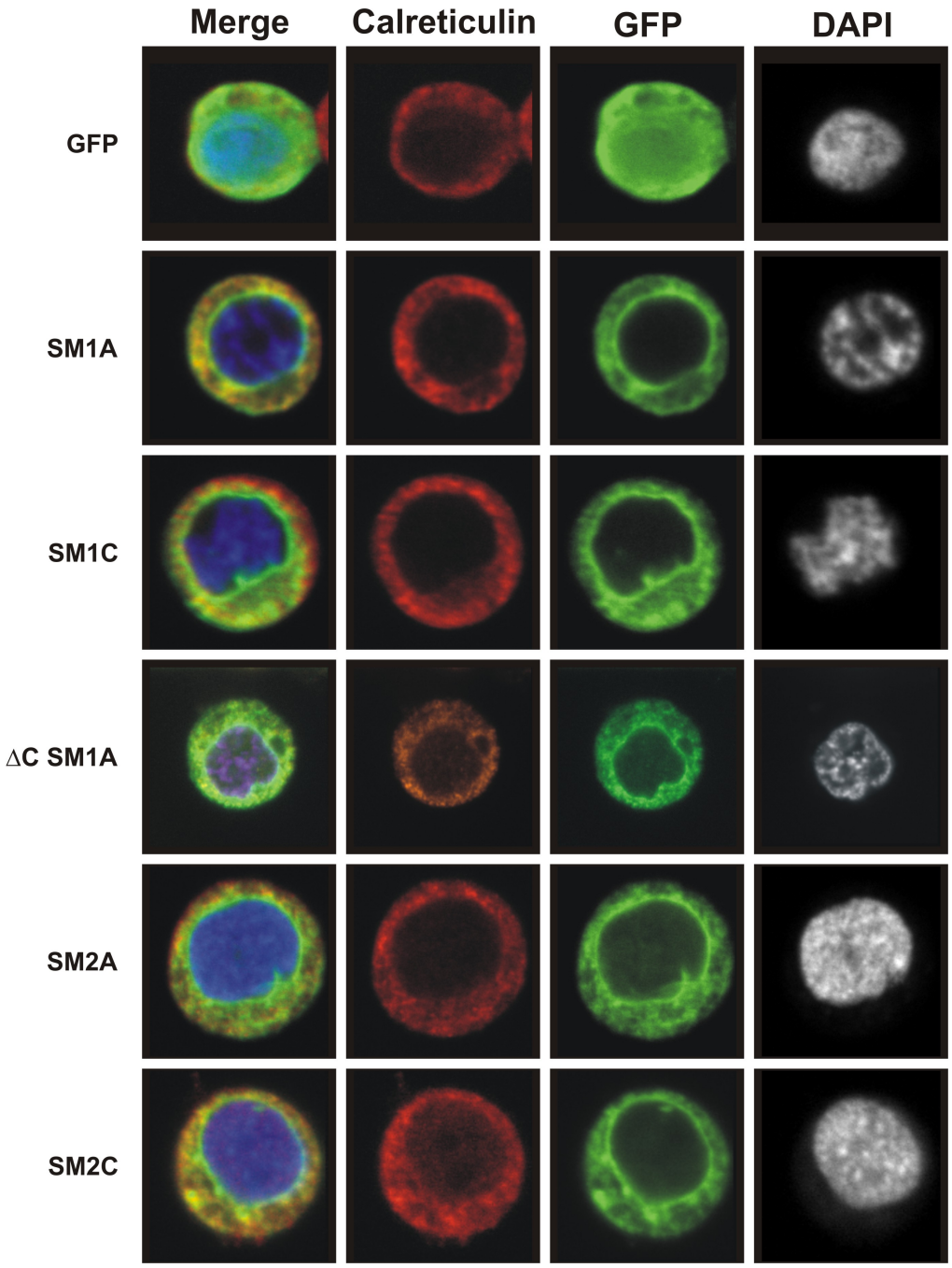

Figure 14. Confocal microscopy images of the Group I SM-fusion proteins expressed in uninfected Sf9 cells. Calreticulin is shown as red, the GFP fusion is shown as green, DAPI is shown as white, and a merge of the three images is shown as "merge," with the DAPI image re-colored blue for contrast.

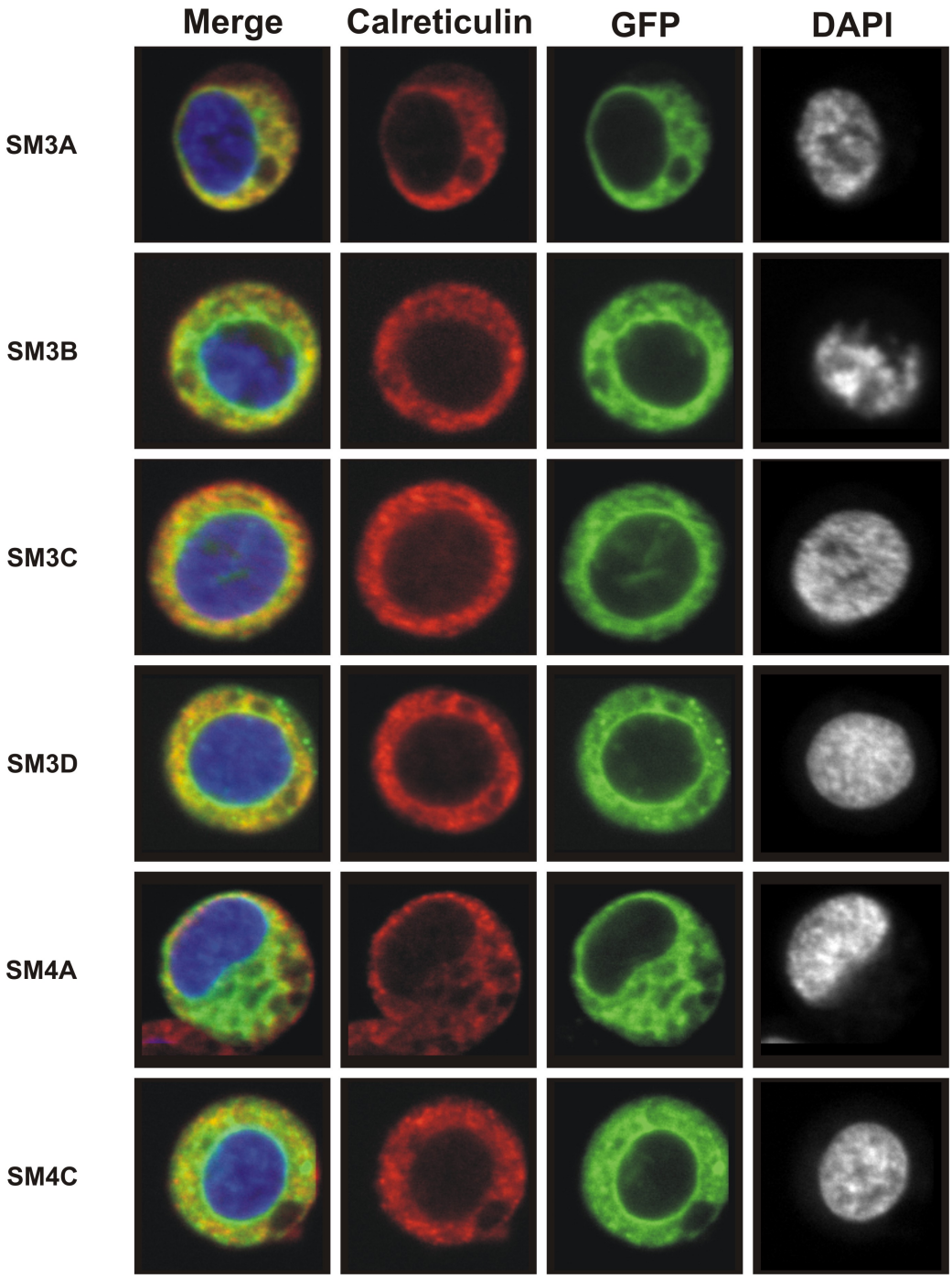

Figure 15. Confocal microscopy images of the Group II SM-fusion proteins expressed in uninfected Sf9 cells. Calreticulin is shown as red, the GFP fusion is shown as green, DAPI is shown as white, and a merge of the three images is shown as "merge," with the DAPI image re-colored blue for contrast.

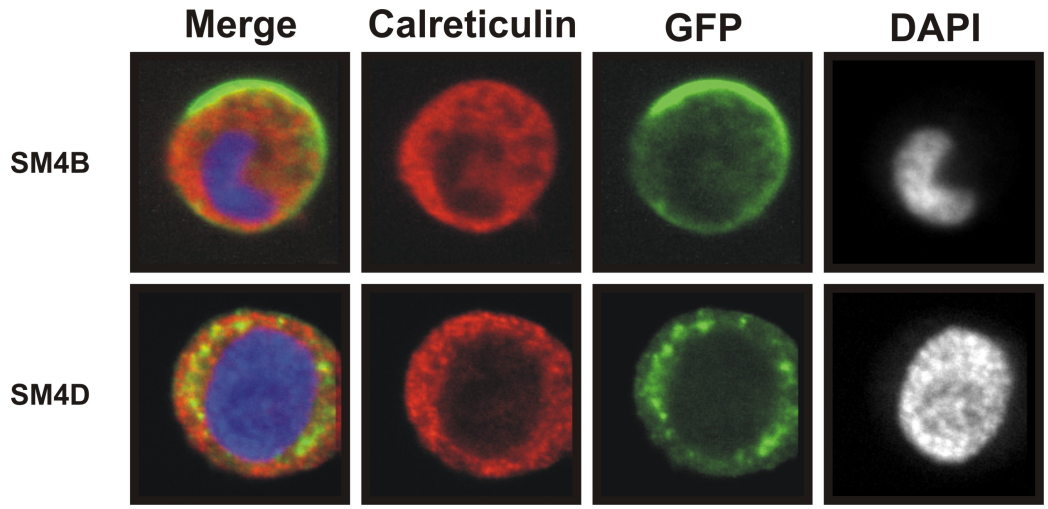

Figure 16. Confocal microscopy images of the Group III SM-fusion proteins expressed in uninfected Sf9 cells. Calreticulin is shown as red, the GFP fusion is shown as green, DAPI is shown as white, and a merge of the three images is shown as "merge," with the DAPI image re-colored blue for contrast.

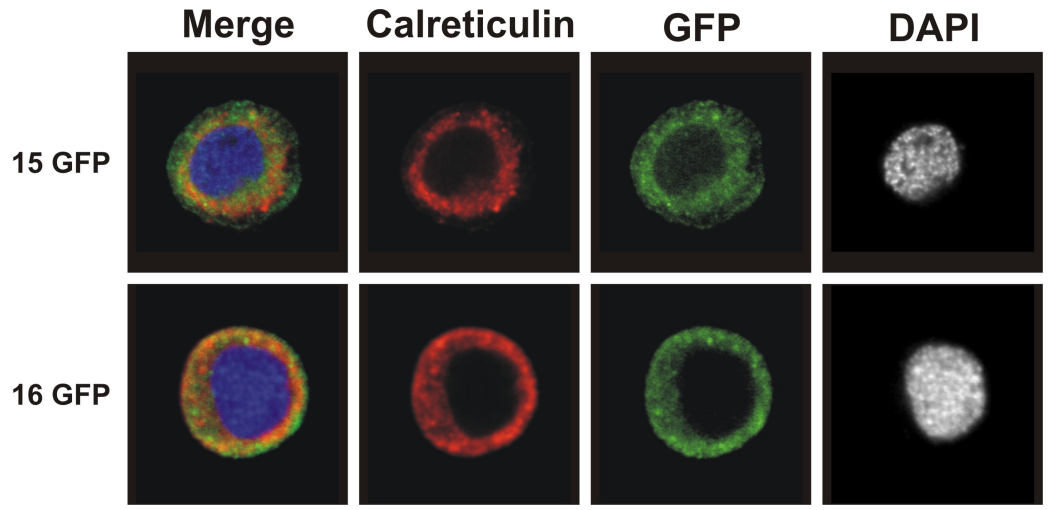

Figure 17. Confocal microscopy images of the Group IV SM-fusion proteins expressed in uninfected Sf9 cells. Calreticulin is shown as red, the GFP fusion is shown as green, DAPI is shown as white, and a merge of the three images is shown as "merge," with the DAPI image re-colored blue for contrast.

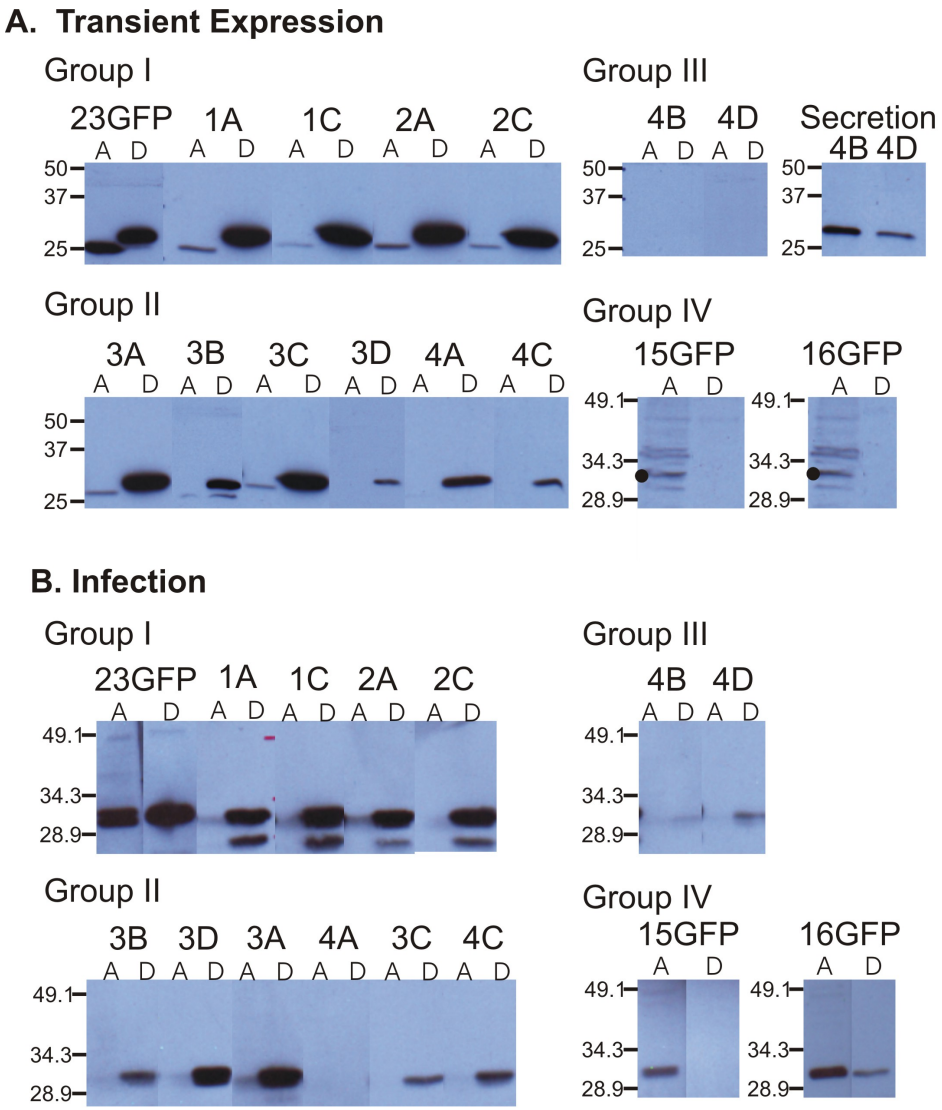

Figure 18. Triton X-114 extraction studies. A.) Triton X-114 extraction of uninfected cells expressing the modified SM fusion proteins. B.) Triton X-114 extraction of infected cells expressing the modified SM fusion proteins. The modified SM fusions were detected on western blot using GFP antibodies. For each designation, "A" represents the aqueous phase from the extractions, and "D" represents the detergent phase. "Secretion" in panel A shows the results from an immuno-precipitation of the media from transfected cells using GFP antibodies from rabbit, and detected using GFP antibodies from goat. These film images were cropped and reordered to show the data in a logical sequence. No data was omitted by cropping.

marker (Fig.17). These fusion proteins were mutated to include polar amino acids in the TM sequence, and shortened the distance from the C-terminus of the TM sequence to the first charged amino acid.

Extraction of cells with Triton X-114 fractionates the proteins into either an aqueous or detergent phase. Proteins that fractionate in the aqueous phase are likely soluble or peripheral membrane proteins, while proteins that fractionate with the detergent phase are likely integral membrane proteins. Since this extraction procedure uses physiological concentrations of salt, peripheral membrane proteins that interact with an integral membrane protein via electrostatic interactions may fractionate with the integral membrane proteins. The results of the Triton X-114 extractions of uninfected cells expressing the SM fusions showed the Group I and II fusion proteins fractionated in the detergent phase (Fig. 18A) suggesting these fusions were integral membrane proteins. The Group IV fusion proteins fractionated in the aqueous fraction (Fig. 18A, see dot) suggesting they were peripheral membrane proteins. The Group III fusion proteins were not detected in the extraction assays. Immuno-precipitation of the culture media from cells expressing the Group III fusion proteins with GFP antibodies showed that these fusion proteins were secreted (Fig. 18A).

The results from uninfected cells show that the aromatic a.a., the cysteine within the TM sequence and/or the polar a.a. did not significantly influence the accumulation of the SM-fusions in the NE. However, altering the distance from the C-terminal end of the TM sequence to the first charged amino acid, and/or

changing the first charged amino acid from a residue with a net positive charge to one with a net negative charge altered the relative ratio of protein detected in the cytoplasmic membranes versus that detected in the nuclear rim. Furthermore, altering the length or chemical character of the TM sequence may also alter the localization of the SM-GFP fusion protein. Therefore, these results showed that the essential features of the SM required for NE localization in uninfected cells (defined by a pronounced fluorescent nuclear rim) are a TM sequence of 18 amino acids (lacking polar and charged a.a.) with a cluster of charged a.a. spaced 5 residues from the end of the TM sequence (Fig. 19).

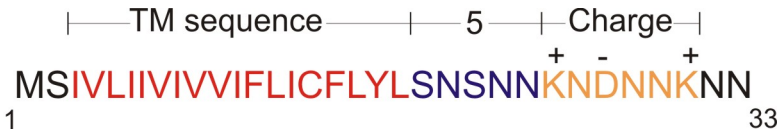

Figure 19. The essential features of the SM as determined by expression and detergent extraction studies in uninfected cells.

These SM fusions were also expressed during infection. Localization was determined using light confocal microscopy and association with the membranes (integral or peripheral) was determined using Triton X-114 extractions. In infected cells expressing the SM fusion proteins, lamin antibodies (Adl67) were used to show the boundary of the nucleoplasm, and the DNA stain, DAPI, was used to identify DNA enriched regions within the nucleus.

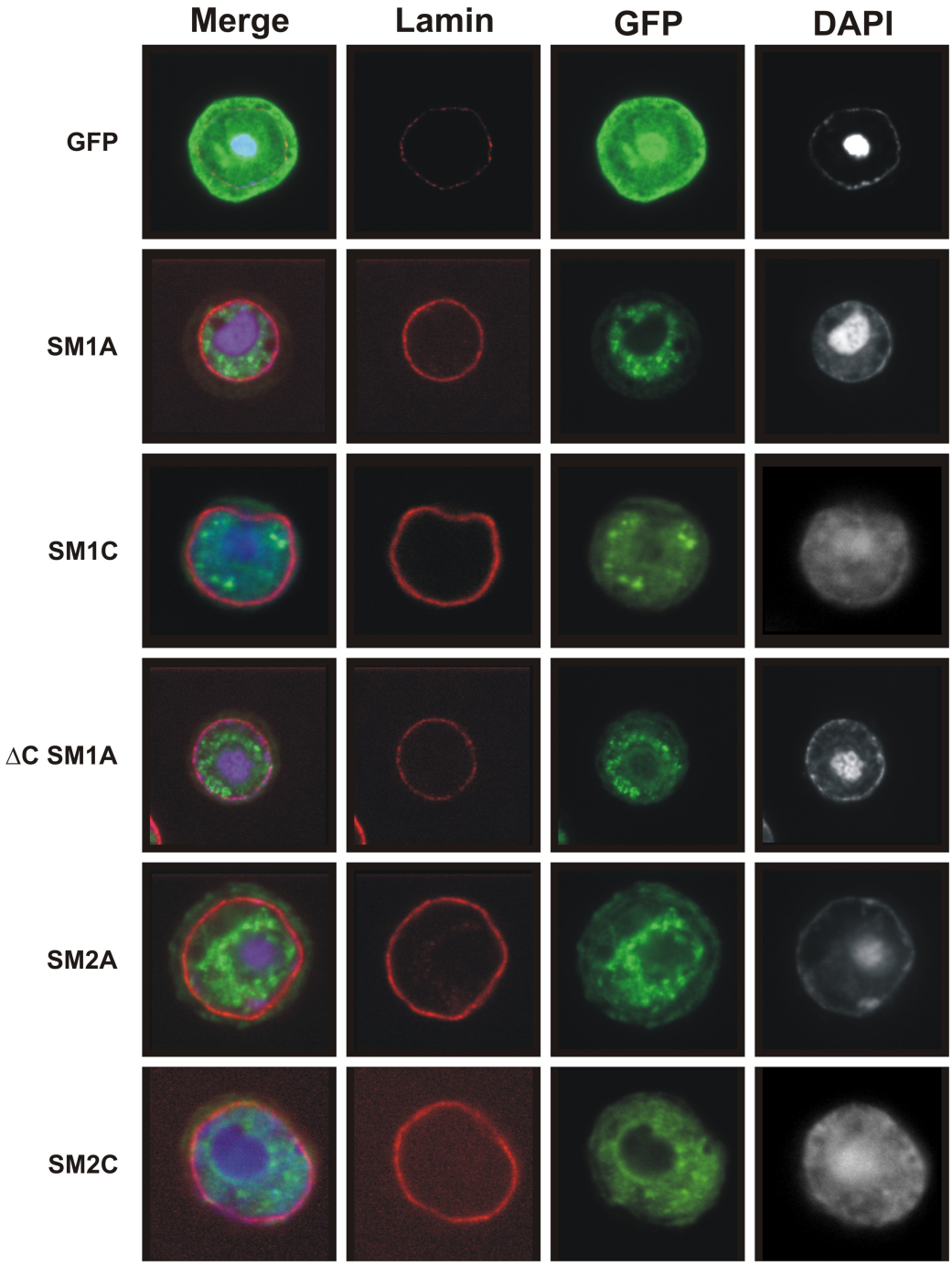

Figure 20. Confocal microscopy images of the Group I SM-fusion proteins expressed in infected cells. Lamin is shown as red, the GFP fusion is shown as green, DAPI is shown as white, and a merge of the three images is shown as "merge," with the DAPI image re-colored blue for contrast.

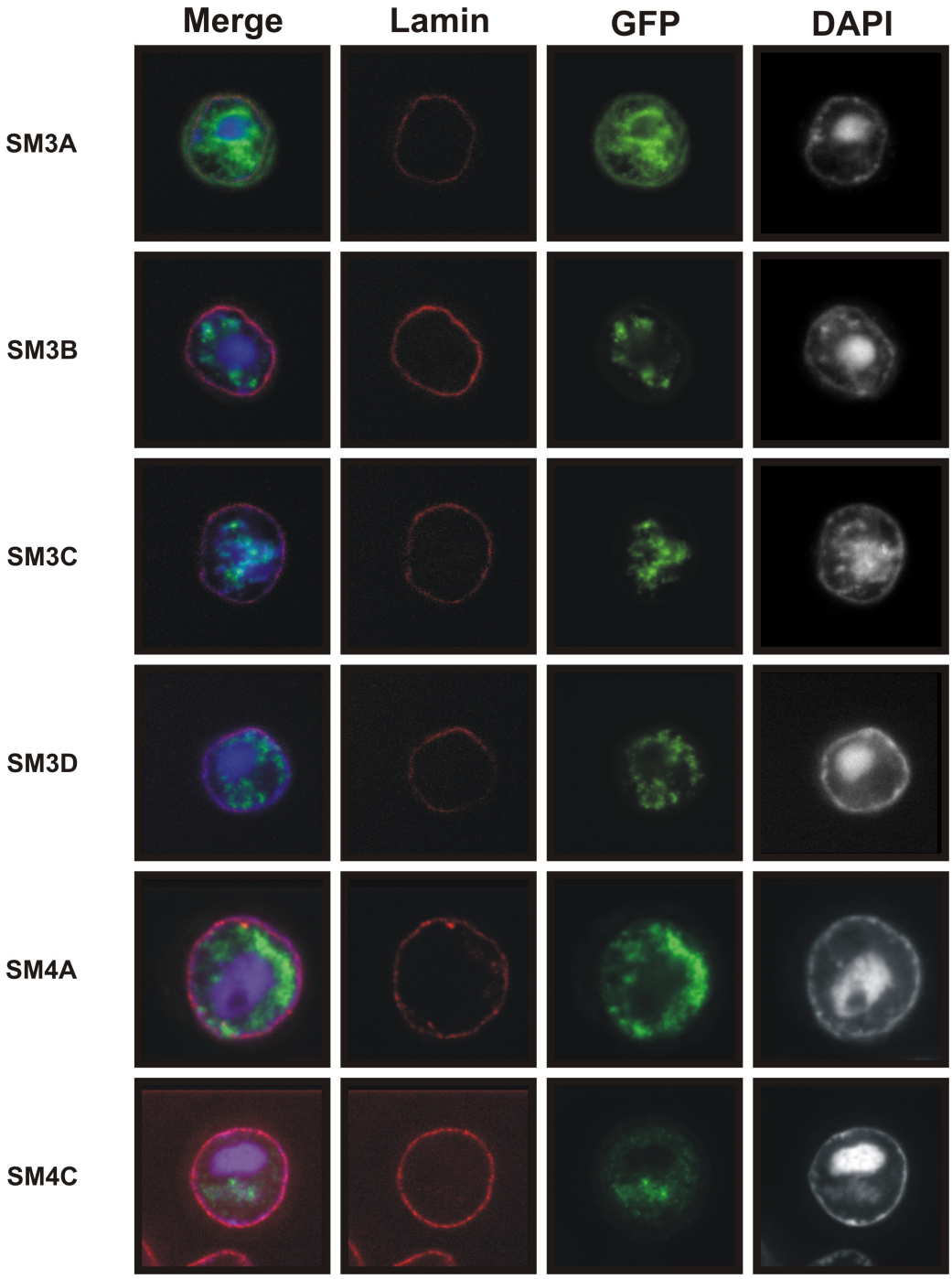

Figure 21. Confocal microscopy images of the Group II SM-fusion proteins expressed in infected cells. Lamin is shown as red, the GFP fusion is shown as green, DAPI is shown as white, and a merge of the three images is shown as "merge," with the DAPI image re-colored blue for contrast.

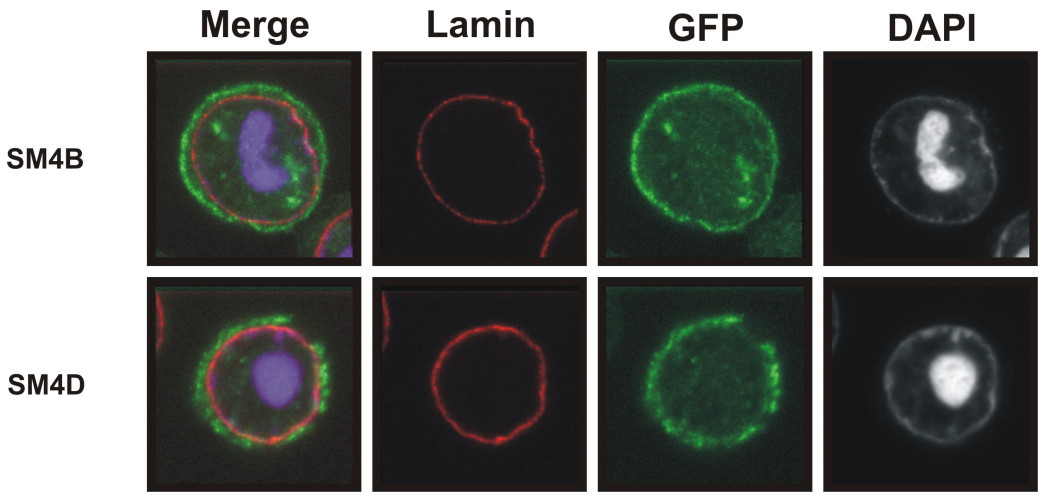

Figure 22. Confocal microscopy images of the Group III SM-fusion proteins expressed in infected cells. Lamin is shown as red, the GFP fusion is shown as green, DAPI is shown as white, and a merge of the three images is shown as "merge," with the DAPI image re-colored blue for contrast.

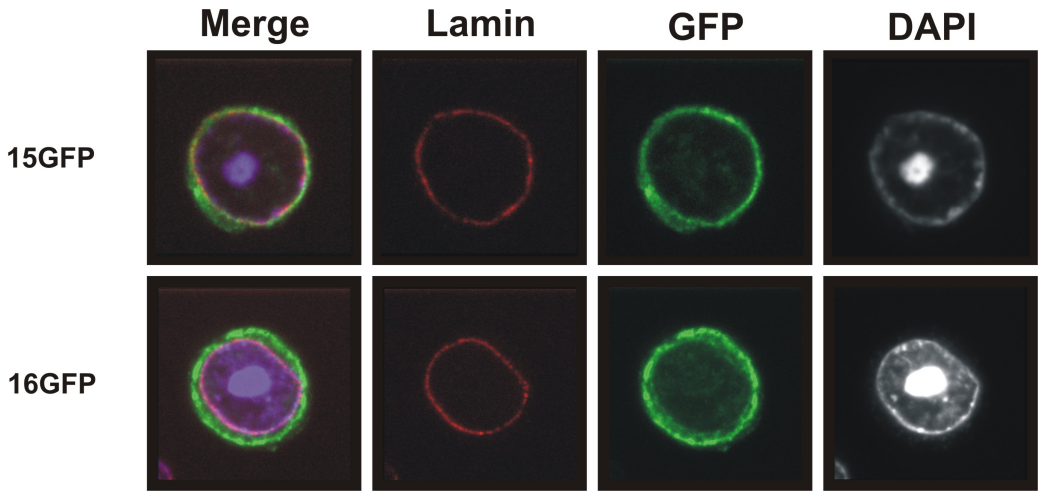

Figure 23. Confocal microscopy images of the Group IV SM-fusion proteins expressed in infected cells. Lamin is shown as red, the GFP fusion is shown as green, DAPI is shown as white, and a merge of the three images is shown as "merge," with the DAPI image re-colored blue for contrast.

The Group I and Group II GFP fusion proteins showed similar fluorescent patterns in infected cells; the proteins were detected within the nucleus. The fluorescent patterns were similar to those reported for ODV envelope proteins and/or SM-GFP (148, 152). This pattern of localization suggested the Group I and II SM fusion proteins localized in the viral-induced intranuclear microvesicles and ODV envelopes (Fig. 20, 21). Triton X-114 extraction data showed that these fusion proteins fractionated mostly with the detergent phase, therefore, suggesting the Group I and II fusion proteins were integral membrane proteins (Fig 18B). In infected cells, the Group III fusion proteins were detected mostly in the cytoplasmic membranes (Fig. 22) with some protein detected in the nucleus. For the two Group III fusion proteins, the majority of the protein fractionated with the detergent phase suggesting that the Group III fusions were integral membrane proteins (Fig. 18B). Since the Group III fusion proteins were readily detected in the cytoplasmic membranes of infected cells, studies to determine if these proteins were secreted during infection were not conducted. The Group IV proteins also localized mostly in the cytoplasmic membranes of the infected cells (Fig 23). The Group IV fusion proteins fractionated mostly in the aqueous phase when extracted with Triton X-114 (Fig. 18B), suggesting that they were peripheral membrane proteins.

The features of the SM required for localization within the nucleus of infected cells were apparently different than the features required for NE

localization in uninfected cells. When the Group I and Group II SM-GFP fusion proteins were expressed in infected cells, there was no detectable difference in the localization patterns between the Group I and Group II proteins. These data suggest that altering the distance to the first charged a.a. did not alter the ability of the SM to direct the GFP fusion proteins to the nucleus. The Group III and Group IV fusion proteins were detected mostly in the cytoplasmic membranes, suggesting that altering the length and/or the chemical character of the TM sequence of the SM did alter the ability of the SM to direct proteins to the nucleus. Combined, these results suggest that during infection the characteristics of the TM sequence of the SM may be the most important feature of the SM.

The role of the charged a.a. within the E66 SM

To further characterize the role of the charged a.a. within the E66 SM, a series of mutations were designed to mutate one or more of the charged a.a. of the SM in full length ODV-E66 (Fig. 24). These mutations changed the selected charged residue(s) to: 1) Alanine; 2) A different a.a. with the same net charge (i.e. K to R); or 3) An a.a. with an opposite net charge (i.e. K to D or D to K). These mutated ODV-E66 sequences were cloned into pIE1 for expression in uninfected Sf9 cells. These experiments were designed such that the differences in the localization of the mutated ODV-E66 would be determined by light confocal microscopy using ODV-E66 antibodies (Ab). In the initial experiments, the E66 Ab could not detect the mutated E66 by confocal

Figure 24 Sorting motif charge mutations within ODV-E66. Mutations of the protein sequence within the SM's cluster of charged a.a. constructed within ODV-E66. Altered a.a. are noted in bold.

microscopy. Furthermore, wild type E66, expressed as a control, was also not detected (data not shown). This indicated that insufficient levels of E66 were produced in transfected cells. Previous studies of a viral protein, FP25K, showed that when the *FP25K* gene is deleted from the viral genome, the translation of E66 during infection is significantly decreased (118) suggesting FP25K may regulate translation of E66. In an effort to boost the translation levels of the E66 in transfected cells, *FP25K* and the wild type or the mutated *E66* were co-transfected into Sf9 cells. FP25K was detected in these cells, however E66 was still not expressed at detectable levels (data not shown). These results suggest that even though the *IE1* promoter is recognized and utilized by the cellular machinery in uninfected cells, E66 translation is possibly regulated by unknown factor(s) during viral infection. As a consequence, these studies could not be completed.

Another approach to determine where proteins containing mutations within the charged a.a. of the SM were sorted was attempted. DNA constructs which coded the first 125 a.a. of E66 (with and without the mutations) fused to GFP were generated (Fig. 25) and expressed transiently in Sf9 cells. When these constructs were transfected into Sf9 cells, the GFP fusion proteins were not expressed at detectable levels (data not shown). Since GFP fusion proteins containing the first 33 a.a. of E66 were expressed at detectable and the GFP fusion proteins containing the first 125 a.a. of E66 were not, it is likely that the a.a. sequence between residues 33 and 125 is important for regulating E66 translation. Since these studies were designed to investigate the role SM charged a.a. in sorting and localization to the INM, the lack of expression in uninfected cells prohibited these studies from being completed. The studies

Figure 25. Charge mutated E66-GFP fusion proteins. Modifications of the protein sequence within SM charged cluster of a.a. constructed within GFP fusion proteins of the first 125 a.a. ODV-E66. Altered a.a. are noted in bold.

using the first 33 a.a. of the SM indicated that the spacing between the TM and the charge a.a. was an important feature of the SM for sorting to the NE in uninfected cells. Further characterization of the charged a.a. was not pursued.

The essential features of the E66 SM are conserved in the cellular INM protein, lamin B receptor

The N-terminal 238 a.a. of LBR are sufficient for localization and accumulation of a GFP fusion ($_{1\text{-}238}$LBR-GFP) to the INM and/or nuclear envelope (NE) of mammalian (199) and plant (219) cells. This region of LBR (Fig. 26) encodes a N-terminal, 200 a.a. nuclear ligand-binding sequence and the first TM sequence. The nuclear ligand-binding sequence binds lamin B (205, 206), DNA (206), chromatin (207), and the chromatin binding protein, HP1 (208). Binding of these immobilized nucleoplasmic components is believed to be responsible for the sorting and retention of LBR in the INM. In addition to the nuclear ligand-binding sequence, the N-terminal 238 a.a. of LBR also contains a SM-like sequence (a.a. 200-238) with chemical characteristics similar to the E66

Figure 26. Amino terminal 238 a.a. of lamin B receptor.

SM (Fig. 26; Braunagel et al. (119) for review). Since the SM features are apparently conserved in LBR, a study was done comparing the sorting and localization of the E66 SM-GFP fusion with the $_{1\text{-}238}$LBR-GFP fusion. To

determine if the SM-like region of LBR could sort proteins to the INM in the absence of the retention domain, two additional LBR-GFP fusions were included in the comparison: $_{200\text{-}238}$LBR-GFP lacked the nuclear ligand-binding sequence, and $_{208\text{-}238}$LBR-GFP lacked the binding sequence and the nucleoplasmic charged a.a. of LBR (Fig. 27).

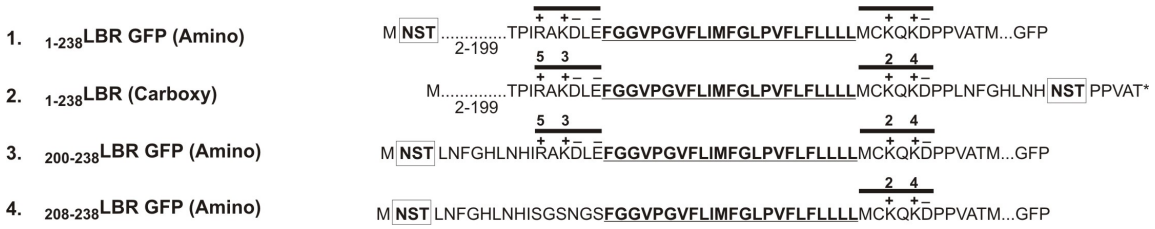

Figure 27. LBR-fusion proteins used for orientation studies. Schematic of the LBR protein sequences and fusions used in the *in vitro* glycosylation assays.

Orientation of the LBR-fusion proteins. Immobilization and retention of LBR via binding to nucleoplasmic components requires that the LBR nuclear ligand-binding sequence be oriented within the nucleoplasm. Since the subsequent experiments were designed to compare the sorting in both insect and mammalian cells, orientation of the LBR GFP fusion proteins was tested to determine if these proteins had the same orientation in each cell type.

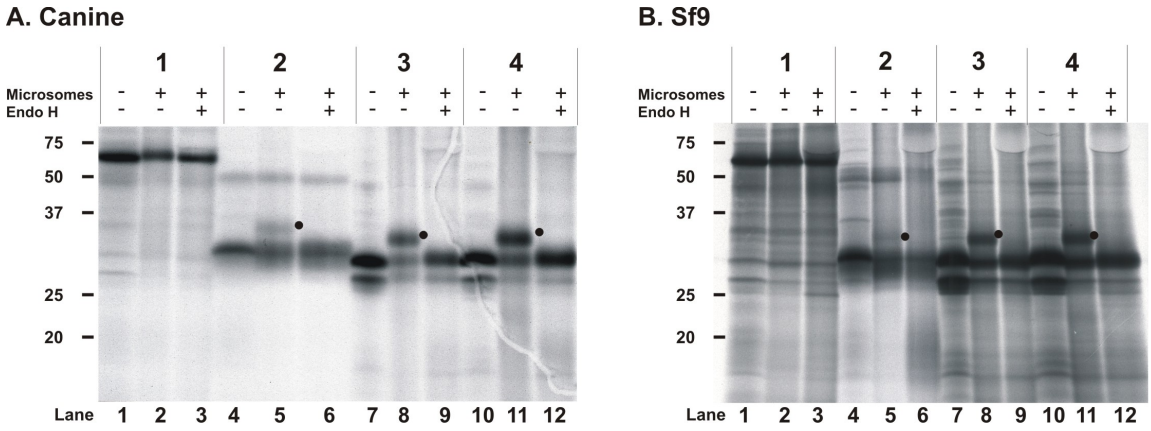

Figure 28. Autoradiographs of SDS-PAGE gels from the orientation studies. A.) Glycosylation assay results from experiments conducted in canine derived microsomal membranes. B.) Glycosylation assay results from experiments conducted in Sf9 derived microsomal membranes. Dots represent glycosylated protein.

Orientation was determined using an *in vitro* glycosylation assay (321, 322). Briefly, mRNAs encoding LBR-fusion proteins with either an engineered amino- or carboxy-terminal consensus glycosylation acceptor sequence, NST, (Fig. 27) were translated, *in vitro*, with or without microsomal membranes. Following translation, one membrane reaction was treated with endoglycosidase H. The translated proteins were analyzed by SDS-PAGE and autoradiography. These experiments were performed using microsomal membranes derived from either canine pancreas or Sf9 cells.

When the NST sequence was placed at the amino terminus of $_{1\text{-}238}$LBR-GFP (Fig. 27; #1), no change in relative mobility (M_r) was observed (Fig. 28A; lanes 1-3). However, when the NST was placed at the carboxy terminus of $_{1\text{-}$

$_{238}$LBR (Fig. 27; #1), a band with a higher M_r was detected, consistent with glycosylation was observed (Fig. 28A; lanes 4-6). Treatment with endoglycosidase H reversed the shift, indicating the higher M_r form was due to the addition of high mannose type oligosaccharides . These data indicate the amino terminus of $_{1-238}$LBR-GFP is oriented on the cytoplasmic side of the microsomal membranes. An endoglycosidase H sensitive band was observed when either $_{200-238}$LBR-GFP or $_{208-238}$LBR-GFP, with an amino-terminal NST, were assayed (Fig. 28A, lanes 7-12). Thus, the orientation of $_{200-238}$LBR-GFP and $_{208-238}$LBR-GFP is opposite of the $_{1-238}$LBR-GFP; the amino terminus of both fusion proteins is oriented on the lumenal side of the microsomal membranes, the same orientation as reported for the E66 SM (119). Orientation assays using microsomal membranes derived from Sf9 cells showed the same results as the canine derived membranes (Fig. 28B). Protease protection assays

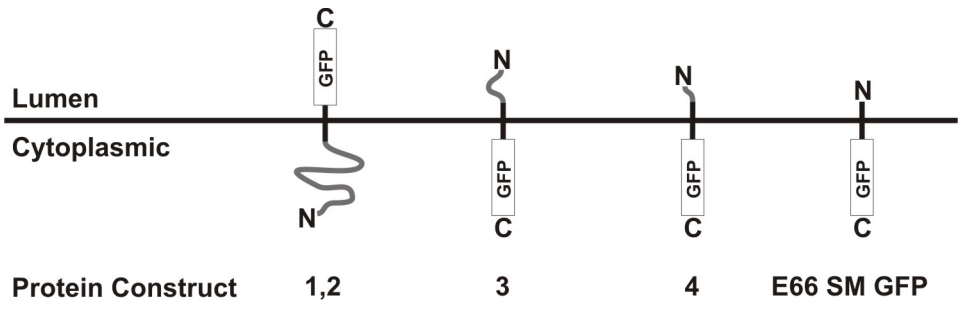

Figure 29. **Orientation of LBR- and SM-fusion proteins**. Orientation as predicted by the site-directed glycosylation and protease protection assays.

confirmed the results of the glycosylation experiments (data not shown). These studies showed that the amino terminal 208 a.a. of LBR are oriented in the cytoplasm (nucleoplasm) in both mammalian and insect cell membranes (Fig. 29). When the amino terminal 200 a.a. of LBR was removed, the first TM sequence of LBR adopted the opposite orientation (Fig. 29). This result suggests that the determinants for the orientation of the first TM sequence of LBR may be within the first 200 a.a. of LBR.

Localization of LBR- and SM-GFP fusion proteins in mammalian and insect cells. Studies of several cellular INM proteins suggest accumulation in the INM requires a nucleoplasmic binding sequence to immobilize or reduce the mobility of the protein via binding to immobilized nuclear ligands or other resident INM proteins (198-200, 231). However, these cellular INM proteins also contain sequences similar to the E66 SM (119). To investigate whether the SM or SM-like sequences are sufficient for accumulation of LBR in the INM, three LBR-fusion proteins and the E66 SM-GFP (Fig. 30) were expressed in CHO-K1 and uninfected Sf9 cells.

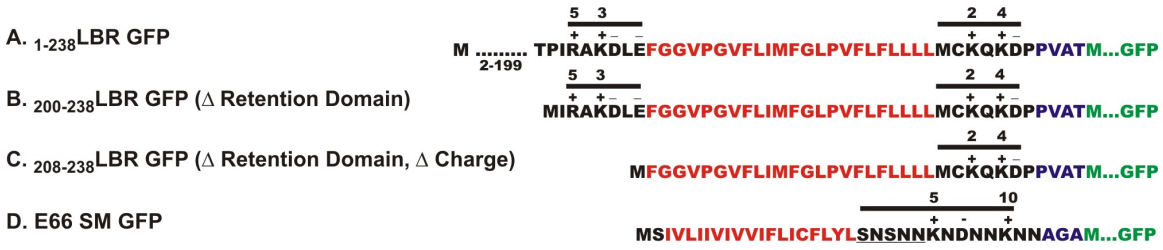

Figure 30. LBR- and SM-GFP fusion proteins used in CHO and Sf9 expression studies.

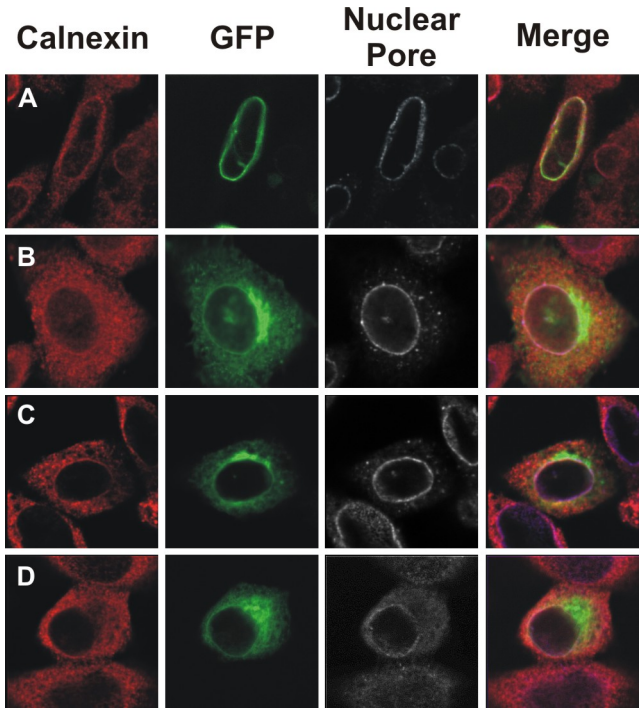

Figure 31. Confocal microscopy images of the GFP-fusion proteins expressed in CHO-K1 cells. Rows A-D are defined by the fusion proteins A-D in Figure 30. Each image represents a single z axis section through the center of the nucleus. Calnexin (red) and mAb414 (white) antibodies were used to label the ER and nuclear pores respectively. The auto-fluorescence of the GFP fusion is shown as green. The merge column shows the three labels overlaid with the nuclear pores re-colored as blue.

When expressed in CHO-K1 cells, $_{1\text{-}238}$LBR-GFP showed a pronounced nuclear rim of fluorescence (Fig. 31A). This pattern is consistent with the results observed by Ellenberg et al. (199). When expressed in Sf9 cells, the $_{1\text{-}238}$LBR-GFP showed a prominent rim of fluorescence around the nucleus as well as being detected within cytoplasmic membranes (Fig. 32A).

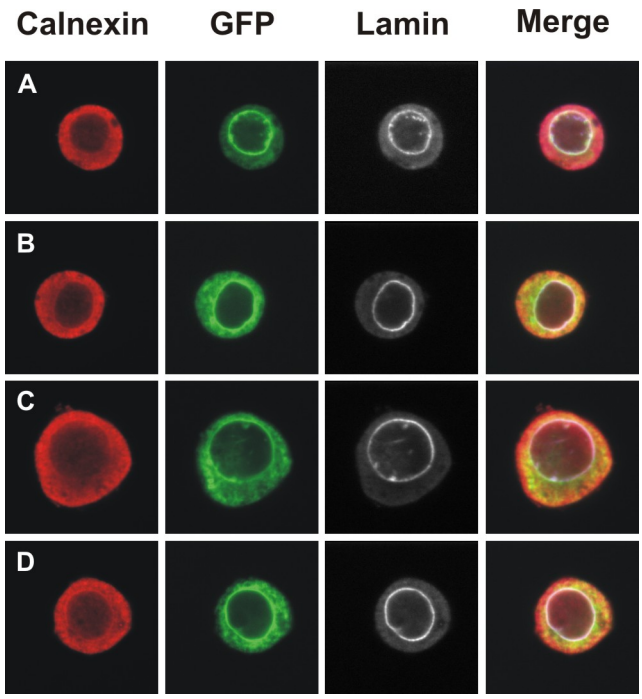

Figure 32. Confocal microscopy images of the GFP-fusion proteins expressed in uninfected Sf9 cells. Rows A-D are defined by the fusion proteins A-D in Figure 30. Calnexin (red) and Adl67 (white) antibodies were used to label the ER and nuclear lamin respectively. The auto-fluorescence of the GFP fusion is shown as green. The merge column represents the three images overlaid with the lamin re-colored as blue.

To determine if the SM-like region of LBR was sufficient to direct GFP fusions to the INM, two additional LBR fusion proteins, $_{200\text{-}238}$LBR-GFP and $_{208\text{-}238}$LBR-GFP (Fig. 30), were constructed and expressed in both CHO-K1 and SF9 cells. The $_{200\text{-}238}$LBR-GFP lacks the nucleoplasmic 200 a.a. nuclear ligand-binding sequence of LBR, and $_{208\text{-}238}$LBR-GFP lacks both the binding sequence

as well as the charged a.a. on the amino terminal side of the TM sequence. When expressed in CHO-K1 cells, $_{200\text{-}238}$LBR-GFP or $_{208\text{-}238}$LBR-GFP (Fig. 31B, 31C), showed: 1) significant localization and accumulation in a subset of ER membranes juxtaposed to the NE; 2) distinct nuclear rimming; and 3) diffuse localization throughout ER membranes. When expressed in Sf9 cells (Fig 32B, 32C), the two LBR-fusions showed a pronounced rim of fluorescence around the nucleus as well as localization throughout the ER membranes (co-localization with calnexin). The prominent rim of fluorescence around the nucleus exhibited by these two LBR-fusions expressed in uninfected Sf9 cells suggests that accumulation in the NE does not require a nuclear ligand-binding sequence and that the SM-like sequence of LBR is sufficient to concentrate membrane proteins in the NE, with a pattern similar to the E66 SM.

The E66 SM-GFP lacks identifiable sequences that bind immobilized nuclear ligands. When expressed in CHO-K1 cells (Fig. 31D), the SM-GFP localization pattern was indistinguishable from the $_{200\text{-}238}$LBR- and $_{208\text{-}238}$LBR-GFP fusions. In Sf9 cells (Fig. 32D), SM-GFP exhibited a pronounced nuclear rim of fluorescence as well as fluorescence in cytoplasmic membranes.

The results of $_{200\text{-}238}$LBR-GFP, $_{208\text{-}238}$LBR-GFP and SM-GFP expression and localization in CHO-K1 and Sf9 cells show that SM or SM-like sequences are sufficient for membrane protein accumulation in or around the NE (as determined by an observed pronounced nuclear rim of fluorescence) in both

mammalian and insect cells. However, when $_{1-238}$LBR-GFP was expressed in either CHO-K1 or Sf9 cells, a larger proportion of the total protein is apparently localized in NE, suggesting that the LBR nuclear ligand-binding sequence may contribute to the relative amount of protein accumulating in the NE.

Nuclear envelope proteins and viral envelope proteins are sorted separately at the INM during viral infection. Recombinant viruses expressing the LBR-GFP and SM-GFP (Fig. 30) fusions under the AcMNPV polyhedrin promoter were used to investigate whether LBR-GFP fusion proteins containing SM-like sequences are sorted differently from the E66 SM fusion during infection. Localization of the GFP fusion was determined using light confocal microscopy at 48 (Fig. 33) and 72 h p.i (data not shown). As reported, the E66 SM-GFP fusion (Fig 30D) co-localized with the viral envelope protein E66, showing this fusion accumulates in the viral-induced intranuclear microvesicles (Fig. 33D) and ODV envelopes (data not shown) during infection (119, 152). The three LBR-GFP fusion proteins (Fig. 30A, 30B, 30C) were detected in both the NE and ER membranes during infection (Fig. 33A, 33B, 33C), although a minimal amount of $_{1-238}$LBR-GFP was also detected in the nucleus of infected cells. These data suggest two possibilities: 1) sorting events induced by infection distinguish the E66 SM sequence from the cellular SM-like sequences in the INM, effectively excluding the cellular SM sequences from sorting to viral induced microvesicles and viral envelopes; or 2) the LBR fusions are immobilized at the INM.

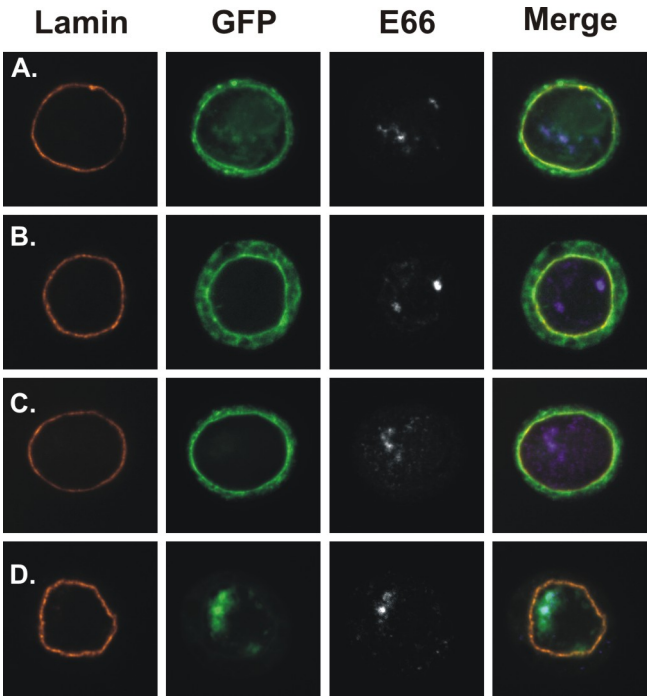

Figure 33. Confocal microscopy images of the GFP-fusion proteins expressed in infected Sf9 cells. The fusion proteins in rows A-D (defined by the fusion proteins A-D in Figure 30) were expressed during infection under the polyhedrin promoter. Infected cells were imaged confocally at 48 h p.i. and a representative z-axis section from the center of the nucleus shown. Adl67 (red) anti-bodies and E66 (white) were used to label the nuclear lamin and the ODV-E66, respectively. GFP auto-fluorescence is represented as green. The merge column represents the three images overlaid, with E66 re-colored as blue.

Localization of proteins to the INM does not require nuclear ligand-binding sequences

While nuclear rimming is considered indicative of protein localization in the NE, it may not necessarily specify if the protein is in the outer, inner, or both membranes of the NE. By immunoelectron microscopy, Ellenberg et al. (199) shows that the nuclear rimming of $_{1\text{-}238}$LBR-GFP expressed in COS-7 cells

represents protein localization in the INM. Several studies use a digitonin permeabilization assay combined with antibody accessibility/detection to determine that a pronounced nuclear rim of fluorescence represents localization of a specific integral membrane protein in the INM [Emerin: Ostlund et al. (200); MANI: Wu et al. (231); Lap I, Maison et al. (220)]. When used at low concentrations, digitonin selectively permeabilizes the plasma membrane without permeabilizing the NE. Therefore, in digitonin permeabilized cells, antibodies will only have access to epitopes that are extracellular or exposed within the cytoplasm (319). Thus, protein localization in the INM can be determined by comparing confocal immuno-localization patterns of digitonin permeabilized cells to either auto-fluorescence patterns in the same cell, or immuno-localization patterns in Triton X-100 permeabilized cells.

Cellular markers were used as internal controls to determine verify the validity of the digitonin permeabilization assay. In CHO-K1 cells, antibody to calreticulin was used as a marker for the ER lumen. Antibody to the cytoplasmic segment of calnexin, an integral membrane protein of the ER, will have equal access to the epitope in digitonin and Triton X-100 permeabilized cells. As expected, in digitonin permeabilized CHO-K1 cells, calreticulin was not detected (Fig. 34A1a); whereas, calreticulin was detected in TX-100 permeabilized cells (Fig. 34A2a). Calnexin was detected in CHO-K1 cells permeabilized with either digitonin or Triton X-100 (Fig. 34A1b, 34A2b). In Sf9 cells, antibody (Adl67) to the insect lamin, Dm_0, were used as a marker for the nucleoplasmic lamina. In

digitonin permeabilized cells the nuclear envelope is intact, and the lamin epitopes are not accessible to antibody, however in Triton X-100 permeabilized cells the nuclear envelope is permeabilized, and therefore the antibody will have access to the lamin epitope. Antibody to the cytoplasmic segment of calnexin (ER) was also used in Sf9 cells. In digitonin permeabilized Sf9 cells, Adl67 did not detect the insect lamina (Fig. 34B1), but did detect the lamina in Triton X-100 permeabilized Sf9 cells (Fig. 34B2). Antibody to calnexin detected the protein in the ER of both digitonin and Triton X-100 permeabilized Sf9 cells. These data verified that the conditions used for digitonin permeabilization in both CHO-K1 and Sf9 cells were suitable.

The N-terminus of $_{1\text{-}238}$LBR-GFP is exposed to the cytoplasm, placing GFP in the lumen of the ER/NE (Fig. 28). Therefore the GFP is not accessible to antibodies in digitonin permeabilized cells. To detect $_{1\text{-}238}$LBR-GFP, a T7 epitope tag was engineered at the N-terminus of $_{1\text{-}238}$LBR GFP (Fig. 34C). In digitonin permeabilized CHO-K1 cells, T7$_{1\text{-}238}$LBR-GFP was not detected by the T7 Ab when expressed at average levels (Fig. 34A1a). However, GFP auto-fluorescence showed a pronounced rim around the nucleus. T7$_{1\text{-}238}$LBR-GFP was detected with T7 Ab in the ER of CHO-K1 cells that expressed high levels of the GFP fusion (Fig. 34A1b). The GFP autofluorescence showed a pronounced rim of fluorescence around the nucleus and detected the T7$_{1\text{-}238}$LBR-GFP

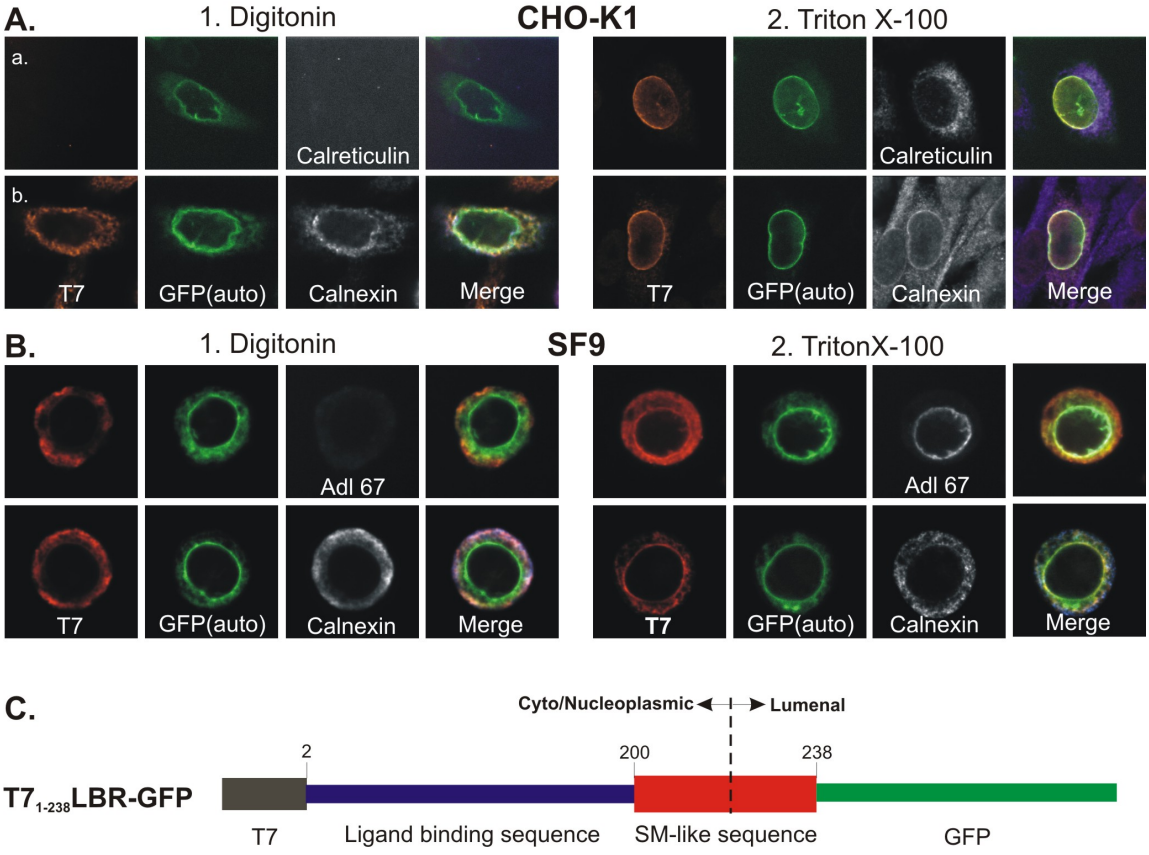

Figure 34. Digitonin permeabilization of cells CHO-K1 or Sf9 cells expressing $_{1\text{-}238}$LBR-GFP. (A) The T7$_{1\text{-}238}$LBR-GFP fusion expressed in CHO-K1 cells. Digitonin or Triton X-100 permeabilized cells were imaged confocally with a representative z-axis section from the center of the nucleus shown. T7 (red) anti-bodies were used to label the fusion protein and calreticulin (white, top panel) or calnexin (white, bottom panel) antibodies were used to label the ER. GFP auto-fluorescence is shown as green. The merge column shows the three images overlaid with calreticulin or calnexin re-colored as blue. Cells expressing low levels of $_{1\text{-}238}$LBR-GFP are shown in row (a). Cells expressing high levels of $_{1\text{-}238}$LBR-GFP are shown in (b). (B) The $_{1\text{-}238}$LBR-GFP fusion expressed uninfected in Sf9 cells, permeabilized and imaged as in panel A. Adl67 (white, top panel) or calnexin (white, bottom panel) antibodies were used to label the lamin or ER, respectively. The merge column shows the three labels overlaid with Adl67 or Calnexin re-colored as blue. (C) Schematic drawing of the T7$_{1\text{-}238}$LBR-GFP fusion.

protein in the ER, when expressed at high levels. Conversely, in Triton X-100 permeabilized CHO-K1 cells, the T7 Ab co-localized with the GFP autofluorescence (Fig. 34A2a, 34A2b) in the nuclear rim and in the ER. Therefore, consistent with the published data (199), the pronounced nuclear rim of $_{1\text{-}238}$LBR-GFP represented protein accumulation in the INM of CHO-K1 cells. In digitonin permeabilized Sf9 cells expressing T7$_{1\text{-}238}$LBR-GFP, the T7 Ab only detected fusion protein in the ER (Fig. 34B1). The GFP auto-fluorescence showed this LBR-fusion accumulating with a pronounced rim of fluorescence around the nucleus and accumulating in the ER (Fig. 34B2). In Triton X-100 permeabilized Sf9 cells, both the T7 Ab and the GFP auto-fluorescence showed T7$_{1\text{-}238}$LBR-GFP accumulating with both a fluorescent nuclear rim pattern and in the ER. Therefore, in Sf9 cells, the results from transient expression studies demonstrated that the nuclear rimming observed for $_{1\text{-}238}$LBR-GFP represented accumulation in the INM.

SM-GFP orientation studies (119) determined the GFP is oriented toward the cytoplasm/nucleoplasm. Therefore, in the permeabilization assay, GFP antibody was used to detect the SM-GFP. In digitonin permeabilized Sf9 cells, GFP antibody detected SM-GFP in the ER, whereas the auto-fluorescence showed the both a fluorescent nuclear rim and fluorescence in the ER (Fig. 35A1). In Triton X-100 permeabilized Sf9 cells, the GFP antibody and GFP auto-fluorescence showed the SM-GFP fluorescence in the ER and rimming the nucleus (Fig. 35A2). These patterns of fluorescence localization showed that

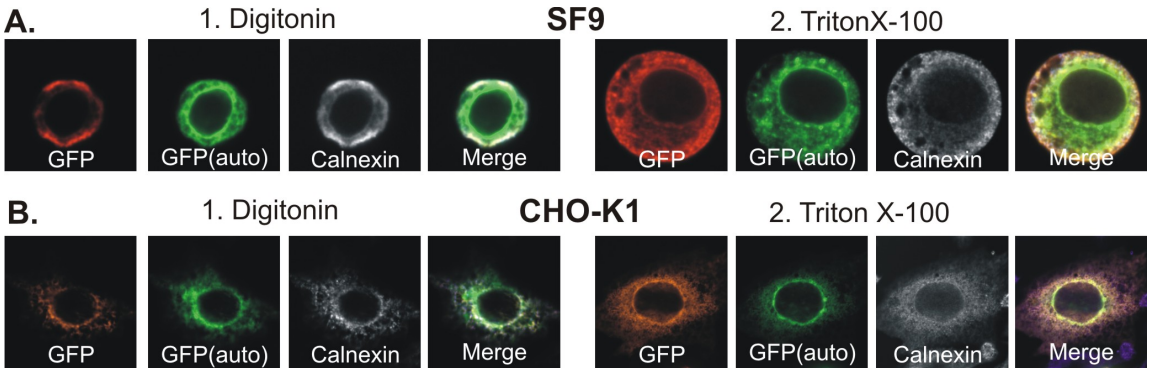

Figure 35. Digitonin permeabilization of CHO-K1 and Sf9 cells expressing the SM-GFP. The SM-GFP fusion expressed in: A.) Sf9 cells or B.) CHO-K1 cells. 1.) Digitonin or 2.) Triton X-100 permeabilized cells were imaged confocally with a representative z-axis section from the center of the nucleus shown. GFP (red) anti-bodies were used to label the fusion protein and calnexin (white) antibodies were used to label the ER. GFP auto-fluorescence is shown as green. The merge column shows the three images overlaid with calreticulin or calnexin re-colored as blue.

the SM-GFP pronounced nuclear rim of fluorescence represented protein accumulation in the INM of Sf9 cells. When expressed in CHO-K1 cells, SM-GFP was detected mostly in regions juxtaposed to the NE, however, a fluorescent nuclear rim was also observed. When CHO-K1 cells were permeabilized with digitonin, GFP antibody detected the protein in the ER membranes juxtaposed to the NE (Fig. 35B1). While in the digitonin permeabilized CHO-K1 cells there may be a minor portion of the SM-GFP in the nuclear rim that was not detected with the GFP antibody, the results were not able to demonstrate such localization.

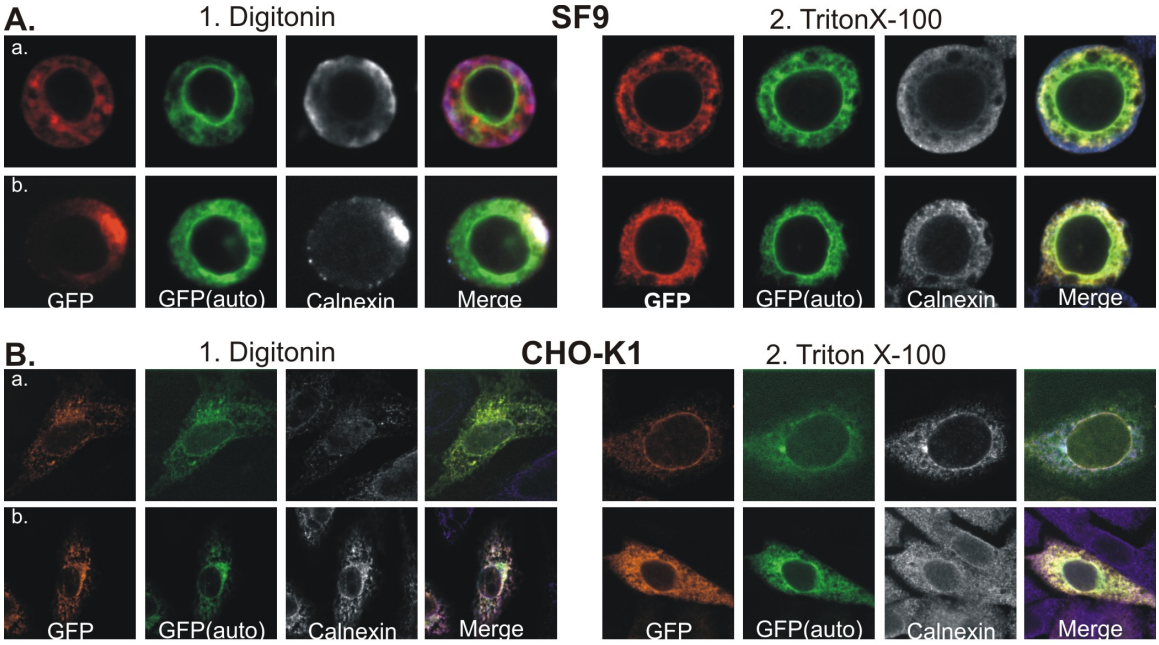

Figure 36. Digitonin permeabilization of CHO-K1 and Sf9 cells expressing the $_{200\text{-}238}$LBR- and $_{208\text{-}238}$LBR-GFP. The a.) $_{200\text{-}238}$LBR-GFP and b.) $_{208\text{-}238}$LBR-GFP fusions (Fig. 30) expressed in: A.) Sf9 cells or B.) CHO-K1 cells. 1.) Digitonin or 2.) Triton X-100 permeabilized cells were imaged confocally with a representative z-axis section from the center of the nucleus shown. GFP (red) anti-bodies were used to label the fusion protein and calnexin (white) antibodies were used to label the ER. GFP auto-fluorescence is shown as green. The merge column shows the three images overlaid with calreticulin or calnexin re-colored as blue.

Orientation studies showed that for $_{200\text{-}238}$LBR- and $_{208\text{-}238}$LBR-GFP fusion proteins, GFP is exposed to the cytoplasm. Therefore, GFP antibodies were used to detect these fusion proteins. In digitonin permeabilized Sf9 cells, the GFP antibody detected $_{200\text{-}238}$LBR- and $_{208\text{-}238}$LBR-GFP colocalized with the ER marker protein, calnexin. The GFP autofluorescence demonstrated a fluorescent nuclear rim and fluorescence in the ER (Fig. 36A1). In Triton X-100

permeabilized Sf9 cells, the GFP antibody and autofluorescence showed the fusion proteins in both the nuclear rim and the ER. These data suggest that the fluorescent nuclear rimming observed for these two fusion proteins represents protein accumulation in the INM of SF9 cells. When CHO-K1 cells expressing either LBR-fusion were permeabilized with digitonin, antibody to GFP detected the fusion proteins in the ER membrane juxtaposed to the NE (Fig. 36B1). Again, while there may have been some portion of the GFP fusions in the nuclear rim that was not detected with the GFP antibodies, the results from these two LBR-GFP fusions were not able to demonstrate such localization.

The results from the digitonin permeabilization studies of CHO-K1 cells expressing the SM-GFP, $_{200\text{-}238}$LBR- and $_{208\text{-}238}$LBR-GFP fusion were not able to demonstrate distinct localization in the INM. However, when these fusions were tested using digitonin permeabilization in Sf9 cells, the data clearly showed that these fusion proteins concentrate in the INM. Therefore, the Sf9 data suggests that protein accumulation in the INM is not necessarily dependent on the presence of a nuclear ligand-binding sequence and is likely mediated, in part, by SM or SM-like sequences.

Accumulation of proteins in the INM can be independent of immobilization

FRAP studies of four INM proteins show that the population of INM protein in the ER is mobile, while that population of protein in the INM is either immobile, or has significantly decreased mobility [Emerin: Ostlund et

al. (200), LBR: Ellenberg et al. (199), MANI: Wu et al. (231), and Nurim: Rolls et al. (198)]. The LBR- and SM-GFP fusions in this study accumulate in the INM when expressed in uninfected SF9 cells. Of these four fusion proteins, only the $_{1-238}$LBR-GFP convincingly accumulates in the INM of CHO-K1 cells. However Sf9 digitonin permeabilization studies of LBR-fusions lacking a nuclear ligand-binding sequence, as well as the SM-GFP, suggest that immobilization via direct binding of nucleoplasmic components is not necessary for sorting and accumulation of all INM proteins to the INM. However, one could argue that these proteins may be immobilized in the INM via interactions in the TM sequence. FRAP was used to determine if there were differences in the mobility of the LBR- or SM-GFP in the ER and the INM/NE when expressed in CHO-K1 or uninfected Sf9 cells. When $_{1-238}$LBR- GFP was expressed in the mammalian cell line, CHO-K1, results consistent with previous reports were obtained (199); the fusion was immobile in the INM and mobile in the ER (recovery profile: Fig. 37A; diffusion constant: Fig. 37C; CHO-K1). However, when $_{1-238}$LBR-GFP was expressed in Sf9 cells the ER and NE populations of this fusion protein were mobile and had similar recovery profiles (Fig 37B). There was no significant difference in the calculated diffusion constants (Fig 37C; Sf9). The $_{200-238}$LBR-GFP, $_{208-238}$LBR-GFP and the viral SM-GFP accumulated in the INM when expressed in uninfected SF9 cells, and in the ER membranes juxtaposed to the NE in CHO-K1 cells. For these proteins, FRAP studies determined that there

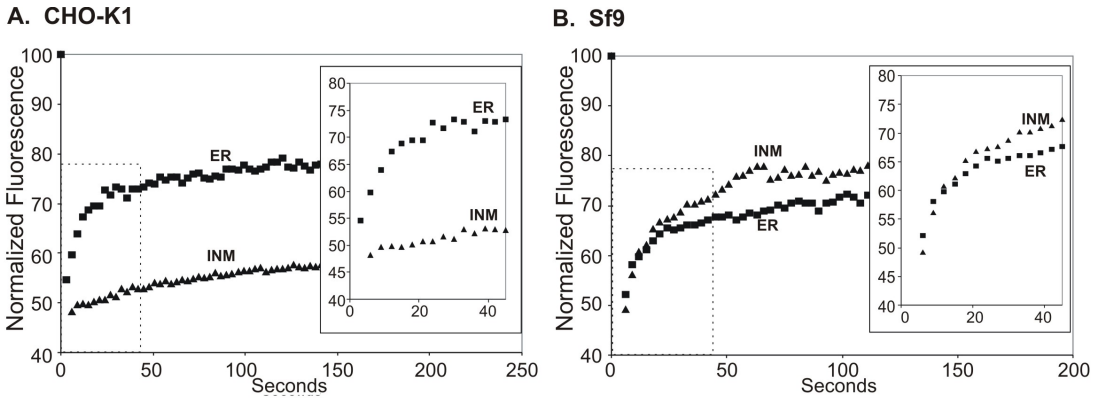

C. Diffusion Constants - ($\mu m^2/s$)

	CHO-K1		Sf9	
	NE/INM	ER	INM	ER
$_{1-238}$LBR GFP	**Immobile** (34)	**0.48** +/- 0.07, (42)	**0.73** +/- 0.07, (49)	**0.77** +/- 0.07, (47)
$_{200-238}$LBR GFP	**0.73** +/- 0.11, (25)	**0.98** +/- 0.13, (29)	**0.60** +/- 0.06, (44)	**0.91** +/- 0.11, (46)
$_{208-238}$LBR GFP	**0.42** +/- 0.05, (28)	**0.46** +/- 0.05, (24)	**0.56** +/- 0.08, (26)	**0.71** +/- 0.06, (28)
$_{1-33}$E66 GFP	**0.79** +/- 0.07, (38)	**0.62** +/- 0.06, (42)	**0.96** +/- 0.08, (50)	**0.92** +/- 0.07, (50)

Figure 37. Fluorescence recovery after photo bleaching. (A) A representative recovery profile of $_{1-238}$LBR-GFP expressed in the ER and INM of CHO-K1 cells. (B) Representative recovery profile of $_{1-238}$LBR-GFP expressed in the ER and INM of Sf9 cells. (C) Diffusion constants (D, $\mu m^2/s$) for the LBR and SM-GFP fusions in the ER and NE/INM of mammalian and insect cells. The fusion proteins were considered mobile if greater than 35% of the fluorescence recovered following photo-bleaching (4 minutes). Simple *t*-test (95% confidence interval) for the remaining assays showed the differences in D values in the NE and ER were not significant. Results are mean +/- std. error for (n) determinations.

was no significant difference in the calculated diffusion constants between the ER and NE/INM populations (Fig. 37C) of either CHO-K1 or Sf9 cells. Combined, the digitonin permeabilization and FRAP data obtained from SF9 cells suggest that sorting and accumulation of proteins to the INM can be independent of immobilization.

The pathway of trafficking proteins to nuclear membranes may be saturated during infection

When the LBR- or SM-GFP fusion proteins were abundantly expressed during infection, an unexpected result was noted; in cells expressing high amounts of E66, a proportion of E66 was detected in cytoplasmic membranes (Fig. 38). This result suggested that trafficking of E66 to the viral induced intranuclear membranes was delayed. One possible explanation for the delay in E66 trafficking is that the abundant SM or SM-like sequences were saturating unidentified factor(s) required for trafficking to nuclear membranes.

To determine if the observed qualitative differences in the localization of E66 were significant, the relative amounts of E66 and the SM-GFP or $_{1\text{-}238}$LBR-GFP in the cytoplasm, nuclear envelope, and intranuclear microvesicles were quantified and compared in wild type virus and recombinant viruses expressing either $_{1\text{-}238}$LBR-GFP or SM-GFP. A macro was written for the KS400 software package that allowed for quantitation of the amount of label localized in each cellular locale (Fig. 39D) as well as the area for each locale. For each label

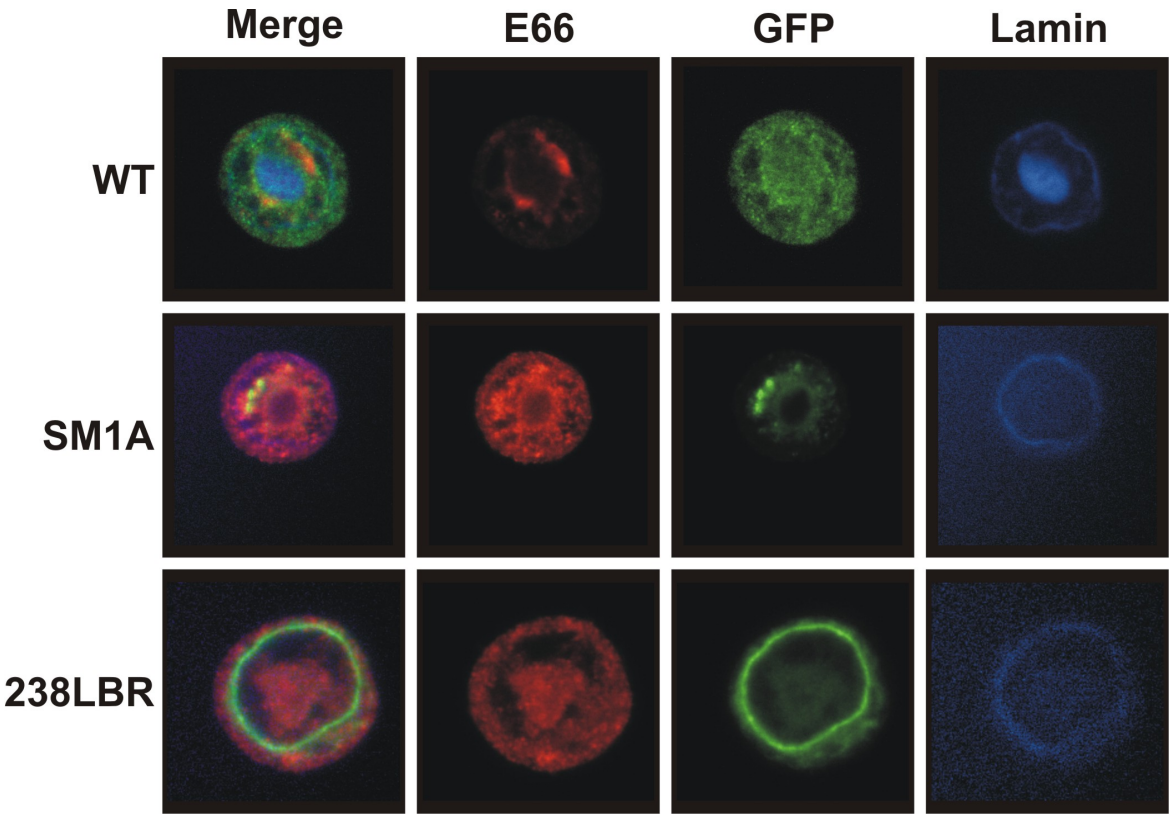

Figure 38. Representative confocal microscopy images from infected cells used in the quantitation assays. Representative images of confocal microscopy from infected cells (48 h pi.) of both wild type and recombinant viruses expressing high levels of ODV-E66. E66 (red) anti-bodies and Lamin (blue) were used to label the ODV-E66 and the nuclear lamin, respectively. GFP auto-fluorescence is represented as green. The merge column represents the three images overlaid.

quantified, a density ratio was calculated (% label/%area). The density ratios were normalized to 100%, and plotted on histograms.

Calnexin and Lamin were used as cellular controls. For calnexin, the histogram (Fig. 39A) showed that the majority of the label was detected within the cytoplasm of the infected cells. The histogram (Fig. 39A) for lamin shows

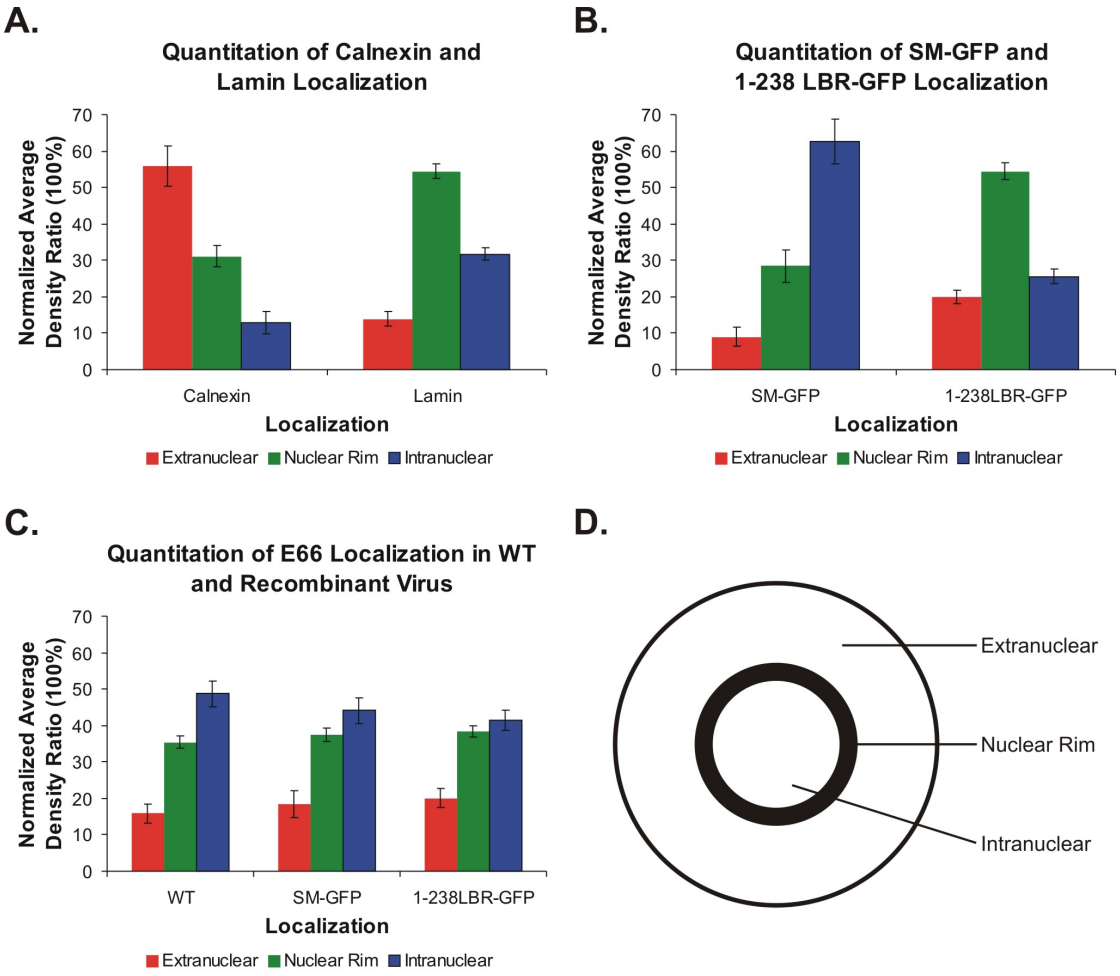

Figure 39. Histogram representation of quantified labels from each cellular compartment. A.) Histogram showing the density ratio of calnexin and lamin localization in each cellular compartment of wt infected cells (n=10). B.) Histogram showing the density ratio of SM-GFP or $_{1\text{-}238}$LBR-GFP localization in each cellular compartment of cells infected with the SM-GFP (n=7) or 1-238LBR-GFP (n=10) recombinant viruses. C.) Histogram showing the density ratio of E66 localization in each cellular compartment of cells infected with the WT (n=10), SM-GFP (n=7) or 1-238LBR-GFP (n=10) recombinant viruses. Histogram error bars represent standard deviation. D.) Pictorial representation of the three cellular compartments defined by the macro used for quantitation.

that the majority of the label is detected within the nuclear rim. This data is consistent with the expected and observed localization (data not shown) of each of these proteins. For the SM-GFP, the histogram (Fig. 39B) shows the majority of the label was localized within the nucleus. This localization is consistent with the microscopy data shown in Fig. 38. For the $_{1\text{-}238}$LBR-GFP, the histogram data showed the majority of the label was localized within the nuclear rim (Fig. 39B). Again, this is consistent with the observed localization shown on Fig. 38.

For the wt, SM-GFP, and $_{1\text{-}238}$LBR-GFP, the histogram (Fig. 39C) shows that the majority of the E66 label is localized within the nucleus. While an increase in the amount of E66 localization within the cytoplasm of cells infected with either the SM-GFP or $_{1\text{-}238}$LBR-GFP recombinant viruses were visually apparent (Fig. 38), the histogram of the quantified E66 localization in each locale showed these visual differences are either not significant or not quantifiable using the available software and/or macro. However, the histogram data does suggest a trend that indicates the amount of E66 excluded from the viral-induced intranuclear microvesicles increases as of amount of protein with SM or SM-like sequences in transit to nuclear membranes increases. This data suggests that the protein trafficking pathway to nuclear membranes may be a saturable process.

DISCUSSION

SM or SM-like sequences can mediate the sorting of integral membrane proteins to the INM independent of immobilization

The N-terminal 33 a.a. E66 sorting motif (SM) (Fig. 23) is sufficient to sort β-galactosidase and GFP fusion proteins to MV and ODV envelopes during infection. When abundantly expressed during infection, the SM-fusion proteins can also be detected in the INM, ONM and ER. These data suggest that SM-fusion proteins sort to the INM, MV and ODV envelopes using a trafficking pathway similar to that of resident INM proteins (152).

To investigate the essential features of the SM, selected mutations that removed or altered one or more of the predicted essential features of the SM were generated (Fig. 13). These mutant SM sequences were fused to GFP and expressed in both uninfected and infected Sf9 cells. The localization and membrane association of each mutant SM fusion was determined. Each of the mutant SM-GFP fusion proteins were classified into one of four groups based on their localization patterns when expressed in uninfected cells.

The Group I fusion proteins colocalized with the ER marker protein, calreticulin, formed a pronounced rim of fluorescence around the nucleus (Fig. 14) and fractionated as integral membrane proteins (Fig. 18). The mutations to the SM fusion proteins classified in this group included: 1. replacing the aromatic a.a. with leucine; 2. replacing the cysteine with leucine; 3. removing the polar

a.a. between the end of the TM sequence and the first charged a.a. In each case the distance between the end of the TM sequence and a positively charged a.a. remained five residues. The results from the Group I SM-fusion proteins suggest that the cysteine and the aromatic amino acids located within the TM sequence are not required for sorting of the SM to the NE of uninfected cells.

The mutations within the Group II SM-GFP fusion proteins all resulted in an increase between the end of the TM sequence and the first charged a.a. to 6 or more residues. Furthermore, the mutations in two of these fusion proteins (SM3B, SM3D) resulted in changing the first charged a.a. from a lysine to a glutamic acid. When expressed in uninfected cells, these mutant SM-GFP fusion proteins were also detected colocalizing with calreticulin and forming a pronounced rim nucleus (Fig. 15). However, the relative ratio of the protein localizing in the nuclear rim vs. the ER membranes decreased; the Group II fusion proteins did not form as strong of a nuclear rim as those in Group I. The Group II fusion proteins also fractionated as integral membrane proteins (Fig. 18). This data suggests that the distance between the end of the TM sequence and the first positively charged a.a. is important for sorting the SM to the NE.

The mutations in the Group III SM-GFP fusion proteins likely resulted in: 1. an increase in the length of the TM sequence from ~18 a.a. to ~34 a.a.; 2. shortening the distance from the end of the TM sequence to less than five a.a.; and 3. changing the first charged a.a. following the TM sequence from a lysine to a glutamic acid. When these mutant fusion proteins were expressed in

uninfected cells, they were detected in the cytoplasmic membranes or the PM (Fig. 16) and were secreted (Fig. 18).

The mutations in the Group IV SM-GFP fusion proteins resulted in: 1. introducing polar a.a. into the TM sequence; and 2. shortening the distance between the end of the TM sequence and the first positively charged a.a. When these fusion proteins were expressed in uninfected cells, the protein(s) accumulated in the ER, but did not concentrate in the NE (Fig. 17). Furthermore, fractionation studies showed that these fusion proteins did not fractionate as integral membrane proteins (Fig. 18). This data suggests that when the SM is only peripherally associated with the membranes, it is not sorted to the NE.

Therefore, the mutational analysis defined the following characteristics as essential features of the SM: 1. an integral membrane protein; 2. a TM sequence lacking polar or charged a.a.; and 3. a positively charged a.a. spaced 5 residues from the end of the TM sequence (Fig. 19). When these essential features of the SM are compared to sequences required for correct localization of either cellular INM or nuclear pore membrane proteins, the features are conserved (119).

When the E66 SM-GFP fusion protein (SM1A) was expressed during infection, the protein was detected in the viral induced intranuclear membranes (Fig. 20) with a pattern similar to that seen for ODV-E66 in cells infected with wt virus. When the Group I and II fusions were expressed in infected cells, the

patterns of localization all resembled that seen for the E66 SM-GFP fusion. This suggests that a 5 residue spacing between the end of the TM and the first positively charged amino acid is not essential in efficient sorting of the SM to the intranuclear membranes. When the Group III fusion proteins were expressed in infected cells, the majority of the protein was detected in the cytoplasmic membranes, although, some protein was also detected in the nucleus (Fig. 22). The Groups I, II, and III fusion proteins fractionated as integral membrane proteins in infected cells (Fig. 18). When the Group IV fusion proteins were expressed in infected cells, the proteins were detected in the cytoplasmic membranes surrounding the nucleus (Fig. 22), and fractionated as peripheral membrane proteins (Fig. 18). Therefore, these data suggest that the minimum requirements for sorting the SM to viral induced membranes were different than that required for sorting to the NE of uninfected cells. The nature of the differences in sorting the SM to the NE in the absence of infection vs. sorting to viral induced intranuclear membranes during infection was beyond the scope of this project.

Studies to further investigate the role of the charged amino acids in sorting proteins to the INM and/or MV and ODV envelope were initiated. These studies were designed to remove or change the chemical characteristics of the cluster of charged a.a. in E66. However, several attempts to express the mutant E66 proteins (or the first 125 a.a. fused to GFP) in uninfected cells were

unsuccessful. Further experiments to fully characterize the cluster of charged a.a. were not pursued.

Braunagel et. al. (119) shows that the essential features of the E66 SM are conserved in several INM proteins. To study the similarities and differences in the sorting of cellular INM proteins and the viral E66 SM to the NE, LBR was chosen as the protein for comparison. This study used a previously characterized LBR-GFP fusion protein, $_{1\text{-}238}$LBR-GFP, that contains the determinants for sorting, localization and retention of LBR in the INM (196, 199). The N-terminal 238 a.a. of LBR include a N-terminal 200 a.a nuclear ligand-binding sequence as well as a SM-like sequence (a.a. 200-238) with charged a.a. positioned on both sides of the TM sequence (Fig. 29). Consistent with published data (199), this LBR fusion concentrated in the INM when expressed in CHO-K1 cells (Fig. 34A). When $_{1\text{-}238}$LBR-GFP was expressed in uninfected Sf9 cells, the fusion protein also concentrated in the INM (Fig. 34B).

Previous reports suggest that concentration of LBR in the INM requires binding to immobilized nucleoplasmic components via the nuclear ligand-binding sequence (199) and/or the first TM sequence plus flanking a.a. residues on either side of the TM sequence (196). The first TM sequence of LBR, plus the flanking charged a.a. residues, have similar chemical characteristics to the a.a. sequence of the E66 SM (Fig. 6). Two LBR-fusion proteins, $_{200\text{-}238}$LBR-GFP and $_{208\text{-}238}$LBR-GFP were constructed and expressed to determine if the SM-like sequence of LBR was sufficient for sorting the fusion protein to the NE. The $_{200\text{-}}$

$_{238}$LBR-GFP lacked the nuclear ligand-binding sequence of LBR, and $_{200-238}$LBR-GFP lacked both the binding sequence and the charged a.a. on the N-terminal side of the TM. These LBR-GFP fusions were similar to the E66 SM-GFP in both chemical characteristics (Fig. 24) and membrane orientation (Fig. 23). When $_{200-238}$LBR-GFP, $_{208-238}$LBR-GFP and SM-GFP were expressed in uninfected Sf9 cells, all three fusion proteins were detected in the ER and the INM (Fig. 35, 36). However, when the fusion proteins expressed in CHO-K1 cells, the data showed the proteins were detected in the ER and membranes juxtaposed to the nucleus, but could not determine if these fusion proteins accumulated in the INM. However, the results from Sf9 cells are consistent with the hypothesis proposed in this study; accumulation of integral membrane proteins in the INM can be mediated by a SM or SM-like sequence.

FRAP was used to determine if there were differences in protein mobility in the ER and NE/INM when the LBR- and SM-GFP fusions were expressed in either CHO-K1 or Sf9 cells. When expressed in CHO-K1 cells, the $_{1-238}$LBR-fusion protein was immobilized in the INM and mobile in the ER (Fig. 37). This result was expected and is consistent with the reported results (199) and the diffusion:retention model. However, when expressed in Sf9 cells, the $_{1-238}$LBR-GFP INM and ER protein populations exhibited no significant difference in the calculated diffusion constant, which showed there was no decrease in mobility of $_{1-238}$LBR-GFP in the INM. This result was unexpected since the $_{1-238}$LBR-fusion localized in the INM of Sf9 cells and contains a binding sequence for the

immobilized nucleoplasmic components lamin B, DNA and/or chromatin (directly or indirectly). The only insect lamin proteins identified to date are the Dm_0 and Lamin C of *Drosophila* cells. *Drosophila* Dm_0 antibodies (Adl67) label the Sf9 lamina (Fig. 31) suggesting the lamins of *Drosophila* may be similar to those in Sf9 cells. While the Dm_0 lamin is considered to be a lamin B equivalent based on expression profiles in their respective species, the two proteins are different in sequence (326, 327). Therefore, it is possible the lamin B binding sequence of LBR does not recognize insect lamin. Despite the possible lack of lamin binding, it was surprising to find that this LBR fusion did not show at least a decreased mobility in the INM mediated by binding DNA and/or chromatin. If LBR did bind either DNA or chromatin in Sf9 cells, this binding was not sufficient to decrease the mobility of the protein in the INM. Mobility data from the two LBR fusions lacking the nuclear ligand-binding sequence, $_{200\text{-}238}$LBR-GFP and $_{208\text{-}238}$LBR-GFP, and from the SM-GFP fusion showed that when expressed in either CHO-K1 or uninfected Sf9 cells, these fusion proteins were mobile in both the NE/INM and the ER (Fig. 37). If diffusion:retention is the only mechanism of INM protein sorting and accumulation, one would expect these fusion proteins to have either a decreased mobility or no accumulation in the INM of Sf9 cells. However, the localization (Figs. 34-36) and FRAP data (Fig. 37) clearly show these proteins do concentrate in the INM of Sf9 cells, yet remain freely mobile.

Given the localization and mobility of the LBR and E66 SM fusions and the data demonstrating that the altered orientation of the truncated LBR fusions

(Fig. 26) did not inhibit accumulation in the INM of Sf9 cells, the results presented in this study suggests that sorting and localization of integral membrane proteins to the INM can be mediated by a SM or SM-like sequence that functions either independent of, or in addition to, immobilization.

Sorting of proteins to the INM can be a signal-mediated process regulated at various steps in the trafficking pathway

Recent reports, combined with the results of this study, support a hypothesis that the sorting of proteins to the INM can be regulated at several steps throughout the protein trafficking pathway and can be independent of diffusion and immobilization. The sorting and localization of membrane proteins to the INM can be regulated at 4 separate checkpoints: 1) co-translational integration in the ER (328); 2) trafficking through the ER and ONM to the nuclear pore (119); 3) trafficking from the ONM to the INM (118); and/or 4) sorting events within the INM that are independent of immobilization.

Co-translational integration in the ER. Saksena et al. (323) demonstrate that sorting of INM proteins may begin as early as co-translational integration into the ER. The authors report that viral (E66, E25) or cellular (LBR, Nurim) derived INM-directed TM sequences crosslink, *in vitro*, to the translocon proteins, Sec61α and TRAM. Furthermore, the authors shows that the INM-directed TM sequences of the viral and cellular proteins are in similar protein environments based on the surfaces of the TM sequences which crosslinked to either Sec61α or TRAM. The authors note that of the ten TM sequences tested, that are sorted

to sites other than the INM, only two crosslink to TRAM using photo-crosslinking methods. Furthermore, of the seven non-INM directed TM sequences that have been studied at high resolution (using probes on several surfaces of the TM sequence), none show a crosslinking pattern similar to the four INM-directed TM sequences studied. Therefore, based on the unique crosslinking pattern demonstrated by the viral and cellular INM-directed TM sequences, the authors propose that INM-directed TM sequences occupy a site in the translocon site that is unique when compared to TM sequences directed to other locations in the cell. These data indicate that sorting of some viral envelope and INM proteins may begin during co-translational integration through the ER translocon.

Trafficking through the ER and ONM to the nuclear pore. Published *in vivo* and *in vitro* protein crosslinking studies suggest that sorting of integral membrane proteins to the INM also may be regulated while the protein is trafficking through the ER/ONM to the INM. Braunagel et al. (119) shows that an E66 SM fusion protein can crosslink two viral proteins, FP25K and E26, when the SM fusion is in the ER. These data suggest that these viral proteins are proximal to SM in the ER and thus may be involved in facilitating the sorting of proteins with SM or SM-like sequences to the INM while the proteins are in the ER/ONM. The specific function of these two viral proteins in the trafficking process requires more direct proof and is currently under investigation. Additionally, studies to identify potential cellular homologues of the viral proteins

are currently underway (Saksena, Ding and Braunagel, personal communication).

Trafficking from the ONM to the INM. Published reports suggest that diffusion of proteins from the ONM to the INM requires that the cytoplasmic/nucleoplasmic domain of a protein must be less than 50 kDa to pass through the 10 nm peripheral channels of the nuclear pore (185, 206). However, the Nesprin family of INM proteins have nucleoplasmic domains that are up to one MDa in size, yet these proteins are detected in the INM (204). ODV-E66 has a nucleoplasmic domain larger than 50 kDa (~63 kDa) but accumulates in the INM derived MV and ODV envelopes during infection. Rosas-Acosta et al. (118) reports that when *FP25K* is deleted from the AcMNPV viral genome, ODV-E66 is detected in clusters in the ONM and does not sort to MV and/or ODV envelopes. These data suggest that FP25K may function, either directly or indirectly, to regulate the efficient transit of E66 from the ONM to the INM. From these data, one could speculate a functional cellular homolog of FP25K may exist that regulates the trafficking of cellular INM proteins with large cytoplasmic/nucleoplasmic domains from the ONM to the INM.

Viral induced sorting at the INM. Localization studies from infected cells demonstrate that sorting events at the INM distinguish viral SM sequences from cellular SM-like sequences (Fig. 33), actively excluding the cellular SM-like sequences from accumulating in viral-induced intranuclear MV and ODV-envelopes. By extrapolation from the studies in uninfected cells, proteins with

SM or SM-like sequences are predicted to be mobile in the INM of infected Sf9 cells. Therefore, the localization data from infected Sf9 cells suggests that sorting events at the INM may exist.

Diffusion:retention may be sufficient to describe the sorting and localization of some integral membrane proteins to the INM. However, the results from this study, combined with recently reported data (119, 323), suggest additional mechanisms. These data predict that sorting and localization of integral membrane proteins to the INM can be mediated via protein sequences that contain the essential features identified in the SM of AcMNPV ODV-E66. Furthermore, this trafficking process can be a sequential and regulated multi-step proteinaceous pathway that is independent of free diffusion and immobilization (119).

SUMMARY

The diffusion:retention model of INM protein sorting and localization predicts that once a protein is integrated into the ER, it freely diffuses within the continuous membrane systems of the ER and NE. Once the protein reaches the INM it binds nucleoplasmic components (via a nuclear ligand binding sequence) (195-197, 199) and/or other resident INM proteins (198) and becomes immobilized and thus retained in the INM. This model infers that immobilization in the INM is the only known sorting event in INM protein trafficking. However, recent studies using viral envelope proteins as markers to investigate the molecular basis and mechanisms involved in the pathway suggest sorting proteins to the INM is a regulated process that can be independent of immobilization.

The amino terminal 33 a.a. of ODV-E66 (the sorting motif, SM) are sufficient for the localization of fusion proteins to viral-induced intranuclear microvesicles (MV) and ODV envelopes during infection (152). When abundantly expressed, SM-fusions are also detected in the INM, ONM and ER, suggesting these SM-fusions use a trafficking pathway similar to that of resident INM proteins. To investigate the essential features of the SM, mutational analyses were performed. From these analyses, the essential features of the SM required for INM protein sorting and accumulation were determined to be a 18 a.a. TM sequence that lacks polar and charged a.a. with a cluster of charged a.a. spaced 5-11 residues from the cyto-/nucleoplasmic side of the TM

sequence. A comparison of the SM with known cellular INM proteins determined that the essential features of the SM were conserved.

Notably, one feature absent from the SM that is present in most INM proteins (except nurim) is a nuclear ligand-binding sequence. These binding sequences interact with immobilized nucleoplasmic components resulting in the immobilization of INM proteins in the INM, and therefore retention. In this study the localization and mobility of the E66 SM was compared with the cellular INM protein lamin B receptor (LBR). Three LBR fusion proteins (with and without the nuclear ligand-binding sequence) were expressed in mammalian and insect cells, and sorting similarities and differences were determined using light confocal microscopy and fluorescence recovery after photo-bleaching (FRAP). Lamin B Receptor is polytopic INM protein with an amino terminal, 200 a.a. nuclear ligand-binding sequence oriented within the nucleoplasm followed by eight TM segments. The INM sorting signals for LBR are contained in the nuclear ligand-binding sequence (218) and/or “the first transmembrane region plus flanking residues on either side” (196). The essential features of the E66 SM are conserved within the region of LBR (a.a. 201-246) identified by Smith and Blobel, (196) as sufficient for LBR sorting to the INM. The data from these studies suggests that localization of proteins to the INM does not require a nuclear ligand-binding sequence. Furthermore, immobilization in the INM is not necessarily a prerequisite for concentration of integral membrane proteins in the INM.

The diffusion:retention model would predict that if the LBR-GFP fusions were not immobilized in the INM of insect cells, these proteins could accumulate in MV and ODV envelopes during infection. However, localization studies show that while an ODV-envelope protein and the SM-GFP fusion partitioned to MV effectively during infection, the LBR-GFP fusion proteins did not. Therefore, this data suggests that there are viral induced sorting events that can occur at the INM that are likely independent of immobilization.

The results of this study, combined with recently reported data (119, 323) suggest that the sorting and localization of proteins to the INM can be directed by sequences which contain the essential features of the viral SM identified in this study. Furthermore trafficking to the INM can be a sequential and regulated, multi-step, proteinaceous pathway independent of free diffusion and immobilization (119).

REFERENCES

1. Lauzon, H. A., Lucarotti, C. J., Krell, P. J., Feng, Q., Retnakaran, A. and Arif, B. M. Sequence and organization of the *Neodiprion lecontei* nucleopolyhedrovirus genome. J Virol 2004;78:7023-35.

2. Hayakawa, T., Ko, R., Okano, K., Seong, S. I., Goto, C. and Maeda, S. Sequence analysis of the *Xestia c-nigrum* granulovirus genome. Virology 1999;262:277-97.

3. Herniou, E. A., Luque, T., Chen, X., Vlak, J. M., Winstanley, D., Cory, J. S. and O'Reilly, D. R. Use of whole genome sequence data to infer baculovirus phylogeny. J Virol 2001;75:8117-26.

4. Hu, Z. H., Arif, B. M., Sun, J. S., Chen, X. W., Zuidema, D., Goldbach, R. W. and Vlak, J. M. Genetic organization of the HindIII-I region of the single-nucleocapsid nucleopolyhedrovirus of *Buzura suppressaria*. Virus Res 1998;55:71-82.

5. Zanotto, P. M., Kessing, B. D. and Maruniak, J. E. Phylogenetic interrelationships among baculoviruses: evolutionary rates and host associations. J Invertebr Pathol 1993;62:147-64.

6. Adams, J. R. and McClintock, J. T. Baculoviridae. Nuclear polyhedrosis virus. In: J. R. Adams and J. R. Bonami. Atlas of invertebrate viruses. Boca Raton, FL:CRC Press; 1991. p. 87-225.

7. Granados, R. R. and Lawler, K. A. *In vivo* pathway of *Autographa californica* baculovirus invasion and infection. Virology 1981;108:297-308.

8. Kawanishi, C., Summers, M. D., Stoltz, D. B. and Arnott, H. J. Entry of an insect virus *in vivo* by fusion of viral envelopes and microvillus membranes. Journal of Invertebrate Pathology 1972;20:104-108.

9. Summers, M. D. Electron microscopic observations on granulosis virus entry, uncoating and replications processes during infection of the midgut cells of *Trichoplusia ni*. Journal of Ultrastructural Research 1971;35:606-625.

10. Harrap, K. and Robertson, J. A possible infection pathway in the development of a nuclear polyhedrosis virus. Journal of General Virology 1968;3:221-225.

11. Keddie, B. A., Aponte, G. W. and Volkman, L. E. The pathway of infection of *Autographa californica* nuclear polyhedrosis virus in an insect host. Science 1989;243:1728-30.

12. Engelhard, E. K., Kam-Morgan, L. N., Washburn, J. O. and Volkman, L. E. The insect tracheal system: a conduit for the systemic spread of *Autographa californica* M nuclear polyhedrosis virus. Proc Natl Acad Sci U S A 1994;91:3224-7.

13. Volkman, L. E., Blissard, G. W., Friesen, P. D., Keddie, B. A., Possee, R. D. and Theilmann, D. A. Baculoviridae. In: F. A. Murphy, C. M. Fauquet, D. H. L. Bishop, S. A. Ghabrial, A. W. Jarvis, G. P. Martelli, M. A. Mayo and M. D. Summers. Sixth report of the International Commitee on Taxonomy of Viruses. New York:Springer-Verlag; 1995. p. 104-113.

14. Volkman, L. E. Nucleopolyhedrovirus interactions with their insect hosts. Adv Virus Res 1997;48:313-48.

15. Luckow, V. A. and Summers, M. D. Signals important for high-level expression of foreign genes in *Autographa californica* nuclear polyhedrosis virus expression vectors. Virology 1988;167:56-71.

16. Smith, G. E., Summers, M. D. and Fraser, M. J. Production of human beta interferon in insect cells infected with a baculovirus expression vector. Mol Cell Biol 1983;3:2156-65.

17. Ayres, M. D., Howard, S. C., Kuzio, J., Lopez-Ferber, M. and Possee, R. D. The complete DNA sequence of *Autographa californica* nuclear polyhedrosis virus. Virology 1994;202:586-605.

18. Luque, T., Finch, R., Crook, N., O'Reilly, D. R. and Winstanley, D. The complete sequence of the *Cydia pomonella* granulovirus genome. J Gen Virol 2001;82:2531-47.

19. Lange, M. and Jehle, J. A. The genome of the *Cryptophlebia leucotreta* granulovirus. Virology 2003;317:220-36.

20. Wormleaton, S., Kuzio, J. and Winstanley, D. The complete sequence of the *Adoxophyes orana* granulovirus genome. Virology 2003;311:350-65.

21. Hashimoto, Y., Hayakawa, T., Ueno, Y., Fujita, T., Sano, Y. and Matsumoto, T. Sequence analysis of the *Plutella xylostella* granulovirus genome. Virology 2000;275:358-72.

22. Ahrens, C. H., Russell, R. L., Funk, C. J., Evans, J. T., Harwood, S. H. and Rohrmann, G. F. The sequence of the *Orgyia pseudotsugata* multinucleocapsid nuclear polyhedrosis virus genome. Virology 1997;229:381-99.

23. Jkel, I. W. F., van Strien, E. A., Heldens, J. G., Broer, R., Zuidema, D., Goldbach, R. W. and Vlak, J. M. Sequence and organization of the *Spodoptera exigua* multicapsid nucleopolyhedrovirus genome. J Gen Virol 1999;80:3289-304.

24. Chen, X., WF, I. J., Tarchini, R., Sun, X., Sandbrink, H., Wang, H., Peters, S., Zuidema, D., Lankhorst, R. K., Vlak, J. M. and Hu, Z. The sequence of the *Helicoverpa armigera* single nucleocapsid nucleopolyhedrovirus genome. J Gen Virol 2001;82:241-57.

25. Chen, X., Zhang, W. J., Wong, J., Chun, G., Lu, A., McCutchen, B. F., Presnail, J. K., Herrmann, R., Dolan, M., Tingey, S., Hu, Z. H. and Vlak, J. M. Comparative analysis of the complete genome sequences of *Helicoverpa zea* and *Helicoverpa armigera* single-nucleocapsid nucleopolyhedroviruses. J Gen Virol 2002;83:673-84.

26. Hyink, O., Dellow, R. A., Olsen, M. J., Caradoc-Davies, K. M., Drake, K., Herniou, E. A., Cory, J. S., O'Reilly, D. R. and Ward, V. K. Whole genome analysis of the *Epiphyas postvittana* nucleopolyhedrovirus. J Gen Virol 2002;83:957-71.

27. Gomi, S., Majima, K. and Maeda, S. Sequence analysis of the genome of *Bombyx mori* nucleopolyhedrovirus. J Gen Virol 1999;80:1323-37.

28. Kuzio, J., Pearson, M. N., Harwood, S. H., Funk, C. J., Evans, J. T., Slavicek, J. M. and Rohrmann, G. F. Sequence and analysis of the genome of a baculovirus pathogenic for *Lymantria dispar*. Virology 1999;253:17-34.

29. Li, Q., Donly, C., Li, L., Willis, L. G., Theilmann, D. A. and Erlandson, M. Sequence and organization of the *Mamestra configurata* nucleopolyhedrovirus genome. Virology 2002;294:106-21.

30. Pang, Y., Yu, J., Wang, L., Hu, X., Bao, W., Li, G., Chen, C., Han, H., Hu, S. and Yang, H. Sequence analysis of the *Spodoptera litura* multicapsid nucleopolyhedrovirus genome. Virology 2001;287:391-404.

31. Garcia-Maruniak, A., Maruniak, J. E., Zanotto, P. M., Doumbouya, A. E., Liu, J. C., Merritt, T. M. and Lanoie, J. S. Sequence analysis of the

genome of the *Neodiprion sertifer* nucleopolyhedrovirus. J Virol 2004;78:7036-51.

32. Afonso, C. L., Tulman, E. R., Lu, Z., Balinsky, C. A., Moser, B. A., Becnel, J. J., Rock, D. L. and Kutish, G. F. Genome sequence of a baculovirus pathogenic for *Culex nigripalpus*. J Virol 2001;75:11157-65.

33. Herniou, E. A., Olszewski, J. A., Cory, J. S. and O'Reilly, D. R. The genome sequence and evolution of baculoviruses. Annu Rev Entomol 2003;48:211-34.

34. Blissard, G. W. and Rohrmann, G. F. Baculovirus diversity and molecular biology. Annu Rev Entomol 1990;35:127-55.

35. Knudson, D. L. and Tinsley, T. W. Replication of a nuclear polyhedrosis virus in a continuous cell line of *Spodoptera frugiperda*: partial characterization of the viral DNA, comparative DNA-DNA hybridization, and patterns of DNA synthesis. Virology 1978;87:42-57.

36. Tija, S. T., Carstens, E. B. and Doerfler, W. Infection of *Spodoptera frugiperda* cells with *Autographa californica* nuclear polyhedrosis virus. II. The viral DNA and the kinetics of its replication. Virology 1979;99:391.

37. Rosinski, M., Reid, S. and Nielsen, L. K. Kinetics of baculovirus replication and release using real-time quantitative polymerase chain reaction. Biotechnol Bioeng 2002;77:476-80.

38. Kool, M., Ahrens, C. H., Goldbach, R. W., Rohrmann, G. F. and Vlak, J. M. Identification of genes involved in DNA replication of the *Autographa californica* baculovirus. Proc Natl Acad Sci U S A 1994;91:11212-6.

39. Braunagel, S. C., Russell, W. K., Rosas-Acosta, G., Russell, D. H. and Summers, M. D. Determination of the protein composition of the occlusion-derived virus of *Autographa califonica* nucleopolyhedrovirus. Proc Natl Acad Sci U S A 2003;100:9797-802.

40. Lu, A., Krell, P. J., Vlak, J. M. and Rohrmann, G. F. Baculovirus DNA replication. In: L. K. Miller. The baculoviruses. New York:Plenum Press; 1997. p. 171-186.

41. Lee, H. and Krell, P. J. Reiterated DNA fragments in defective genomes of *Autographa californica* nuclear polyhedrosis virus are competent for AcMNPV-dependent DNA replication. Virology 1994;202:418-29.

42. Friesen, P. D. and Miller, L. K. The regulation of baculovirus gene expression. Curr Top Microbiol Immunol 1986;131:31-49.

43. Blissard, G. W. and Rohrmann, G. F. Baculovirus gp64 gene expression: analysis of sequences modulating early transcription and transactivation by IE1. J Virol 1991;65:5820-7.

44. Huh, N. E. and Weaver, R. F. Identifying the RNA polymerases that synthesize specific transcripts of the *Autographa californica* nuclear polyhedrosis virus. J Gen Virol 1990;71:195-201.

45. Hoopes, R. R., Jr. and Rohrmann, G. F. In vitro transcription of baculovirus immediate early genes: accurate mRNA initiation by nuclear extracts from both insect and human cells. Proc Natl Acad Sci U S A 1991;88:4513-7.

46. Rice, W. C. and Miller, L. K. Baculovirus transcription in the presence of inhibitors and in nonpermissive *Drosophila* cells. Virus Res 1986;6:155-72.

47. Huh, N. E. and Weaver, R. F. Categorizing some early and late transcripts directed by the *Autographa californica* nuclear polyhedrosis virus. J Gen Virol 1990;71:2195-200.

48. Carson, D. D., Summers, M. D. and Guarino, L. A. Molecular analysis of a baculovirus regulatory gene. Virology 1991;182:279-86.

49. Guarino, L. A. and Summers, M. D. Functional mapping of a trans-activating gene required for expression of a baculovirus delayed-early gene. J Virol 1986;57:563-71.

50. Guarino, L. A. and Summers, M. D. Functional mapping of *Autographa california* nuclear polyhedrosis virus genes required for late gene expression. J Virol 1988;62:463-71.

51. Nissen, M. S. and Friesen, P. D. Molecular analysis of the transcriptional regulatory region of an early baculovirus gene. J Virol 1989;63:493-503.

52. Kovacs, G. R., Guarino, L. A. and Summers, M. D. Novel regulatory properties of the IE1 and IE0 transactivators encoded by the baculovirus *Autographa californica* multicapsid nuclear polyhedrosis virus. J Virol 1991;65:5281-8.

53. Pearson, M. N. and Rohrmann, G. F. Splicing is required for transactivation by the immediate early gene 1 of the *Lymantria dispar* multinucleocapsid nuclear polyhedrosis virus. Virology 1997;235:153-65.

54. Theilmann, D. A., Willis, L. G., Bosch, B. J., Forsythe, I. J. and Li, Q. The baculovirus transcriptional transactivator IE0 produces multiple products by internal initiation of translation. Virology 2001;290:211-23.

55. Dai, X., Willis, L. G., Huijskens, I., Palli, S. R. and Theilmann, D. A. The acidic activation domains of the baculovirus transactivators IE1 and IE0 are functional for transcriptional activation in both insect and mammalian cells. J Gen Virol 2004;85:573-82.

56. Huijskens, I., Li, L., Willis, L. G. and Theilmann, D. A. Role of AcMNPV IE0 in baculovirus very late gene activation. Virology 2004;323:120-30.

57. Carson, D. D., Guarino, L. A. and Summers, M. D. Functional mapping of an AcNPV immediately early gene which augments expression of the IE-1 trans-activated 39K gene. Virology 1988;162:444-51.

58. Carson, D. D., Summers, M. D. and Guarino, L. A. Transient expression of the *Autographa californica* nuclear polyhedrosis virus immediate-early gene, IE-N, is regulated by three viral elements. J Virol 1991;65:945-51.

59. Yoo, S. and Guarino, L. A. The *Autographa californica* nuclear polyhedrosis virus ie2 gene encodes a transcriptional regulator. Virology 1994;202:746-53.

60. Prikhod'ko, E. A. and Miller, L. K. Role of baculovirus IE2 and its RING finger in cell cycle arrest. J Virol 1998;72:684-92.

61. Murges, D., Quadt, I., Schroer, J. and Knebel-Morsdorf, D. Dynamic nuclear localization of the baculovirus proteins IE2 and PE38 during the infection cycle: the promyelocytic leukemia protein colocalizes with IE2. Exp Cell Res 2001;264:219-32.

62. Krappa, R. and Knebel-Morsdorf, D. Identification of the very early transcribed baculovirus gene PE-38. J Virol 1991;65:805-12.

63. Prikhod'ko, E. A. and Miller, L. K. The baculovirus PE38 protein augments apoptosis induced by transactivator IE1. J Virol 1999;73:6691-9.

64. Wang, W., Davison, S. and Krell, P. J. Identification and characterization of a major early-transcribed gene of *Trichoplusia ni* single nucleocapsid

nucleopolyhedrovirus using the baculovirus expression system. Virus Genes 2004;29:19-29.

65. Steglitz-Morsdorf, U., Morsdorf, G. and Kaltwasser, H. Cloning, heterologous expression, and sequencing of the *Proteus vulgaris* glnAntrBC operon and implications of nitrogen control on heterologous urease expression. FEMS Microbiol Lett 1993;106:157-64.

66. Blissard, G. W. and Rohrmann, G. F. Location, sequence, transcriptional mapping, and temporal expression of the gp64 envelope glycoprotein gene of the *Orgyia pseudotsugata* multicapsid nuclear polyhedrosis virus. Virology 1989;170:537-55.

67. Guarino, L. A. and Smith, M. Regulation of delayed-early gene transcription by dual TATA boxes. J Virol 1992;66:3733-9.

68. Kogan, P. H. and Blissard, G. W. A baculovirus gp64 early promoter is activated by host transcription factor binding to CACGTG and GATA elements. J Virol 1994;68:813-22.

69. Krappa, R., Behn-Krappa, A., Jahnel, F., Doerfler, W. and Knebel-Morsdorf, D. Differential factor binding at the promoter of early baculovirus gene PE38 during viral infection: GATA motif is recognized by an insect protein. J Virol 1992;66:3494-503.

70. Rodems, S. M. and Friesen, P. D. The hr5 transcriptional enhancer stimulates early expression from the *Autographa californica* nuclear polyhedrosis virus genome but is not required for virus replication. J Virol 1993;67:5776-85.

71. McLachlin, J. R. and Miller, L. K. Identification and characterization of vlf-1, a baculovirus gene involved in very late gene expression. J Virol 1994;68:7746-56.

72. Miller, L. K. and Lu, A. Regulation of baculovirus late and very late gene expression. In: L. K. Miller. The baculoviruses. New York:Plenum Press; 1997. p. 193-216.

73. Rapp, J. C., Wilson, J. A. and Miller, L. K. Nineteen baculovirus open reading frames, including LEF-12, support late gene expression. J Virol 1998;72:10197-206.

74. Lu, A. and Miller, L. K. The roles of eighteen baculovirus late expression factor genes in transcription and DNA replication. J Virol 1995;69:975-82.

75. Morris, T. D. and Miller, L. K. Mutational analysis of a baculovirus major late promoter. Gene 1994;140:147-53.

76. Possee, R. D. and Howard, S. C. Analysis of the polyhedrin gene promoter of the *Autographa californica* nuclear polyhedrosis virus. Nucleic Acids Res 1987;15:10233-48.

77. Braunagel, S. C. and Summers, M. D. *Autographa californica* nuclear polyhedrosis virus, PDV, and ECV viral envelopes and nucleocapsids: structural proteins, antigens, lipid and fatty acid profiles. Virology 1994;202:315-28.

78. Funk, C. J., Braunagel, S. C. and Rohrmann, G. F. Baculovirus structure. In: L. K. Miller. The baculoviruses. New York:Plenum Press; 1997. p. 7-32.

79. Hess, R. T. and Tanada, Y. Baculoviridae. Granulosis viruses. In: J. R. Adama and J. R. Bonami. Atlas of invertebrate viruses. Boca Raton:CRC Press, Inc.; 1991. p. 227-257.

80. Altschul, S. F., Madden, T. L., Schaffer, A. A., Zhang, J., Zhang, Z., Miller, W. and Lipman, D. J. Gapped BLAST and PSI-BLAST: a new generation of protein database search programs. Nucleic Acids Res 1997;25:3389-402.

81. Bideshi, D. K., Bigot, Y. and Federici, B. A. Molecular characterization and phylogenetic analysis of the *Harrisina brillians* granulovirus granulin gene. Arch Virol 2000;145:1933-45.

82. Rohrmann, G. F. Baculovirus structural proteins. J Gen Virol 1992;73:749-61.

83. Summers, M. D. and Smith, G. E. A Manual of Methods for Baculovirus vectors and Insect Cell Culture Procedures. College Station, TX USA:Texas Agricultural Experiment Station; Bulletin #1555, 1987.

84. Minion, F., Coons, L. and Broome, J. Characterization of the polyhedral envelope of the nuclear polyhedrosis virus *Heliothis virescens*. Journal of Invertebrate Pathology 1979;34:303.

85. Russell, R. L. and Rohrmann, G. F. A baculovirus polyhedron envelope protein: immunogold localization in infected cells and mature polyhedra. Virology 1990;174:177-84.

86. Whitt, M. A. and Manning, J. S. A phosphorylated 34-kDa protein and a subpopulation of polyhedrin are thiol linked to the carbohydrate layer surrounding a baculovirus occlusion body. Virology 1988;163:33-42.

87. Gombart, A. F., Pearson, M. N., Rohrmann, G. F. and Beaudreau, G. S. A baculovirus polyhedral envelope-associated protein: genetic location, nucleotide sequence, and immunocytochemical characterization. Virology 1989;169:182-93.

88. Bjornson, R. M. and Rohrmann, G. F. Nucleotide sequence of the polyhedron envelope protein gene region of the *Lymantria dispar* nuclear polyhedrosis virus. J Gen Virol 1992;73:1499-504.

89. Gross, C. H., Russell, R. L. and Rohrmann, G. F. *Orgyia pseudotsugata* baculovirus p10 and polyhedron envelope protein genes: analysis of their relative expression levels and role in polyhedron structure. J Gen Virol 1994;75:1115-23.

90. Ignoffo, C. M., Garcia, C., Zuidema, D. and Vlak, J. M. Relative *in vivo* activity and simulated sunlight -uv stability of inclusion bodies of a wild-type and an engineered polyhedral envelope-negative isolate of the nucleopolyhedrosis virus of *Autographa californica*. Journal of Invertebrate Pathology 1995;66:212-213.

91. Zuidema, D., Klinge-Roode, E. C., van Lent, J. W. and Vlak, J. M. Construction and analysis of an Autographa californica nuclear polyhedrosis virus mutant lacking the polyhedral envelope. Virology 1989;173:98-108.

92. Bianchi, F. J., Snoeijing, I., van der Werf, W., Mans, R. M., Smits, P. H. and Vlak, J. M. Biological activity of SeMNPV, AcMNPV, and three AcMNPV deletion mutants against Spodoptera exigua larvae (Lepidoptera: noctuidae). J Invertebr Pathol 2000;75:28-35.

93. Bianchi, F. J. J. A., Joosten, N. N., Gutierrez, S., Reijnen, T. M., Werf, W. V. D. and Vlak, J. M. The polyhedral membrane does not protect polyhedra of AcMNPV against inactivation on greenhouse *Chrysanthemum*. Biocontrol Science and Technology 1999;9:523-27.

94. Vialard, J., Lalumiere, M., Vernet, T., Briedis, D., Alkhatib, G., Henning, D., Levin, D. and Richardson, C. Synthesis of the membrane fusion and hemagglutinin proteins of measles virus, using a novel baculovirus vector containing the beta-galactosidase gene. J Virol 1990;64:37-50.

95. King, L. A. and Possee, R. D. The baculovirus expression system. A laboratory guide. London:Chapman & Hall; 1992.

96. Scheper, G. C., Vries, R. G., Broere, M., Usmany, M., Voorma, H. O., Vlak, J. M. and Thomas, A. A. Translational properties of the untranslated regions of the p10 messenger RNA of *Autographa californica* multicapsid nucleopolyhedrovirus. J Gen Virol 1997;78:687-96.

97. van Oers, M. M., Vlak, J. M., Voorma, H. O. and Thomas, A. A. Role of the 3' untranslated region of baculovirus p10 mRNA in high-level expression of foreign genes. J Gen Virol 1999;80:2253-62.

98. van Oers, M. M., Flipsen, J. T., Reusken, C. B., Sliwinsky, E. L., Goldbach, R. W. and Vlak, J. M. Functional domains of the p10 protein of *Autographa californica* nuclear polyhedrosis virus. J Gen Virol 1993;74:563-74.

99. Wilson, J. A., Hill, J. E., Kuzio, J. and Faulkner, P. Characterization of the baculovirus *Choristoneura fumiferana* multicapsid nuclear polyhedrosis virus p10 gene indicates that the polypeptide contains a coiled-coil domain. J Gen Virol 1995;76:2923-32.

100. Cheley, S., Kosik, K. S., Paskevich, P., Bakalis, S. and Bayley, H. Phosphorylated baculovirus p10 is a heat-stable microtubule-associated protein associated with process formation in Sf9 cells. J Cell Sci 1992;102:739-52.

101. Van Oers, M. M., Flipsen, J. T., Reusken, C. B. and Vlak, J. M. Specificity of baculovirus p10 functions. Virology 1994;200:513-23.

102. Bergold, G. H. Fine Structure of some insect viruses. J. Insect Pathol 1963;5:111-128.

103. Balhorn, R. A model for the structure of chromatin in mammalian sperm. J Cell Biol 1982;93:298-305.

104. Nakano, M., Kasai, K., Yoshida, K., Tanimoto, T., Tamaki, Y. and Tobita, T. Conformation of the fowl protamine, galline, and its binding properties to DNA. J Biochem (Tokyo) 1989;105:133-7.

105. Funk, C. J. and Consigli, R. A. Phosphate cycling on the basic protein of *Plodia interpunctella* granulosis virus. Virology 1993;193:396-402.

106. Oppenheimer, D. I. and Volkman, L. E. Proteolysis of p6.9 induced by cytochalasin D in *Autographa californica* M nuclear polyhedrosis virus-infected cells. Virology 1995;207:1-11.

107. Thiem, S. M. and Miller, L. K. Identification, sequence, and transcriptional mapping of the major capsid protein gene of the baculovirus *Autographa californica* nuclear polyhedrosis virus. J Virol 1989;63:2008-18.

108. Russell, R. L., Pearson, M. N. and Rohrmann, G. F. Immunoelectron microscopic examination of *Orgyia pseudotsugata* multicapsid nuclear polyhedrosis virus-infected *Lymantria dispar* cells: time course and localization of major polyhedron-associated proteins. J Gen Virol 1991;72:275-83.

109. Bateman, A., Coin, L., Durbin, R., Finn, R. D., Hollich, V., Griffiths-Jones, S., Khanna, A., Marshall, M., Moxon, S., Sonnhammer, E. L., Studholme, D. J., Yeats, C. and Eddy, S. R. The Pfam protein families database. Nucleic Acids Res 2004;32:D138-41.

110. Yang, S. and Miller, L. K. Expression and mutational analysis of the baculovirus very late factor 1 (vlf-1) gene. Virology 1998;245:99-109.

111. Yang, S. and Miller, L. K. Control of baculovirus polyhedrin gene expression by very late factor 1. Virology 1998;248:131-8.

112. Olszewski, J. and Miller, L. K. Identification and characterization of a baculovirus structural protein, VP1054, required for nucleocapsid formation. J Virol 1997;71:5040-50.

113. Hink, W. and Vail, P. A plaque assy for titration of alfalfa looper nuclear polyhedrosis virus in a cabbage looper (TN-368) cell line. J. Invert. Patholo. 1973;22:168-174.

114. Fraser, M. J., Smith, G. E. and Summers, M. D. Aquisition of host cell DNA sequences by baculovirus: relationship between DNA host cell insertions and FP mutants on *Autographa californica* and *Galleria mellonella* nuclear polyhedrosis virus. J. Virol 1983;47:287-300.

115. Beames, B. and Summers, M. D. Location and nucleotide sequence of the 25K protein missing from baculovirus few polyhedra (FP) mutants. Virology 1989;168:344-53.

116. Harrison, R. L. and Summers, M. D. Mutations in the *Autographa californica* multinucleocapsid nuclear polyhedrosis virus 25 kDa protein

gene result in reduced virion occlusion, altered intranuclear envelopment and enhanced virus production. J Gen Virol 1995;76:1451-9.

117. Braunagel, S. C., Burks, J. K., Rosas-Acosta, G., Harrison, R. L., Ma, H. and Summers, M. D. Mutations within the *Autographa californica* nucleopolyhedrovirus FP25K gene decrease the accumulation of ODV-E66 and alter its intranuclear transport. J Virol 1999;73:8559-70.

118. Rosas-Acosta, G., Braunagel, S. C. and Summers, M. D. Effects of Deletion and Overexpression of the *Autographa californica* Nuclear Polyhedrosis Virus FP25K Gene on Synthesis of Two Occlusion-Derived Virus Envelope Proteins and Their Transport into Virus-Induced Intranuclear Membranes. J Virol 2001;75:10829-42.

119. Braunagel, S. C., Williamson, S. T., Saksena, S., Zhong, Z., Russell, W. K., Russell, D. H. and Summers, M. D. Trafficking of ODV-E66 is mediated via a sorting motif and other viral proteins: facilitated trafficking to the inner nuclear membrane. Proc Natl Acad Sci U S A 2004;101:8372-77.

120. Vialard, J. E. and Richardson, C. D. The 1,629-nucleotide open reading frame located downstream of the *Autographa californica* nuclear polyhedrosis virus polyhedrin gene encodes a nucleocapsid-associated phosphoprotein. J Virol 1993;67:5859-66.

121. Kitts, P. A. and Possee, R. D. A method for producing recombinant baculovirus expression vectors at high frequency. Biotechniques 1993;14:810-7.

122. Russell, R. L., Funk, C. J. and Rohrmann, G. F. Association of a baculovirus-encoded protein with the capsid basal region. Virology 1997;227:142-52.

123. Braunagel, S. C., Guidry, P. A., Rosas-Acosta, G., Engelking, L. and Summers, M. D. Identification of BV/ODV-C42, an *Autographa californica* nucleopolyhedrovirus orf101-encoded structural protein detected in infected-cell complexes with ODV-EC27 and p78/83. J Virol 2001;75:12331-8.

124. Lanier, L. M. and Volkman, L. E. Actin binding and nucleation by *Autographa california* M nucleopolyhedrovirus. Virology 1998;243:167-77.

125. Iorio, C., Vialard, J. E., McCracken, S., Lagace, M. and Richardson, C. D. The late expression factors 8 and 9 and possibly the phosphoprotein p78/83 of *Autographa californica* multicapsid nucleopolyhedrovirus are

components of the virus-induced RNA polymerase. Intervirology 1998;41:35-46.

126. Braunagel, S. C., He, H., Ramamurthy, P. and Summers, M. D. Transcription, translation, and cellular localization of three *Autographa californica* nuclear polyhedrosis virus structural proteins: ODV-E18, ODV-E35, and ODV-EC27. Virology 1996;222:100-14.

127. Belyavskyi, M., Braunagel, S. C. and Summers, M. D. The structural protein ODV-EC27 of *Autographa californica* nucleopolyhedrovirus is a multifunctional viral cyclin. Proc Natl Acad Sci U S A 1998;95:11205-10.

128. Wolgamot, G. M., Gross, C. H., Russell, R. L. and Rohrmann, G. F. Immunocytochemical characterization of p24, a baculovirus capsid-associated protein. J Gen Virol 1993;74:103-7.

129. Lu, A. and Carstens, E. B. Nucleotide sequence and transcriptional analysis of the p80 gene of *Autographa californica* nuclear polyhedrosis virus: a homologue of the *Orgyia pseudotsugata* nuclear polyhedrosis virus capsid-associated gene. Virology 1992;190:201-9.

130. Whitford, M. and Faulkner, P. A structural polypeptide of the baculovirus *Autographa californica* nuclear polyhedrosis virus contains O-linked N-acetylglucosamine. J Virol 1992;66:3324-9.

131. Whitford, M. and Faulkner, P. Nucleotide sequence and transcriptional analysis of a gene encoding gp41, a structural glycoprotein of the baculovirus *Autographa californica* nuclear polyhedrosis virus. J Virol 1992;66:4763-8.

132. Olszewski, J. and Miller, L. K. A role for baculovirus GP41 in budded virus production. Virology 1997;233:292-301.

133. Volkman, L. E. and Goldsmith, P. A. Mechansims of nuetralization of budded *Autographa californica* nuclear polyhedrosis virus by a monoclonal antibody: inhibition of entry by absorptive endocytosis. Virology 1985;143:185.

134. Pearson, M. N., Groten, C. and Rohrmann, G. F. Identification of the *Lymantria dispar* nucleopolyhedrovirus envelope fusion protein provides evidence for a phylogenetic division of the Baculoviridae. J Virol 2000;74:6126-31.

135. Blissard, G. W. and Wenz, J. R. Baculovirus gp64 envelope glycoprotein is sufficient to mediate pH-dependent membrane fusion. J Virol 1992;66:6829-35.

136. Whitford, M., Stewart, S., Kuzio, J. and Faulkner, P. Identification and sequence analysis of a gene encoding gp67, an abundant envelope glycoprotein of the baculovirus *Autographa californica* nuclear polyhedrosis virus. J Virol 1989;63:1393-9.

137. Volkman, L. E. and Goldsmith, P. A. Budded *Autographa californica* NPV 64K protein: further biochemical analysis and effects of postimmunoprecipitation sample preparation conditions. Virology 1984;139:295.

138. Monsma, S. A. and Blissard, G. W. Identification of a membrane fusion domain and an oligomerization domain in the baculovirus GP64 envelope fusion protein. J Virol 1995;69:2583-95.

139. Monsma, S. A., Oomens, A. G. and Blissard, G. W. The GP64 envelope fusion protein is an essential baculovirus protein required for cell-to-cell transmission of infection. J Virol 1996;70:4607-16.

140. Roberts, T. E. and Faulkner, P. Fatty acid acylation of the 67K envelope glycoprotein of a baculovirus: *Autographa californica* nuclear polyhedrosis virus. Virology 1989;172:377-81.

141. Zhang, S. X., Han, Y. and Blissard, G. W. Palmitoylation of the *Autographa californica* multicapsid nucleopolyhedrovirus envelope glycoprotein GP64: mapping, functional studies, and lipid rafts. J Virol 2003;77:6265-73.

142. Oomens, A. G., Monsma, S. A. and Blissard, G. W. The baculovirus GP64 envelope fusion protein: synthesis, oligomerization, and processing. Virology 1995;209:592-603.

143. Washburn, J. O., Chan, E. Y., Volkman, L. E., Aumiller, J. J. and Jarvis, D. L. Early synthesis of budded virus envelope fusion protein GP64 enhances *Autographa californica* multicapsid nucleopolyhedrovirus virulence in orally infected Heliothis virescens. J Virol 2003;77:280-90.

144. Pearson, M. N., Russell, R. L. and Rohrmann, G. F. Characterization of a baculovirus-encoded protein that is associated with infected-cell membranes and budded virions. Virology 2001;291:22-31.

145. Lung, O. Y., Cruz-Alvarez, M. and Blissard, G. W. Ac23, an envelope fusion protein homolog in the baculovirus *Autographa californica* multicapsid nucleopolyhedrovirus, is a viral pathogenicity factor. J Virol 2003;77:328-39.

146. Lung, O., Westenberg, M., Vlak, J. M., Zuidema, D. and Blissard, G. W. Pseudotyping *Autographa californica* multicapsid nucleopolyhedrovirus (AcMNPV): F proteins from group II NPVs are functionally analogous to AcMNPV GP64. J Virol 2002;76:5729-36.

147. Fraser, M. J. Ultrastructural observations of virion maturation in *Autographa californica* nuclear polyhedrosis virus infected *Spodoptera frugiperda* cell cultures. J. Ultrastruct. Mol. Struct. Res. 1986;95:189-195.

148. Hong, T., Braunagel, S. C. and Summers, M. D. Transcription, translation, and cellular localization of PDV-E66: a structural protein of the PDV envelope of *Autographa californica* nuclear polyhedrosis virus. Virology 1994;204:210-22.

149. Stoltz, D. B., Pavan, C. and Da Cunha, A. B. Nuclear polyhedrosis virus: a possible example of de novo intranuclear membrane morphogenesis. Journal of General Virology 1973;19:145-50.

150. Summers, M. D. and Arnott, H. J. Ultrastuctural studies on inclusion formation and virus occlusion in nuclear polyhedrosis and granulosis virus-infected cells of *Trichoplusia ni*. J. Ultrastruct. Res. 1969;28:462-480.

151. Braunagel, S. C., Elton, D. M., Ma, H. and Summers, M. D. Identification and analysis of an *Autographa californica* nuclear polyhedrosis virus structural protein of the occlusion-derived virus envelope: ODV-E56. Virology 1996;217:97-110.

152. Hong, T., Summers, M. D. and Braunagel, S. C. N-terminal sequences from *Autographa californica* nuclear polyhedrosis virus envelope proteins ODV-E66 and ODV-E25 are sufficient to direct reporter proteins to the nuclear envelope, intranuclear microvesicles and the envelope of occlusion derived virus. Proc Natl Acad Sci U S A 1997;94:4050-5.

153. Russell, R. L. and Rohrmann, G. F. A 25-kDa protein is associated with the envelopes of occluded baculovirus virions. Virology 1993;195:532-40.

154. Theilmann, D. A., Chantler, J. K., Stweart, S., Flipsen, H. T., Vlak, J. M. and Crook, N. E. Characterization of a highly conserved baculovirus

structural protein that is specific for occlusion-derived virions. Virology 1996;218:148-58.

155. Ma, H. Studies of ODV-E56, an envelope protein of *Autographa californica* nucleopolyhedrovirus. College Station:Texas A&M University; 1998.

156. Faulkner, P., Kuzio, J., Williams, G. V. and Wilson, J. A. Analysis of p74, a PDV envelope protein of *Autographa californica* nucleopolyhedrovirus required for occlusion body infectivity in vivo. J Gen Virol 1997;78:3091-100.

157. Kuzio, J., Jaques, R. and Faulkner, P. Identification of p74, a gene essential for virulence of baculovirus occlusion bodies. Virology 1989;173:759-63.

158. Yao, L., Zhou, W., Xu, H., Zheng, Y. and Qi, Y. The *Heliothis armigera* single nucleocapsid nucleopolyhedrovirus envelope protein P74 is required for infection of the host midgut. Virus Res 2004;104:111-21.

159. Slack, J. M., Dougherty, E. M. and Lawrence, S. D. A study of the *Autographa californica* multiple nucleopolyhedrovirus ODV envelope protein p74 using a GFP tag. J Gen Virol 2001;82:2279-87.

160. Haas-Stapleton, E. J., Washburn, J. O. and Volkman, L. E. P74 mediates specific binding of *Autographa californica* M nucleopolyhedrovirus occlusion-derived virus to primary cellular targets in the midgut epithelia of *Heliothis virescens* larvae. J Virol 2004;78:6786-91.

161. Fang, M., Wang, H., Yuan, L., Chen, X., Vlak, J. M. and Hu, Z. Open reading frame 94 of *Helicoverpa armigera* single nucleocapsid nucleopolyhedrovirus encodes a novel conserved occlusion-derived virion protein, ODV-EC43. J Gen Virol 2003;84:3021-7.

162. Russell, R. L. and Rohrmann, G. F. Characterization of P91, a protein associated with virions of an *Orgyia pseudotsugata* baculovirus. Virology 1997;233:210-23.

163. Beniya, H., Braunagel, S. C. and Summers, M. D. *Autographa californica* nuclear polyhedrosis virus: subcellular localization and protein trafficking of BV/ODV-E26 to intranuclear membranes and viral envelopes. Virology 1998;240:64-75.

164. Imai, N., Kurihara, M., Matsumoto, S. and Kang, W. K. *Bombyx mori* nucleopolyhedrovirus orf8 encodes a nucleic acid binding protein that colocalizes with IE1 during infection. Arch Virol 2004;149:1581-94.

165. Gutierrez, S., Kikhno, I. and Lopez Ferber, M. Transcription and promoter analysis of pif, an essential but low-expressed baculovirus gene. J Gen Virol 2004;85:331-41.

166. Kikhno, I., Gutierrez, S., Croizier, L., Croizier, G. and Ferber, M. L. Characterization of pif, a gene required for the per os infectivity of *Spodoptera littoralis* nucleopolyhedrovirus. J Gen Virol 2002;83:3013-22.

167. Pijlman, G. P., Pruijssers, A. J. and Vlak, J. M. Identification of pif-2, a third conserved baculovirus gene required for per os infection of insects. J Gen Virol 2003;84:2041-9.

168. Lapointe, R., Popham, H. J., Straschil, U., Goulding, D., O'Reilly, D. R. and Olszewski, J. A. Characterization of two *Autographa californica* nucleopolyhedrovirus proteins, Ac145 and Ac150, which affect oral infectivity in a host-dependent manner. J Virol 2004;78:6439-48.

169. Gerace, L. and Burke, B. Functional organization of the nuclear envelope. Annu Rev Cell Biol 1988;4:335-74.

170. Burke, B. and Stewart, C. L. Life at the edge: the nuclear envelope and human disease. Nat Rev Mol Cell Biol 2002;3:575-85.

171. Goldberg, M. W. and Allen, T. D. Structural and functional organization of the nuclear envelope. Curr Opin Cell Biol 1995;7:301-9.

172. Gruenbaum, Y., Wilson, K. L., Harel, A., Goldberg, M. and Cohen, M. Review: nuclear lamins--structural proteins with fundamental functions. J Struct Biol 2000;129:313-23.

173. Worman, H. J. and Courvalin, J. C. The nuclear lamina and inherited disease. Trends Cell Biol 2002;12:591-8.

174. Nakielny, S. and Dreyfuss, G. Transport of proteins and RNAs in and out of the nucleus. Cell 1999;99:677-90.

175. Hinshaw, J. E., Carragher, B. O. and Milligan, R. A. Architecture and design of the nuclear pore complex. Cell 1992;69:1133-41.

176. Rout, M. P., Aitchison, J. D., Suprapto, A., Hjertaas, K., Zhao, Y. and Chait, B. T. The yeast nuclear pore complex: composition, architecture, and transport mechanism. J Cell Biol 2000;148:635-51.

177. Vasu, S. K. and Forbes, D. J. Nuclear pores and nuclear assembly. Curr Opin Cell Biol 2001;13:363-75.

178. Rout, M. P. and Aitchison, J. D. The nuclear pore complex as a transport machine. J Biol Chem 2001;276:16593-6.

179. Allen, T. D., Cronshaw, J. M., Bagley, S., Kiseleva, E. and Goldberg, M. W. The nuclear pore complex: mediator of translocation between nucleus and cytoplasm. J Cell Sci 2000;113:1651-9.

180. Talcott, B. and Moore, M. S. Getting across the nuclear pore complex. Trends Cell Biol 1999;9:312-8.

181. Miller, B. R. and Forbes, D. J. Purification of the vertebrate nuclear pore complex by biochemical criteria. Traffic 2000;1:941-51.

182. Bastos, R., Lin, A., Enarson, M. and Burke, B. Targeting and function in mRNA export of nuclear pore complex protein Nup153. J Cell Biol 1996;134:1141-56.

183. Moroianu, J., Blobel, G. and Radu, A. RanGTP-mediated nuclear export of karyopherin alpha involves its interaction with the nucleoporin Nup153. Proc Natl Acad Sci U S A 1997;94:9699-704.

184. Shah, S., Tugendreich, S. and Forbes, D. Major binding sites for the nuclear import receptor are the internal nucleoporin Nup153 and the adjacent nuclear filament protein Tpr. J Cell Biol 1998;141:31-49.

185. Paine, P. L., Moore, L. C. and Horowitz, S. B. Nuclear envelope permeability. Nature 1975;254:109-14.

186. Peters, R. Fluorescence microphotolysis to measure nucleocytoplasmic transport and intracellular mobility. Biochim Biophys Acta 1986;864:305-59.

187. Schwamborn, K., Albig, W. and Doenecke, D. The histone H1(0) contains multiple sequence elements for nuclear targeting. Exp Cell Res 1998;244:206-17.

188. Kalderon, D., Roberts, B. L., Richardson, W. D. and Smith, A. E. A short amino acid sequence able to specify nuclear location. Cell 1984;39:499-509.

189. Dingwall, C., Sharnick, S. V. and Laskey, R. A. A polypeptide domain that specifies migrationof nucleoplasmin into the nucleus. Cell 1982;30:449-458.

190. Fridell, R. A., Bogerd, H. P. and Cullen, B. R. Nuclear export of late HIV-1 mRNAs occurs via a cellular protein export pathway. Proc Natl Acad Sci U S A 1996;93:4421-4.

191. Yoneda, Y., Hieda, M., Nagoshi, E. and Miyamoto, Y. Nucleocytoplasmic protein transport and recycling of Ran. Cell Struct Funct 1999;24:425-33.

192. Macara, I. G. Transport into and out of the nucleus. Microbiol Mol Biol Rev 2001;65:570-94.

193. Bayliss, R., Corbett, A. H. and Stewart, M. The molecular mechanism of transport of macromolecules through nuclear pore complexes. Traffic 2000;1:448-56.

194. Kaffman, A. and O'Shea, E. K. Regulation of nuclear localization: a key to a door. Annu Rev Cell Dev Biol 1999;15:291-339.

195. Worman, H. J. and Courvalin, J. C. The inner nuclear membrane. J Membr Biol 2000;177:1-11.

196. Smith, S. and Blobel, G. The first membrane spanning region of the lamin B receptor is sufficient for sorting to the inner nuclear membrane. J Cell Biol 1993;120:631-7.

197. Soullam, B. and Worman, H. J. Signals and structural features involved in integral membrane protein targeting to the inner nuclear membrane. J Cell Biol 1995;130:15-27.

198. Rolls, M. M., Stein, P. A., Taylor, S. S., Ha, E., McKeon, F. and Rapoport, T. A. A visual screen of a GFP-fusion library identifies a new type of nuclear envelope membrane protein. J Cell Biol 1999;146:29-44.

199. Ellenberg, J., Siggia, E. D., Moreira, J. E., Smith, C. L., Presley, J. F., Worman, H. J. and Lippincott-Schwartz, J. Nuclear membrane dynamics and reassembly in living cells: targeting of an inner nuclear membrane protein in interphase and mitosis. J Cell Biol 1997;138:1193-206.

200. Ostlund, C., Ellenberg, J., Hallberg, E., Lippincott-Schwartz, J. and Worman, H. J. Intracellular trafficking of emerin, the Emery-Dreifuss muscular dystrophy protein. J Cell Sci 1999;112:1709-19.

201. Lin, F., Blake, D. L., Callebaut, I., Skerjanc, I. S., Holmer, L., McBurney, M. W., Paulin-Levasseur, M. and Worman, H. J. MAN1, an inner nuclear membrane protein that shares the LEM domain with lamina-associated polypeptide 2 and emerin. J Biol Chem 2000;275:4840-7.

202. Apel, E. D., Lewis, R. M., Grady, R. M. and Sanes, J. R. Syne-1, a dystrophin- and Klarsicht-related protein associated with synaptic nuclei at the neuromuscular junction. J Biol Chem 2000;275:31986-95.

203. Mislow, J. M., Kim, M. S., Davis, D. B. and McNally, E. M. Myne-1, a spectrin repeat transmembrane protein of the myocyte inner nuclear membrane, interacts with lamin A/C. J Cell Sci 2002;115:61-70.

204. Zhang, Q., Skepper, J. N., Yang, F., Davies, J. D., Hegyi, L., Roberts, R. G., Weissberg, P. L., Ellis, J. A. and Shanahan, C. M. Nesprins: a novel family of spectrin-repeat-containing proteins that localize to the nuclear membrane in multiple tissues. J Cell Sci 2001;114:4485-98.

205. Worman, H. J., Yuan, J., Blobel, G. and Georgatos, S. D. A lamin B receptor in the nuclear envelope. Proc Natl Acad Sci U S A 1988;85:8531-4.

206. Ye, Q. and Worman, H. J. Primary structure analysis and lamin B and DNA binding of human LBR, an integral protein of the nuclear envelope inner membrane. J Biol Chem 1994;269:11306-11.

207. Pyrpasopoulou, A., Meier, J., Maison, C., Simos, G. and Georgatos, S. D. The lamin B receptor (LBR) provides essential chromatin docking sites at the nuclear envelope. EMBO J 1996;15:7108-19.

208. Ye, Q. and Worman, H. J. Interaction between an integral protein of the nuclear envelope inner membrane and human chromodomain proteins homologous to *Drosophila* HP1. J Biol Chem 1996;271:14653-6.

209. Foisner, R. and Gerace, L. Integral membrane proteins of the nuclear envelope interact with lamins and chromosomes, and binding is modulated by mitotic phosphorylation. Cell 1993;73:1267-79.

210. Yorifuji, H., Tadano, Y., Tsuchiya, Y., Ogawa, M., Goto, K., Umetani, A., Asaka, Y. and Arahata, K. Emerin, deficiency of which causes Emery-

Dreifuss muscular dystrophy, is localized at the inner nuclear membrane. Neurogenetics 1997;1:135-40.

211. Clements, L., Manilal, S., Love, D. R. and Morris, G. E. Direct interaction between emerin and lamin A. Biochem Biophys Res Commun 2000;267:709-14.

212. Sakaki, M., Koike, H., Takahashi, N., Sasagawa, N., Tomioka, S., Arahata, K. and Ishiura, S. Interaction between emerin and nuclear lamins. J Biochem (Tokyo) 2001;129:321-7.

213. Schuler, E., Lin, F. and Worman, H. J. Characterization of the human gene encoding LBR, an integral protein of the nuclear envelope inner membrane. J Biol Chem 1994;269:11312-7.

214. Silve, S., Dupuy, P. H., Ferrara, P. and Loison, G. Human lamin B receptor exhibits sterol C14-reductase activity in Saccharomyces cerevisiae. Biochim Biophys Acta 1998;1392:233-44.

215. Prakash, A., Sengupta, S., Aparna, K. and Kasbekar, D. P. The erg-3 (sterol delta14,15-reductase) gene of *Neurospora crassa*: generation of null mutants by repeat-induced point mutation and complementation by proteins chimeric for human lamin B receptor sequences. Microbiology 1999;145:1443-51.

216. Holmer, L. and Worman, H. J. Inner nuclear membrane proteins: functions and targeting. Cell Mol Life Sci 2001;58:1741-7.

217. Worman, H. J., Evans, C. D. and Blobel, G. The lamin B receptor of the nuclear envelope inner membrane: a polytopic protein with eight potential transmembrane domains. J Cell Biol 1990;111:1535-42.

218. Soullam, B. and Worman, H. J. The amino-terminal domain of the lamin B receptor is a nuclear envelope targeting signal. J Cell Biol 1993;120:1093-100.

219. Irons, S. L., Evans, D. E. and Brandizzi, F. The first 238 amino acids of the human lamin B receptor are targeted to the nuclear envelope in plants. J Exp Bot 2003;54:943-50.

220. Maison, C., Pyrpasopoulou, A., Theodoropoulos, P. A. and Georgatos, S. D. The inner nuclear membrane protein LAP1 forms a native complex with B- type lamins and partitions with spindle-associated mitotic vesicles. Embo J 1997;16:4839-50.

221. Senior, A. and Gerace, L. Integral membrane proteins specific to the inner nuclear membrane and associated with the nuclear lamina. J Cell Biol 1988;107:2029-36.

222. Martin, L., Crimaudo, C. and Gerace, L. cDNA cloning and characterization of lamina-associated polypeptide 1C (LAP1C), an integral protein of the inner nuclear membrane. J Biol Chem 1995;270:8822-8.

223. Kondo, Y., Kondoh, J., Hayashi, D., Ban, T., Takagi, M., Kamei, Y., Tsuji, L., Kim, J. and Yoneda, Y. Molecular cloning of one isotype of human lamina-associated polypeptide 1s and a topological analysis using its deletion mutants. Biochem Biophys Res Commun 2002;294:770-8.

224. Furukawa, K. LAP2 binding protein 1 (L2BP1/BAF) is a candidate mediator of LAP2-chromatin interaction. J Cell Sci 1999;112:2485-92.

225. Furukawa, K., Fritze, C. E. and Gerace, L. The major nuclear envelope targeting domain of LAP2 coincides with its lamin binding region but is distinct from its chromatin interaction domain. J Biol Chem 1998;273:4213-9.

226. Dechat, T., Gotzmann, J., Stockinger, A., Harris, C. A., Talle, M. A., Siekierka, J. J. and Foisner, R. Detergent-salt resistance of LAP2alpha in interphase nuclei and phosphorylation-dependent association with chromosomes early in nuclear assembly implies functions in nuclear structure dynamics. EMBO J 1998;17:4887-902.

227. Dechat, T., Vlcek, S. and Foisner, R. Review: lamina-associated polypeptide 2 isoforms and related proteins in cell cycle-dependent nuclear structure dynamics. J Struct Biol 2000;129:335-45.

228. Liu, J., Lee, K. K., Segura-Totten, M., Neufeld, E., Wilson, K. L. and Gruenbaum, Y. MAN1 and emerin have overlapping function(s) essential for chromosome segregation and cell division in *Caenorhabditis elegans*. Proc Natl Acad Sci U S A 2003;100:4598-603.

229. Tsuchiya, Y., Hase, A., Ogawa, M., Yorifuji, H. and Arahata, K. Distinct regions specify the nuclear membrane targeting of emerin, the responsible protein for Emery-Dreifuss muscular dystrophy. Eur J Biochem 1999;259:859-65.

230. Wolff, N., Gilquin, B., Courchay, K., Callebaut, I., Worman, H. J. and Zinn-Justin, S. Structural analysis of emerin, an inner nuclear membrane

protein mutated in X-linked Emery-Dreifuss muscular dystrophy. FEBS Lett 2001;501:171-6.

231. Wu, W., Lin, F. and Worman, H. J. Intracellular trafficking of MAN1, an integral protein of the nuclear envelope inner membrane. J Cell Sci 2002;115:1361-71.

232. Hofemeister, H. and O'Hare, P. Analysis of the localization and topology of nurim, a polytopic protein tightly associated with the inner nuclear membrane. J Biol Chem 2005;280:2512-21.

233. Holaska, J. M., Wilson, K. L. and Mansharamani, M. The nuclear envelope, lamins and nuclear assembly. Curr Opin Cell Biol 2002;14:357-64.

234. Delaunay, J. Genetic disorders of the red cell membranes. FEBS Lett 1995;369:34-7.

235. Mansharamani, M., Hewetson, A. and Chilton, B. S. Cloning and characterization of an atypical Type IV P-type ATPase that binds to the RING motif of RUSH transcription factors. J Biol Chem 2001;276:3641-9.

236. Dreger, M., Bengtsson, L., Schoneberg, T., Otto, H. and Hucho, F. Nuclear envelope proteomics: novel integral membrane proteins of the inner nuclear membrane. Proc Natl Acad Sci U S A 2001;98:11943-8.

237. Malone, C. J., Fixsen, W. D., Horvitz, H. R. and Han, M. UNC-84 localizes to the nuclear envelope and is required for nuclear migration and anchoring during *C. elegans* development. Development 1999;126:3171-81.

238. Lee, K. K., Starr, D., Cohen, M., Liu, J., Han, M., Wilson, K. L. and Gruenbaum, Y. Lamin-dependent localization of UNC-84, a protein required for nuclear migration in *Caenorhabditis elegans*. Mol Biol Cell 2002;13:892-901.

239. Starr, D. A., Hermann, G. J., Malone, C. J., Fixsen, W., Priess, J. R., Horvitz, H. R. and Han, M. unc-83 encodes a novel component of the nuclear envelope and is essential for proper nuclear migration. Development 2001;128:5039-50.

240. Fitzgerald, J., Kennedy, D., Viseshakul, N., Cohen, B. N., Mattick, J., Bateman, J. F. and Forsayeth, J. R. UNCL, the mammalian homologue of UNC-50, is an inner nuclear membrane RNA-binding protein. Brain Res 2000;877:110-23.

241. Ashery-Padan, R., Weiss, A. M., Feinstein, N. and Gruenbaum, Y. Distinct regions specify the targeting of otefin to the nucleoplasmic side of the nuclear envelope. J Biol Chem 1997;272:2493-9.

242. Goldberg, M., Lu, H., Stuurman, N., Ashery-Padan, R., Weiss, A. M., Yu, J., Bhattacharyya, D., Fisher, P. A., Gruenbaum, Y. and Wolfner, M. F. Interactions among *Drosophila* nuclear envelope proteins lamin, otefin, and YA. Mol Cell Biol 1998;18:4315-23.

243. Harel, A., Zlotkin, E., Nainudel-Epszteyn, S., Feinstein, N., Fisher, P. A. and Gruenbaum, Y. Persistence of major nuclear envelope antigens in an envelope-like structure during mitosis in *Drosophila melanogaster* embryos. J Cell Sci 1989;94:463-70.

244. Lin, H. and Wolfner, M. F. Cloning and analysis of fs(1) Ya, a maternal effect gene required for the initiation of *Drosophila* embryogenesis. Mol Gen Genet 1989;215:257-65.

245. Lopez, J. M. and Wolfner, M. F. The developmentally regulated *Drosophila* embryonic nuclear lamina protein 'Young Arrest' (fs(1)Ya) is capable of associating with chromatin. J Cell Sci 1997;110:643-51.

246. Gilbert, R. and Ghosh, H. P. Immunoelectron microscopic localization of herpes simplex virus glycoprotein gB in the nuclear envelope of infected cells. Virus Res 1993;28:217-31.

247. Gilbert, R., Ghosh, K., Rasile, L. and Ghosh, H. P. Membrane anchoring domain of herpes simplex virus glycoprotein gB is sufficient for nuclear envelope localization. J Virol 1994;68:2272-85.

248. Torrisi, M. R., Cirone, M., Pavan, A., Zompetta, C., Barile, G., Frati, L. and Faggioni, A. Localization of Epstein-Barr virus envelope glycoproteins on the inner nuclear membrane of virus-producing cells. J Virol 1989;63:828-32.

249. Scaria, A., Tollefson, A. E., Saha, S. K. and Wold, W. S. The E3-11.6K protein of adenovirus is an Asn-glycosylated integral membrane protein that localizes to the nuclear membrane. Virology 1992;191:743-53.

250. Schirmer, E. C., Florens, L., Guan, T., Yates, J. R., 3rd and Gerace, L. Nuclear membrane proteins with potential disease links found by subtractive proteomics. Science 2003;301:1380-2.

251. Stuurman, N., Heins, S. and Aebi, U. Nuclear lamins: their structure, assembly, and interactions. J Struct Biol 1998;122:42-66.

252. Stuurman, N., Sasse, B. and Fisher, P. A. Intermediate filament protein polymerization: molecular analysis of *Drosophila* nuclear lamin head-to-tail binding. J Struct Biol 1996;117:1-15.

253. Klapper, M., Exner, K., Kempf, A., Gehrig, C., Stuurman, N., Fisher, P. A. and Krohne, G. Assembly of A- and B-type lamins studied *in vivo* with the baculovirus system. J Cell Sci 1997;110:2519-32.

254. Hennekes, H. and Nigg, E. A. The role of isoprenylation in membrane attachment of nuclear lamins. A single point mutation prevents proteolytic cleavage of the lamin A precursor and confers membrane binding properties. J Cell Sci 1994;107:1019-29.

255. McKeon, F. D., Kirschner, M. W. and Caput, D. Homologies in both primary and secondary structure between nuclear envelope and intermediate filament proteins. Nature 1986;319:463-8.

256. Furukawa, K. and Hotta, Y. cDNA cloning of a germ cell specific lamin B3 from mouse spermatocytes and analysis of its function by ectopic expression in somatic cells. Embo J 1993;12:97-106.

257. Goldberg, M., Jenkins, H., Allen, T., Whitfield, W. G. and Hutchison, C. J. *Xenopus* lamin B3 has a direct role in the assembly of a replication competent nucleus: evidence from cell-free egg extracts. J Cell Sci 1995;108:3451-61.

258. Fisher, D. Z., Chaudhary, N. and Blobel, G. cDNA sequencing of nuclear lamins A and C reveals primary and secondary structural homology to intermediate filament proteins. Proc Natl Acad Sci U S A 1986;83:6450-4.

259. Weber, K., Plessmann, U. and Traub, P. Maturation of nuclear lamin A involves a specific carboxy-terminal trimming, which removes the polyisoprenylation site from the precursor; implications for the structure of the nuclear lamina. FEBS Lett 1989;257:411-4.

260. Smith, D. E., Gruenbaum, Y., Berrios, M. and Fisher, P. A. Biosynthesis and interconversion of *Drosophila* nuclear lamin isoforms during normal growth and in response to heat shock. J Cell Biol 1987;105:771-90.

261. Bossie, C. A. and Sanders, M. M. A cDNA from *Drosophila melanogaster* encodes a lamin C-like intermediate filament protein. J Cell Sci 1993;104:1263-72.

262. Riemer, D., Stuurman, N., Berrios, M., Hunter, C., Fisher, P. A. and Weber, K. Expression of *Drosophila* lamin C is developmentally

regulated: analogies with vertebrate A-type lamins. J Cell Sci 1995;108:3189-98.

263. Bione, S., Maestrini, E., Rivella, S., Mancini, M., Regis, S., Romeo, G. and Toniolo, D. Identification of a novel X-linked gene responsible for Emery-Dreifuss muscular dystrophy. Nat Genet 1994;8:323-7.

264. Bonne, G., Di Barletta, M. R., Varnous, S., Becane, H. M., Hammouda, E. H., Merlini, L., Muntoni, F., Greenberg, C. R., Gary, F., Urtizberea, J. A., Duboc, D., Fardeau, M., Toniolo, D. and Schwartz, K. Mutations in the gene encoding lamin A/C cause autosomal dominant Emery-Dreifuss muscular dystrophy. Nat Genet 1999;21:285-8.

265. Fatkin, D., MacRae, C., Sasaki, T., Wolff, M. R., Porcu, M., Frenneaux, M., Atherton, J., Vidaillet, H. J., Jr., Spudich, S., De Girolami, U., Seidman, J. G., Seidman, C., Muntoni, F., Muehle, G., Johnson, W. and McDonough, B. Missense mutations in the rod domain of the lamin A/C gene as causes of dilated cardiomyopathy and conduction-system disease. N Engl J Med 1999;341:1715-24.

266. Muchir, A., Bonne, G., van der Kooi, A. J., van Meegen, M., Baas, F., Bolhuis, P. A., de Visser, M. and Schwartz, K. Identification of mutations in the gene encoding lamins A/C in autosomal dominant limb girdle muscular dystrophy with atrioventricular conduction disturbances (LGMD1B). Hum Mol Genet 2000;9:1453-9.

267. Speckman, R. A., Garg, A., Du, F., Bennett, L., Veile, R., Arioglu, E., Taylor, S. I., Lovett, M. and Bowcock, A. M. Mutational and haplotype analyses of families with familial partial lipodystrophy (Dunnigan variety) reveal recurrent missense mutations in the globular C-terminal domain of lamin A/C. Am J Hum Genet 2000;66:1192-8.

268. Novelli, G., Muchir, A., Sangiuolo, F., Helbling-Leclerc, A., D'Apice, M. R., Massart, C., Capon, F., Sbraccia, P., Federici, M., Lauro, R., Tudisco, C., Pallotta, R., Scarano, G., Dallapiccola, B., Merlini, L. and Bonne, G. Mandibuloacral dysplasia is caused by a mutation in LMNA-encoding lamin A/C. Am J Hum Genet 2002;71:426-31.

269. De Sandre-Giovannoli, A., Chaouch, M., Kozlov, S., Vallat, J. M., Tazir, M., Kassouri, N., Szepetowski, P., Hammadouche, T., Vandenberghe, A., Stewart, C. L., Grid, D. and Levy, N. Homozygous defects in LMNA, encoding lamin A/C nuclear-envelope proteins, cause autosomal recessive axonal neuropathy in human (Charcot-Marie-Tooth disorder type 2) and mouse. Am J Hum Genet 2002;70:726-36.

270. Sullivan, T., Escalante-Alcalde, D., Bhatt, H., Anver, M., Bhat, N., Nagashima, K., Stewart, C. L. and Burke, B. Loss of A-type lamin expression compromises nuclear envelope integrity leading to muscular dystrophy. J Cell Biol 1999;147:913-20.

271. Kleinschmidt, J. H. Membrane protein folding on the example of outer membrane protein A of *Escherichia coli*. Cell Mol Life Sci 2003;60:1547-58.

272. Henderson, R., Baldwin, J. M., Ceska, T. A., Zemlin, F., Beckmann, E. and Downing, K. H. Model for the structure of bacteriorhodopsin based on high-resolution electron cryo-microscopy. J Mol Biol 1990;213:899-929.

273. Luecke, H., Schobert, B., Richter, H. T., Cartailler, J. P. and Lanyi, J. K. Structure of bacteriorhodopsin at 1.55 A resolution. J Mol Biol 1999;291:899-911.

274. Alberts, B., Bray, D., Lewis, J., Raff, M., Roberts, K. and Watson, J. D. Molecular biology of the cell. New York:Garland Publishing, Inc.; 1994.

275. Borgese, N., Brambillasca, S., Soffientini, P., Yabal, M. and Makarow, M. Biogenesis of tail-anchored proteins. Biochem Soc Trans 2003;31:1238-42.

276. Johnson, A. E. and van Waes, M. A. The translocon: a dynamic gateway at the ER membrane. Annu Rev Cell Dev Biol 1999;15:799-842.

277. Alder, N. N. and Johnson, A. E. Cotranslational membrane protein biogenesis at the endoplasmic reticulum. J Biol Chem 2004;279:22787-90.

278. Gorlich, D., Hartmann, E., Prehn, S. and Rapoport, T. A. A protein of the endoplasmic reticulum involved early in polypeptide translocation. Nature 1992;357:47-52.

279. Goder, V. and Spiess, M. Topogenesis of membrane proteins: determinants and dynamics. FEBS Lett 2001;504:87-93.

280. Nelson, D. L. and Cox, M. M. Lehninger principles of biochemistry. New York:Worth Publishers; 2000.

281. von Heijne, G. Membrane protein structure prediction. Hydrophobicity analysis and the positive-inside rule. J Mol Biol 1992;225:487-94.

282. Hartmann, E., Rapoport, T. A. and Lodish, H. F. Predicting the orientation of eukaryotic membrane-spanning proteins. Proc Natl Acad Sci U S A 1989;86:5786-90.

283. Abell, B. M., Pool, M. R., Schlenker, O., Sinning, I. and High, S. Signal recognition particle mediates post-translational targeting in eukaryotes. EMBO J 2004;23:2755-64.

284. Denzer, A. J., Nabholz, C. E. and Spiess, M. Transmembrane orientation of signal-anchor proteins is affected by the folding state but not the size of the N-terminal domain. EMBO J 1995;14:6311-7.

285. Wahlberg, J. M. and Spiess, M. Multiple determinants direct the orientation of signal-anchor proteins: the topogenic role of the hydrophobic signal domain. J Cell Biol 1997;137:555-62.

286. Liu, L. P. and Deber, C. M. Uncoupling hydrophobicity and helicity in transmembrane segments. Alpha-helical propensities of the amino acids in non-polar environments. J Biol Chem 1998;273:23645-8.

287. Harley, C. A., Holt, J. A., Turner, R. and Tipper, D. J. Transmembrane protein insertion orientation in yeast depends on the charge difference across transmembrane segments, their total hydrophobicity, and its distribution. J Biol Chem 1998;273:24963-71.

288. van Vliet, C., Thomas, E. C., Merino-Trigo, A., Teasdale, R. D. and Gleeson, P. A. Intracellular sorting and transport of proteins. Prog Biophys Mol Biol 2003;83:1-45.

289. Emanuelsson, O. and von Heijne, G. Prediction of organellar targeting signals. Biochim Biophys Acta 2001;1541:114-9.

290. Chatterjee, S. and Mayor, S. The GPI-anchor and protein sorting. Cell Mol Life Sci 2001;58:1969-87.

291. Martin, P. E. and Evans, W. H. Incorporation of connexins into plasma membranes and gap junctions. Cardiovasc Res 2004;62:378-87.

292. Killian, J. A. Hydrophobic mismatch between proteins and lipids in membranes. Biochim Biophys Acta 1998;1376:401-15.

293. Cosson, P. and Letourneur, F. Coatomer interaction with di-lysine endoplasmic reticulum retention motifs. Science 1994;263:1629-31.

294. Letourneur, F., Gaynor, E. C., Hennecke, S., Demolliere, C., Duden, R., Emr, S. D., Riezman, H. and Cosson, P. Coatomer is essential for retrieval of dilysine-tagged proteins to the endoplasmic reticulum. Cell 1994;79:1199-207.

295. Schutze, M. P., Peterson, P. A. and Jackson, M. R. An N-terminal double-arginine motif maintains type II membrane proteins in the endoplasmic reticulum. EMBO J 1994;13:1696-705.

296. Bonifacino, J. S. and Dell'Angelica, E. C. Molecular bases for the recognition of tyrosine-based sorting signals. J Cell Biol 1999;145:923-6.

297. Folsch, H., Ohno, H., Bonifacino, J. S. and Mellman, I. A novel clathrin adaptor complex mediates basolateral targeting in polarized epithelial cells. Cell 1999;99:189-98.

298. Folsch, H., Pypaert, M., Schu, P. and Mellman, I. Distribution and function of AP-1 clathrin adaptor complexes in polarized epithelial cells. J Cell Biol 2001;152:595-606.

299. Miranda, K. C., Khromykh, T., Christy, P., Le, T. L., Gottardi, C. J., Yap, A. S., Stow, J. L. and Teasdale, R. D. A dileucine motif targets E-cadherin to the basolateral cell surface in Madin-Darby canine kidney and LLC-PK1 epithelial cells. J Biol Chem 2001;276:22565-72.

300. Keller, P. and Simons, K. Post-Golgi biosynthetic trafficking. J Cell Sci 1997;110:3001-9.

301. Fiedler, K., Parton, R. G., Kellner, R., Etzold, T. and Simons, K. VIP36, a novel component of glycolipid rafts and exocytic carrier vesicles in epithelial cells. EMBO J 1994;13:1729-40.

302. Machamer, C. E. Golgi retention signals: do membranes hold the key? Trends Cell Biol 1991;1:141-4.

303. Nilsson, T., Hoe, M. H., Slusarewicz, P., Rabouille, C., Watson, R., Hunte, F., Watzele, G., Berger, E. G. and Warren, G. Kin recognition between medial Golgi enzymes in HeLa cells. Embo J 1994;13:562-74.

304. van Meer, G. Lipid traffic in animal cells. Annu Rev Cell Biol 1989;5:247-75.

305. Lundbaek, J. A., Andersen, O. S., Werge, T. and Nielsen, C. Cholesterol-induced protein sorting: an analysis of energetic feasibility. Biophys J 2003;84:2080-9.

306. Bretscher, M. S. and Munro, S. Cholesterol and the Golgi apparatus. Science 1993;261:1280-1.

307. Munro, S. An investigation of the role of transmembrane domains in Golgi protein retention. EMBO J 1995;14:4695-704.

308. Munro, S. A comparison of the transmembrane domains of Golgi and plasma membrane proteins. Biochem Soc Trans 1995;23:527-30.

309. Yang, M., Ellenberg, J., Bonifacino, J. S. and Weissman, A. M. The transmembrane domain of a carboxyl-terminal anchored protein determines localization to the endoplasmic reticulum. J Biol Chem 1997;272:1970-5.

310. Brandizzi, F., Frangne, N., Marc-Martin, S., Hawes, C., Neuhaus, J. M. and Paris, N. The destination for single-pass membrane proteins is influenced markedly by the length of the hydrophobic domain. Plant Cell 2002;14:1077-92.

311. Yuan, Z. and Teasdale, R. D. Prediction of Golgi Type II membrane proteins based on their transmembrane domains. Bioinformatics 2002;18:1109-15.

312. Szczesna-Skorupa, E. and Kemper, B. Endoplasmic reticulum retention determinants in the transmembrane and linker domains of cytochrome P450 2C1. J Biol Chem 2000;275:19409-15.

313. Hallberg, E., Wozniak, R. W. and Blobel, G. An integral membrane protein of the pore membrane domain of the nuclear envelope contains a nucleoporin-like region. J Cell Biol 1993;122:513-21.

314. Sambrook, J., Fritsch, E. F. and Maniatis, T. Molecular cloning: a laboratory manual. Cold Spring Harbor, NY:Cold Spring Harbor Laboratory Press; 1989.

315. Vaughn, J. L., Goodwin, R. H., Tompkins, G. J. and McCawley, P. The establishment of two cell lines from the insect *Spodoptera frugiperda* (Lepidoptera; Noctuidae). In Vitro 1977;13:213-7.

316. Grace, T. D. C. Establishment of four strains of cells from insect tissue grown *in vitro*. Nature 1962;195:788-789.

317. Bordier, C. Phase separation of integral membrane proteins in Triton X-114 solution. J Biol Chem 1981;256:1604-7.

318. Rosenberg, I. M. Protein analysis and purification:bentchtop techniques. Boston, MA:Birkhauser; 1996.

319. Adam, S. A., Sterne-Marr, R. and Gerace, L. Nuclear protein import using digitonin-permeabilized cells. Methods Enzymol 1992;219:97-110.

320. Yguerabide, J., Schmidt, J. A. and Yguerabide, E. E. Lateral mobility in membranes as detected by fluorescence recovery after photobleaching. Biophys J 1982;40:69-75.

321. Hasler, U., Greasley, P. J., von Heijne, G. and Geering, K. Determinants of topogenesis and glycosylation of type II membrane proteins. Analysis of Na,K-ATPase beta 1 AND beta 3 subunits by glycosylation mapping. J Biol Chem 2000;275:29011-22.

322. Nilsson, I., Saaf, A., Whitley, P., Gafvelin, G., Waller, C. and von Heijne, G. Proline-induced disruption of a transmembrane alpha-helix in its natural environment. J Mol Biol 1998;284:1165-75.

323. Saksena, S., Shao, Y., Braunagel, S. C., Summers, M. D. and Johnson, A. E. Cotranslational integration and initial sorting at the endoplasmic reticulum translocon of proteins destined for the inner nuclear membrane. Proc Natl Acad Sci U S A 2004;101:12537-42.

324. Laemmli, U. K. Cleavage of structural proteins during the assembly of the head of bacteriophage T4. Nature 1970;227:680-5.

325. Kozak, M. At least six nucleotides preceding the AUG initiator codon enhance translation in mammalian cells. J Mol Biol 1987;196:947-50.

326. Gruenbaum, Y., Landesman, Y., Drees, B., Bare, J. W., Saumweber, H., Paddy, M. R., Sedat, J. W., Smith, D. E., Benton, B. M. and Fisher, P. A. *Drosophila* nuclear lamin precursor Dm0 is translated from either of two developmentally regulated mRNA species apparently encoded by a single gene. J Cell Biol 1988;106:585-96.

327. Pollard, K. M., Chan, E. K., Grant, B. J., Sullivan, K. F., Tan, E. M. and Glass, C. A. *In vitro* posttranslational modification of lamin B cloned from a human T-cell line. Mol Cell Biol 1990;10:2164-75.

328. Saksena, S., Shao, Y., C., B. S., Summers, M. D. and Johnson, A. E. Cotranslational integration and initial sorting at the endoplasmic reticulum translocon of proteins destined for the inner nuclear membrane. Proc Natl Acad Sci U S A 2004;101:12537-42.

APPENDIX A

Quantitation Macro

```
#  This is a modified version of the TEXASAM.MCR macro.
#5/12/2001 RSU
#This macro allows the user to measure specific regions within an image.

! imgsetpath "d:\"

imgdelete "*"
Gclear 0
MBok "Place images into appropiate image channels: 1-Red, 5-Green, 6-Blue
and 7-Brightfield"
showwindow "Display",1
showwindow "Gallery",1
showwindow "Messages",1
! MSload "basic"
write "@"

write "Load Red Channel"
! imgload "d:\",1
imgcopy 1,4

write "Load Green Channel"
! imgload "d:\",2
imgcopy 2,5

write "Load Blue Channel"
! imgload "d:\",3
imgcopy 3,6

write "Load Brightfield Channel"
! imgload "d:\",7
imgdisplay 7

write "Circle drawn around plasma membrane Part F."
MBok  "Draw a circle around plasma membrane, Part F, at cutlink command."

cutlink 7,255,1
imgdisplay 7
dislev 7,8,254,255,1
binscrap 8,8,0,20,0
binfill 8,9
```

```
binand 9,6,10

write "Circle drawn around inner nuclear membrane marker Part E."
MBok  "Draw a circle around inner nuclear membrane marker, Part E, at cutlink
command."

imgdisplay 3
cutlink 3,255,1
dislev 3,14,254,255,1
binscrap 14,14,0,20,0
binfill 14,15
binand 15,6,16

write "The computer will draw a circle to define the outer nuclear membrane."
MBok "The computer will draw a circle to define the outer nuclear membrane,
Part D"

macro DoThick(Input=1,GreyLev=255,Thick=3,OvColor=12)
   dislev 3,92,GreyLev,GreyLev
   bindilate 92,93,7,Thick
   binfill 92,94
   binnot 94,94
   binand 93,94,94
   Gextract 94,1,255,OvColor

binxor 16,94,17

MSsetprop "REGIONFEAT","AREA,SUMD"
write "Now we can measure Cytoplasmic Localization, Image 18, Part A"
MBok "Now we can measure Cytoplasmic Localization, Image 18, Part A"
! dislev 10,18,1,255,1
binscrap 18,18,0,20,0

write "Now we can measure Nuclear Membrane Localization, Image 19, Part B"
MBok  "Now we can measure Nuclear Membrane Localization, Image 19, Part
B"
! dislev 17,19,4,255,1
binscrap 19,19,0,20,0

write "Now we can measure Nuclear Protein Localization, Image 20, Part C"
MBok "Now we can measure Nuclear Protein Localization, Image 20, Part C"
! dislev 16,20,4,255,1
binscrap 20,20,0,20,0
```

```
MSmeasmask 18,1,"dataR",0,1,10
MSmeasmask 18,2,"dataG",0,1,10
MSmeasmask 18,3,"dataB",0,1,10

MSmeasmask 19,1,"dataR",1,1,10
MSmeasmask 19,2,"dataG",1,1,10
MSmeasmask 19,3,"dataB",1,1,10

MSmeasmask 20,1,"dataR",1,1,10
MSmeasmask 20,2,"dataG",1,1,10
MSmeasmask 20,3,"dataB",1,1,10

MBok  "The first measurement is Part A , 2nd is Part B, 3rd is Part C."
datalist "dataR",0,0
pause "Make sure to print out the database!!"
datalist "dataG",0,0
pause "Make sure to print out the database!!"
datalist "dataB",0,0
pause "Make sure to print out the database!!"

MBok "These next several lines are for creating the 3 circles, pseudo-colored."
imgnew 100,256,256,1,"Grey"
Gclear 0
Gextract 8,254,255,12
Gextract 14,254,255,14
Gextract 94,254,255,6
Gmerge 100,255
imgdelete 100
imgnew 100,256,256,1,"Colour"
Gmerge 95,255
Gclear 0
#!imgsetpath "d:\"
!imgsave 95,"d:\circles.tif"
#MBok "Try function in line 118 or 119 to give you the best results."
#combine 95,2,102,1.00,0.82,0
#add 95,2,101,2

write "Done"
MBok "Thank you Roger!!!"
```

APPENDIX B

DNA construct information and clone maps

B1: ΔXbaI, NarI pUC 18.

Description:

Δ XbaI, NarI pUC18 was generated by digestion of each site followed by polymerase fill. With the exception of the destroyed restriction sites, this version of pUC18 remains unaltered. This vector is used as the pUC backbone for the sorting motif GFP fusions.

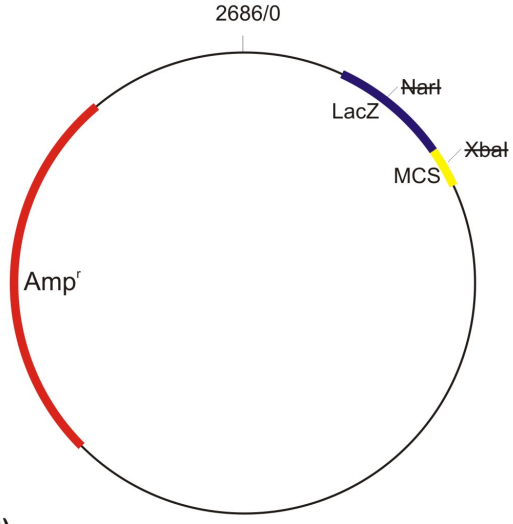

New multiple cloning site(MCS)

```
                                  Sal I
                                  Hinc II                                    Kpn I                EcoR I
HindIII                           Acc I                  Bam HI              Acc65 I              Apo I
5' AAGCTTGCATGCCTGCAGGTCGACTCTACTAGAGGATCCCCGGGTACCGAGCTCGAATTC 3'
      SphI    SbfI                                                 Ava I          Ban II
              PstI                                                 Xma I          Ecl136 II
                                                                   Sma I          Sac I
```

B2: ΔXbaI, NarI pUC 18 EGFP/Alt. EGFP.

Description:

EGFP or Alt. EGFP was PCR amplified from the pEGFP(Clontech Laboratories) using the oligonucleotides shown below. This yielded two forms of the EGFP gene flanked on either side with BamHI sites. Alt. EGFP lacks the coding seqeunce for the N-terminal 7 amino acids to yield a protein with the N-terminal charges deleted. The 5' end of these products have an Xba I and Nar I site between the Bam HI and the methionine start codon of the EGFP. The PCR product was cloned into ΔXbaI, NarI pUC18. This clone will be used subsequently for cloning the modified sorting motif fusion proteins. The PCR product is underlined in the MCS sequence shown below.

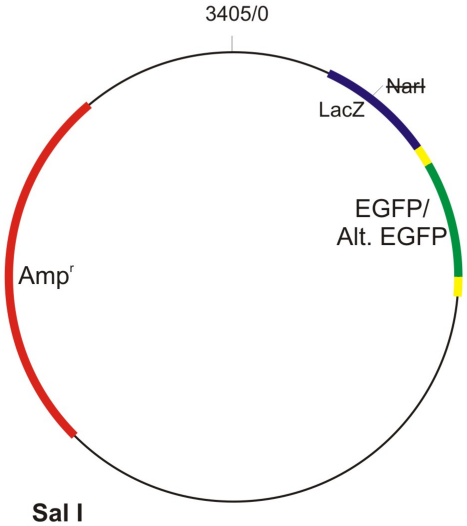

EGFP MCS:

HindIII SphI SbfI PstI Sal I Hinc II Acc I Bam HI XbaI NarI

5′ AAGCTTGCATGCCTGCAGGTCGACTCTACTAGAGGATCCTCTAGATGGCGCC

EGFP Sequence

ATG GTG AGC AAG GGC GAG ... ... GAC GAGCTG TAC AAG TAA

Bam HI Kpn I Sac I Eco RI

GGATCCCCGGGTACCGAGCTCGAATTC 3′

Sma I

Alt. EGFP MCS:

HindIII SphI SbfI PstI Sal I Hinc II Acc I Bam HI XbaI NarI

5′ AAGCTTGCATGCCTGCAGGTCGACTCTACTAGAGGATCCTCTAGATGGCGCC

Alternate EGFP Sequence

ATG TTA TCG CTG TTC ACC GGG ... ... GAC GAGCTG TAC AAG TAA

Bam HI Kpn I Sac I Eco RI

GGATCCCCGGGTACCGAGCTCGAATTC 3′

Oligonucleotides for PCR:

EGFP Forward 5′ cg ggatcc tctaga atg ggcggg ATGGTGAGCAAGGGCGAG 3′
(BamHI; XbaI; NarI; Met Codon; EGFP sequence)

Alt. EGFP Forward 5′ cg ggatcc tctaga atg ggcgcc atgttatcg CTGTTCACCGGGGTGG 3′
(BamHI; XbaI; NarI; Met Codon; EGFP sequence)

EGFP Reverse 5′ gcg ggatcc TTACTTGTACAGCTCGTCC 3′
(BamHI; EGFP sequence)

B3: Sorting Motif clones.

Description:

The annealed complementary oligonucleotides shown below were cloned into the XbaI, NarI site of the EGFP vectors in Appendix B1. A unique NaeI was also added to the coding sequence and used to screen for insertion of the annealed oligonucleotides. These base clones were then used to generate pIE1, pGEM-4z, pBACgus, and pcDNA3.1/zeo(+) constructs for expression in insect and mammalian cells, and *in vitro* transcription.

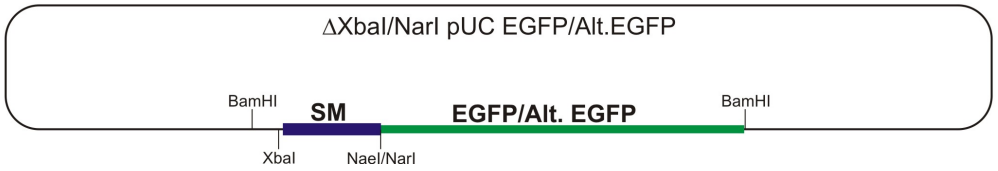

Amino acid sequences and Oligonucleotides:

E66

```
 M  S  I  V  L  I  I  V  I  V  V  I  F  L  I  C  F  L  Y  L  S  N  S  N  N
ATGTCTATCGTATTGATTATTGTCATAGTTGTAATATTTTTAATATGTTTTTTGTACCTATCAAATAGCAATAAT
TACAGATAGCATAACTAATAACAGTATCAACATTATAAAAATTATACAAAAAACATGGATAGTTTATCGTTATTA

 K  N  D  A  N  K  N  N  A  F  I  D
AAAAATGATGCCAATAAAAACAATGCTTTTATTGAT
TTTTTACTACGGTTATTTTTGTTACGAAAATAACTA
```

SM1A

```
          M  S  I  V  L  I  I  V  I  V  V  I  F  L  I  C  F  L  Y  L  S  N
5′ ctaga ATGTCTATCGTATTGATTATTGTCATAGTTGTAATATTTTTAATATGTTTTTTGTACCTATCAAAT
3′     t TACAGATAGCATAACTAATAACAGTATCAACATTATAAAAATTATACAAAAAACATGGATAGTTTA

 S  N  N  K  N  D  A  N  K  N  N   A  G   A   M-EGFP
AGCAATAATAAAAATGATGCCAATAAAAACAAT gccgg   3′
TCGTTATTATTTTTACTACGGTTATTTTTGTTA cggccgc 5′
```

SM1C

```
          M  S  I  V  L  I  I  V  I  V  V  I  L  L  I  C  L  L  L  L  S  N
5′ ctaga ATGTCTATCGTATTGATTATTGTCATAGTTGTAATATTGTTAATATGTTTGTTGTTGCTATCAAAT
3′     t TACAGATAGCATAACTAATAACAGTATCAACATTATAACAATTATACAAACAACAACGATAGTTTA

 S  N  N  K  N  D  A  N  K  N  N   A  G   A   M-EGFP
AGCAATAATAAAAATGATGCCAATAAAAACAAT gccgg   3′
TCGTTATTATTTTTACTACGGTTATTTTTGTTA cggccgc 5′
```

SM2A

```
          M  S  I  V  L  I  I  V  I  V  V  I  F  L  I  C  F  L  Y  L
5′ ctaga ATGTCTATCGTATTGATTATTGTCATAGTTGTAATATTGTTAATATGTTTGTTGTTGCTA
3′     t TACAGATAGCATAACTAATAACAGTATCAACATTATAACAATTATACAAACAACAACGAT

 K  N  D  A  N  K  N  N   A  G   A   M-EGFP
AAAAATGATGCCAATAAAAACAAT gccgg   3′
TTTTTACTACGGTTATTTTTGTTA cggccgc 5′
```

SM2C

```
          M  S  I  V  L  I  I  V  I  V  V  I  L  L  I  C  L  L  L  L
5′ ctaga ATGTCTATCGTATTGATTATTGTCATAGTTGTAATATTTTTAATATGTTTTTTGTACCTA
3′     t TACAGATAGCATAACTAATAACAGTATCAACATTATAAAAATTATACAAAAAACATGGAT

 K  N  D  A  N  K  N  N   A  G   A   M-EGFP
AAAAATGATGCCAATAAAAACAAT gccgg   3′
TTTTTACTACGGTTATTTTTGTTA cggccgc 5′
```

SM3A/B

```
                M  S  I  V  L  I  I  V  I  V  V  I  F  L  I  C  F  L  Y  L  S  N
5′ ctaga ATGTCTATCGTATTGATTATTGTCATAGTTGTAATATTTTTAATATGTTTTTTGTACCTATCAAAT
3′     t TACAGATAGCATAACTAATAACAGTATCAACATTATAAAAATTATACAAAAAACATGGATAGTTTA

 S  N  N   A  G   A   M-EGFP/Alt.EGFP
AGCAATAAT gccgg   3′
TCGTTATTA cggccgc 5′
```

SM3C/D

```
                M  S  I  V  L  I  I  V  I  V  V  I  L  L  I  C  L  L  L  L  S  N
5′ ctaga ATGTCTATCGTATTGATTATTGTCATAGTTGTAATATTGTTAATATGTTTGTTGTTGCTATCAAAT
3′     t TACAGATAGCATAACTAATAACAGTATCAACATTATAACAATTATACAAACAACAACGATAGTTTA

 S  N  N   A  G   A   M-EGFP/Alt.EGFP
AGCAATAAT gccgg   3′
TCGTTATTA cggccgc 5′
```

SM4A/B

```
                M  S  I  V  L  I  I  V  I  V  V  I  F  L  I  C  F  L  Y  L  S  N
5′ ctaga ATGTCTATCGTATTGATTATTGTCATAGTTGTAATATTTTTAATATGTTTTTTGTACCTATCAAAT
3′     t TACAGATAGCATAACTAATAACAGTATCAACATTATAAAAATTATACAAAAAACATGGATAGTTTA

 S  N  N  K  N  D  A  N  K  N  N   A  G   A   M-EGFP/Alt.EGFP
AGCAATAATAAAAATGATGCCAATAAAAACAAT gccgg   3′
TCGTTATTATTTTTACTACGGTTATTTTTGTTA cggccgc 5′
```

SM4C/D

```
                M  S  I  V  L  I  I  V  I  V  V  I  L  L  I  C  L  L  L  L
5′ ctaga ATGTCTATCGTATTGATTATTGTCATAGTTGTAATATTGTTAATATGTTTGTTGTTGCTA
3′     t TACAGATAGCATAACTAATAACAGTATCAACATTATAACAATTATACAAACAACAACGAT

 A  G   A   M-EGFP/Alt.EGFP
gccgg   3′
cggccgc 5′
```

ΔC SM1A

```
                M  S  I  V  L  I  I  V  I  V  V  I  F  L  I  L  F  L  Y  L  S  N
5′ ctaga ATGTCTATCGTATTGATTATTGTCATAGTTGTAATATTTTTAATATTGTTTTTGTACCTATCAAAT
3′     t TACAGATAGCATAACTAATAACAGTATCAACATTATAAAAATTATAACAAAAACATGGATAGTTTA

 S  N  N  K  N  D  A  N  K  N  N   A  G   A   M-EGFP
AGCAATAATAAAAATGATGCCAATAAAAACAAT gccgg   3′
TCGTTATTATTTTTACTACGGTTATTTTTGTTA cggccgc 5′
```

Sorting motif amino acid sequences and corresponding complementary oligonucleotides used for construction of the EGFP/Alt. EGFP fusion proteins. “A” and “B” represent native E66 sequences, while “C” and “D” have the aromatic amino acid codons (bold text) replaced with a leucine codon. The transmembrane sequences are shown in red. The aromatic amino acids or the leucines substituted in their place are bolded. The polar amino acids are shown in blue. The charged cluster of amino acids is shown in purple. The EGFP of Alt.EGFP sequences are shown in green. In ΔC SM1A, the cystiene to leucine mutation is underlined.

B4: E66 Charge Modification of E66.

Description:

E66 with mutated charge residues within the SM region were PCR using the oligos listed below. The PCR products were cloned into the SacI/MluI of site of Δ33 Clone 60 T7S to generate a copy of a mutated E66 with the noted changes in the charge residues. These base clones were then used to generate pIE1 variants for expression in insect cells.

E66 charge modifications base clones:

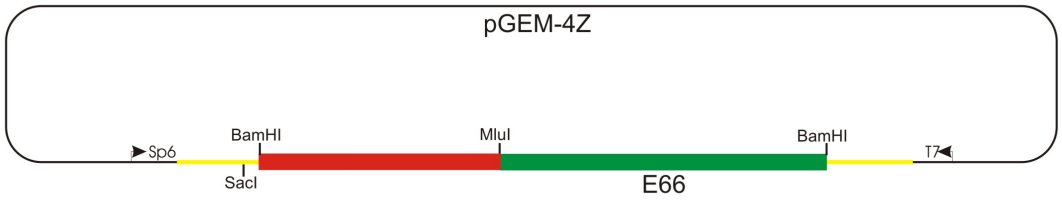

E66 charge modificagtions MCS:

SacI **BamHI** **MluI** **BamHI**

...GAGCTC GGATCC **ATG**TTCATCGTA.....TCCCTC ACGCGT TACTGG.....TAAGGATCC...

Met Start

Amino acid sequences and Oligonucleotides:

E66

M S I V L I I V I V V I F L I C F L Y L S N S N N

ATGTCTATCGTATTGATTATTGTCATAGTTGTAATATTTTTAATATGTTTTTTGTACCTATCAAATAGCAATAAT

K N D A N K N N A F I D

AAAAATGATGCCAATAAAAACAATGCTTTTATTGAT

E66 GGG FW

M S I V L I I V I V V I F L I C F L Y

5′ cccgagctcggatcc ATGTCTATCGTATTGATTATTGTCATAGTTGTAATATTTTTAATATGTTTTTTGTAC

L S N S N N **G** N **G** A N **G** N N A F I D L

CTATCAAATAGCAATAAT**GGG**AAT**GGG**GCCAAT**GGG** AACAATGCTTTTATTGATCTC 3′

E66 AAA FW

M S I V L I I V I V V I F L I C F L Y

5′ cccgagctcggatcc ATGTCTATCGTATTGATTATTGTCATAGTTGTAATATTTTTAATATGTTTTTTGTAC

L S N S N N **A** N **A** A N **A** N N A F I D L

CTATCAAATAGCAATAAT**GCG**AAT**GCG**GCCAAT**GCG** AACAATGCTTTTATTGATCTC 3′

E66 KKK FW

M S I V L I I V I V V I F L I C F L Y

5′ cccgagctcggatcc ATGTCTATCGTATTGATTATTGTCATAGTTGTAATATTTTTAATATGTTTTTTGTAC

L S N S N N **K** N **K** A N **K** N N A F I D L

CTATCAAATAGCAATAAT**AAA**AAT**AAA**GCCAAT**AAA** AACAATGCTTTTATTGATCTC 3′

E66 DDD FW

M S I V L I I V I V V I F L I C F L Y

5′ cccgagctcggatcc ATGTCTATCGTATTGATTATTGTCATAGTTGTAATATTTTTAATATGTTTTTTGTAC

L S N S N N **D** N **D** A N **D** N N A F I D L

CTATCAAATAGCAATAAT**GAT**AAT**GAT**GCCAAT**GAT** AACAATGCTTTTATTGATCTC 3′

M S I V L I I V I V V I F L I C F L Y
E66 KDA FW 5′ cccgagctcggatcc ATGTCTATCGTATTGATTATTGTCATAGTTGTAATATTTTTAATATGTTTTTTGTAC

L S N S N N **K** N **D** A N **A** N N A F I D L
CTATCAAATAGCAATAAT**AAA**AAT**GAT**GCCAAT**GCG** AACAATGCTTTTATTGATCTC 3′

M S I V L I I V I V V I F L I C F L Y
E66 ADK FW 5′ cccgagctcggatcc ATGTCTATCGTATTGATTATTGTCATAGTTGTAATATTTTTAATATGTTTTTTGTAC

L S N S N N **A** N **D** A N **K** N N A F I D L
CTATCAAATAGCAATAAT**GCG**AAT**GAT**GCCAAT**AAA** AACAATGCTTTTATTGATCTC 3′

M S I V L I I V I V V I F L I C F L Y
E66 ADA FW 5′ cccgagctcggatcc ATGTCTATCGTATTGATTATTGTCATAGTTGTAATATTTTTAATATGTTTTTTGTAC

L S N S N N **A** N **D** A N **A** N N A F I D L
CTATCAAATAGCAATAAT**GCG**AAT**GAT**GCCAAT**GCG** AACAATGCTTTTATTGATCTC 3′

M S I V L I I V I V V I F L I C F L Y
E66 RDR FW 5′ cccgagctcggatcc ATGTCTATCGTATTGATTATTGTCATAGTTGTAATATTTTTAATATGTTTTTTGTAC

L S N S N N **R** N **D** A N **R** N N A F I D L
CTATCAAATAGCAATAAT**CGC**AAT**GAT**GCCAAT**CGC** AACAATGCTTTTATTGATCTC 3′

M S I V L I I V I V V I F L I C F L Y
E66 KEK FW 5′ cccgagctcggatcc ATGTCTATCGTATTGATTATTGTCATAGTTGTAATATTTTTAATATGTTTTTTGTAC

L S N S N N **K** N **E** A N **K** N N A F I D L
CTATCAAATAGCAATAAT**AAA**AAT**GAA**GCCAAT**AAA** AACAATGCTTTTATTGATCTC 3′

M S I V L I I V I V V I F L I C F L Y
E66 RER FW 5′ cccgagctcggatcc ATGTCTATCGTATTGATTATTGTCATAGTTGTAATATTTTTAATATGTTTTTTGTAC

L S N S N N **R** N **E** A N **R** N N A F I D L
CTATCAAATAGCAATAAT**CGC**AAT**GAA**GCCAAT**CGC** AACAATGCTTTTATTGATCTC 3′

E66 RV **5′** CAGATACAAGCCGAGCCAGTAACGGCGGTGAGGACGAGC 3′

Amino acid sequences and PCR oligonucleotides for the amplification of ODV-E66 with the charged a.a.of the sorting motif changed to the noted amino acid. Text in lowercase denotes nucleotides added for cloning purposes, text in uppercase denotes the nucleotides corresponding to the E66 sequence, bolded text corresponds to the codons that were changed to yield the noted amino acid, and underlined text corresponds to the complementary sequence of E66 used the PCR amplification.

B5: 125 amino acid Charge Modification of E66 fused to EGFP.

Description:

PCR products amplified from the pGEM E66 charge modification clones using the oligos listed below were cloned into the XbaI, NarI site of the EGFP vector in Appendix B1. These base clones were then used to generate pIE1 variants for expression in insect cells.

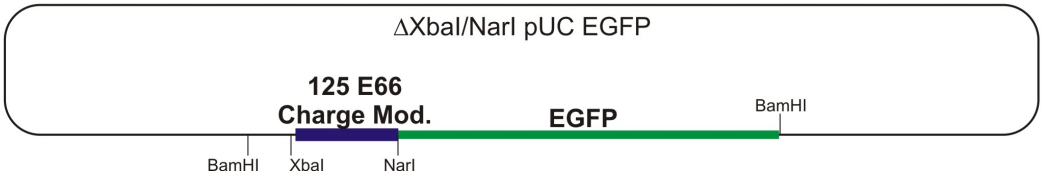

Amino acid sequence and Oligonucleotides:

```
                    SacII  AflII  XbaI  Kozak  M  S  I   V  L  I  I  V  I  V
125 new FW  5' cta ccgcgg cttaag tctaga ccacc atgtctata GTATTGTTATTGGTCATAGTTG 3'

                      NarI   KpnI   F  D  P   V  S  T  W  P  S
125 gfp RV  5' atctac ggcgcc ggtacc aaagtccgg AACGCTTGTCCACGGACTC 3'
```

The amino acid sequence and PCR oligonucleotides used for the amplification of the sequence corresponding to the first 125 amino acids of E66 with the charge modifications (appendix B5). Text in uppercase corresponds to the sequence that is complementary to E66.

Appendix B6: Sorting Motif plus Kozak

Description:

For mammalian expression, a Kozak site needed to be inserted 5' of the methionine start of the SM-GFP coding seqeunce. PCR (oligonucleotides 125FW (ori), and EGFP Reverse (appendix B2) was used to amplify the coding seqeunce with the inserted 5' Kozak. The PCR product was inserted into the pcDNA3.1/Zeo(+) vector via the AflII/BamHI sites.

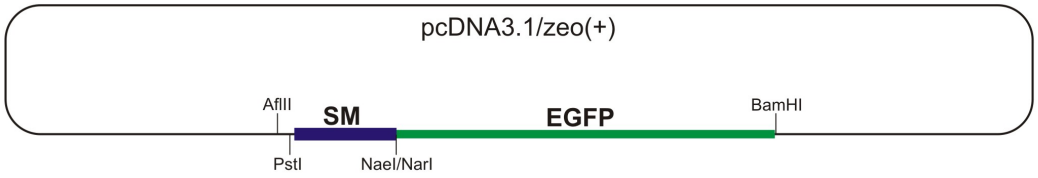

pcDNA3.1 SM-GFP (K) MCS:

PmeI AflII PstI Kozak M S I Y K STOP BamHI
...GCGTTTAAACTTAAG T CTTAAG T CCACC ATGTCTATA.....TAC AAG TAA GGATCC ACTAG...
SM-GFP

Amino acid sequence and Oligonucleotide:

SacII AflII PstI Kozak M S I V L I I V I V
125 FW (ori) 5' cta ccgcgg cttaag t cgatcg t ccacc ATGTCTATTGTATTGTTATTGGTCATAGTTG 3'

The amino acid sequence and PCR oligonucleotides used for the amplification of the SM with a 5' Kozak consensus transcription initiation site. Text in uppercase corresponds to the sequence that is complementary to E66.

B7: **N-terminal deletion of LBR-EGFP clones.**

Description:

Two LBR-EGFP fusion clones were generated using PCR (oligonucleotides shown below) from the phLBR 1TM-EGFP provided by Ellenberg. These PCR products were cloned into the BamHI/HindIII sites of pUC18. Subsequent cloning into pIE1, pBACgus, pCMVblue, and pGEM-4z was done for expression studies.

N-terminal deletion of LBR-EGFP clones MCS:

SmaI BamHI NotI HindIII
...CCCGGG GGATCC GCGT ATG.....TACAAGTAA GCGGCCGC AAGCTT...
LBR EGFP

Oligonucleotides:

		BamHI
LBR-GFP-F-C	5′ cgc ggatcc gcgt atg ATCCGGGCAAAGGGACTTGG 3′	
		Met Codon
		BamHI
LBR-GFP-F-H	5′ cgc ggatcc gcgt atg TTTGGAGGAGTACCTGGTG 3′	
		Met Codon
		Hind III
LBR-GFP-R	5′ gacccaagctt GCGGCCGCTTACTTGTACAGCTCG 3′	

PCR oligonucleotides for amplification of the coding sequence for LBR EGFP minus the N-terminal binding domain. LBR-GFP-F-C is the forward oligonucleotide used to generate the $_{200\text{-}238}$LBR-GFP clone construct, LBR-GFP-F-H is the forward oligonucleotide used to generate the $_{208\text{-}238}$LBR-GFP clone construct, and LBR-GFP-R is the reverse oligonucleotides used to generate both the $_{200\text{-}238}$LBR-GFP and $_{208\text{-}238}$LBR-GFP clone constructs.

B8: LBR-EGFP Kozak clones.

Description:

For mammalian expression, a Kozak site needed to be inserted 5' of the methionine start of the LBR-GFP coding seqeunce. PCR (oligonucleotides below) was used to amplify the coding seqeunce with the inserted 5' Kozak. The PCR product was inserted into the pcDNA3.1/Zeo(+) vector via the BamHI/NotI sites.

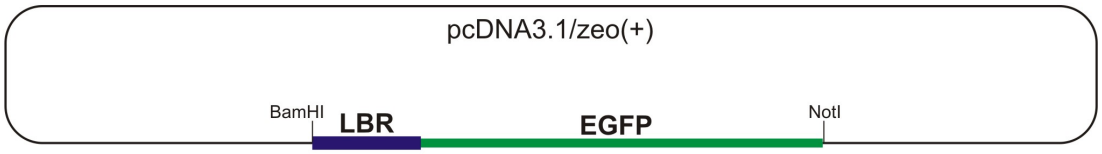

pcDNA3.1 LBR-GFP (K) MCS:

Amino acid Sequence and Oligonucleotides:

	BamHI M I R A K D L
200-238 LBR-Kozak FW	5' gcg ggatccacc ATGATTCGGCAAAGGACTTG 3'
	Kozak
	BamHI M F G G V P
208-238 LBR-Kozak FW	5' gcg ggatccacc ATGTTTGGAGGAGTACCTG 3'
	Kozak
	BamHI
EGFP RV NotI	5' ata gcgggccgc TTACTTGTACAGCTCGTC 3'

The amino acid sequence and PCR oligonucleotides used for the amplification of $_{200\text{-}238}$LBR- and $_{208\text{-}238}$LBR-GFP with a 5' Kozak consensus transcription initiation site. Text in uppercase corresponds to the sequence that is complementary to $_{200\text{-}238}$LBR- and $_{208\text{-}238}$LBR-GFP.

B9: $T7_{1-238}$LBR-EGFP.

Description:

For digitonin permemabilization studies, a T7 epitope tag was inserted between the methionine start and amino acid 2 of the 1-238 LBR-GFP coding seqeunce. PCR (forward oligonucleotide below, reverse oligonucleotide, Appendix B9) was used to amplify the coding seqeunce with the inserted T7 epitope tag coding sequence. The PCR product was inserted into the pcDNA3.1/Zeo(+) vector via the BamHI/NotI sites.

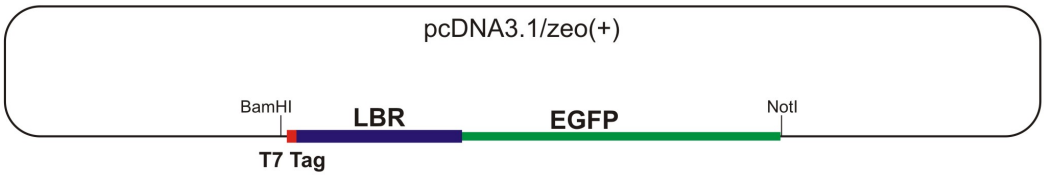

pcDNA3.1 $T7_{1-238}$LBR-GFP:

KpnI **BamHI** **Kozak**
...GGTACCGAGCTC GGATCC CCACC
T7 Epitope Tag sequence
ATG GCTTCTATGACCGGCGGACAGCAGATGGGAACATTCACA
LBR-EGFP **NotI**
CCTAGTAGG.....TAC AAG TAA T GCGGCCGC TCG...

1-238 LBR FW T7N

BamHI M A S M T G G Q Q M E H S H
5′ gcg ggatccacc ATGGCTTCTATGACCGGCGGACAGCAGATGGAACATTCACAC
Kozak

S S R K F A D
CCTAGTAGGAAATTTGCCGAT 3′

The amino acid sequence and PCR oligonucleotides used for the amplification of $_{1-238}$LBR-GFP with a N-terminal T7 epitope tag. Underlined in uppercase corresponds to the sequence that is complementary to $_{1-238}$LBR-GFP.

VITA

Shawn T. Williamson
2411 De Lee #25
Bryan, TX 77802
979 324 0658
stwilliamson@cox.net

EDUCATION
September 1994 - December 1996

Texas A&M University--College of Science
College Station, Texas
Bachelor of Science, December 1996, Microbiology

RESEARCH EXPERIENCE
January 1997 - August 1998

Texas A&M University--Department of Entomology
Research Assistant, Full Time
While in Dr. Max Summers laboratory as a research assistant I aided in the research of *Autographa californica* multi-nucleopolyhedrovirus (AcMNPV), a baculovirus.

TEACHING EXPERIENCE
September 1998-May 1999

Texas A&M University-Department of Biology
Graduate Teaching Assistant
As a graduate teaching assistant I taught, Diagnostic Bacteriology and Immunology Laboratory under the direction of Dr. Rita Moyes.

RESEARCH PRESENTATIONS

Entomology Graduate Student Forum, August 2003
"AcMNPV ODV-E66 encodes a nuclear targeting sequence that is sufficient for nuclear envelope and microvesicle localization of integral membrane proteins."

American Society of Virology, July 2004
"Sorting and localization of proteins to the inner nuclear membrane."

PUBLICATIONS

Williamson, S. T., Braunagel, S. C. & Summers, M. D. Sorting of proteins to the inner nuclear membrane is independent of immobilization. *Traffic* 2005; Submitted.

Braunagel, S. C., Williamson, S. T., Saksena, S., Zhong, Z., Russell, W. K., Russell, D. H. & Summers, M. D. Trafficking of ODV-E66 is mediated via a sorting motif and other viral proteins: facilitated trafficking to the inner nuclear membrane. *Proc Natl Acad Sci U S A* 2004; 101:8372-77.